A Simplified Multi-Zone Model for Determining the Placement of Bio-Defense Sensors in Large Buildings
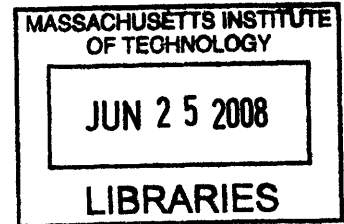
by

Scott B. Van Broekhoven

B.S., Mechanical Engineering

Northwestern University (2001)

Submitted to the Engineering Systems Division as Partial Fulfillment of the

Requirements for the Degree of Masters of Science in Engineering Systems

at the

Massachusetts Institute of Technology

June 2008

© 2008 Massachusetts Institute of Technology

Signature of Auth

Engineering Systems Division

May 9, 2008

Certified by..........

Annalisa Weigel Ph.D.

Jerome C. Hunsacker Assistant Professor of

Aeronautics and Astronautics and Engineering Systems

Thesis Supervisor

Accepted by...........

Richard Larson Ph.D.

Mitsui Professor of

Civil and Environmental Engineering and Engineering Systems

Acting Chair, ESD Education Committee

A Simplified Multi-Zone Model for Determining the Placement of Bio-Defense Sensors in Large Buildings

by

Scott B. Van Broekhoven

Submitted to the Engineering Systems Division as Partial Fulfillment of the
Requirements for the Degree of Masters of Science in Engineering Systems

ABSTRACT

The anthrax mailings of 2001 increased public and government awareness to the threat of bio-terrorism. Particularly vulnerable to a bio-terrorist event are large indoor facilities such as convention centers, office buildings, transportation centers, and sports arenas with their high population densities and limited physical security. Under heightened threat levels deploying bio-aerosol sensors inside these facilities provides added protection to the occupants. The challenge is determining the number and placement of sensors needed to guarantee the detection of a release inside a particular building.

The methodology proposed here aims to simplify the analysis of contamination transport within buildings and provide first-order sensing requirements for dose dependant sensors in large facilities. A reduced-order model is developed that allows buildings to be subdivided into larger sections while maintaining a higher degree of accuracy than building analysis models with the same level of granularity. The problem is formulated as a network model with the nodes representing possible sensor locations and the path lengths equal to the reduction in dose as a contaminant travels between sensor locations. Techniques borrowed from network theory are then used to determine the minimum cost set of sensors that provides full building coverage.

The reduced-order model estimates sensing requirements in hours or days for problems that would take months to analyze with fine grained multi-zone models and that are too large to be considered with computational fluid dynamics. Models of an office building, a convention center, and an airport terminal are constructed and their underlying network graph is employed to understand how the structure of the indoor environment affects the placement of sensors. Additionally, the equations derived to formulate the network model are used to quantify the optimal tradeoff between sensor sensitivity and cost as a function of building parameters. Future efforts will continue on this path, focusing on how easily discernible building properties such as size, HVAC layout, and air exchange rates can be used to predict the sensing requirements in large indoor spaces.

Thesis Supervisor: Annalisa Weigel
Title: Assistant Professor of Aeronautics and Astronautics and Engineering Systems

TABLE OF CONTENTS

LIST OF FIGURES

1. INTRODUCTION

The 2001 anthrax attack on the Hart Senate Office Building in Washington DC is only the most recent example of the use biological organisms as agents of combat. One hundred and fifty-eight countries ratified the 1972 Biological Weapons Convention prohibiting the development, production, and stockpiling of biological weapons. Active bio-weapons research continued, however, in countries such as the Soviet Union and Iraq through the early 1990's (Davis, 1999). In comparison to other weapons of mass destruction, biological warfare agents are inexpensive to produce and easy to transport making it likely that terrorists and rogue states will continue to employ biological weapons as a means to inflict mass causalities and create widespread fear.

Early warning in the case of an attack is absolutely critical towards reducing casualties. The time from anthrax inhalation until the first symptoms begin to present can vary anywhere from 1-15 days depending largely on the inhalation dose. The early symptoms for inhalation anthrax are similar to those for the flu, further complicating diagnosis. The efficacy of medical treatment depends on its speed because medical treatment is most effective when delivered before or just after the onset of symptoms. Over 90% of the population can be saved if treatment begins 2-3 days after a release but the survival rate drops off considerably if treatment takes longer (Wilkening, 2006). For contagious biological agents reducing detection time is even more important because the disease will continue to spread until medical personnel can quarantine those infected.

Recognizing the bio-terrorism threat, the United States government has begun to work with local municipalities to deploy sensors capable of detecting the release of an aerosolized biological agent. These sensors oftentimes take the form of air filters that are deployed around an urban area and are collected at regular intervals then sent to a laboratory for analysis (Miller, 2003). During periods of heightened threat levels multiple sensors may be placed in specific buildings to provide full coverage in the event of a release inside the building. Because there are numerous potential targets ranging from transportation hubs to large office buildings, sports arenas, and convention centers a rigorous analysis to determine to determine the sensing requirements in all possible facilities is not plausible. A need exists for a simple analysis tool that can provide a first-order set of sensing requirements for a variety of different indoor spaces.

Current research focuses on techniques that would be appropriate for the defense of one particular facility but are too computationally intensive to be applied to multiple large buildings. Computational Fluid Dynamics, which approximates the Navier-Stokes equations for fluid transport, provides the highest degree of accuracy in determining the transport of contaminants in interior spaces, but is too computationally complex to easily be applied in large buildings. In recent years researchers have adapted building analysis codes such as CONTAM and COMIS that were originally created for energy and fire protection research to analyze bio-defense related problems. Even using these simplified models, however, it can take weeks or months to fully analyze a large complex building such as an airport or skyscraper.

The methodology proposed here aims to further simplify the analysis of contamination transport within buildings and provide first-order sensing requirements for dose dependant sensors in large facilities. A reduced-order model is developed that allows buildings to be subdivided into larger sections while maintaining a higher degree of accuracy than building analysis models with the same level of granularity. The problem can then be formulated as a network model which lends itself to a broad range of analysis techniques. This approach aims to shorten the time needed to analyze a complex building to a few days.
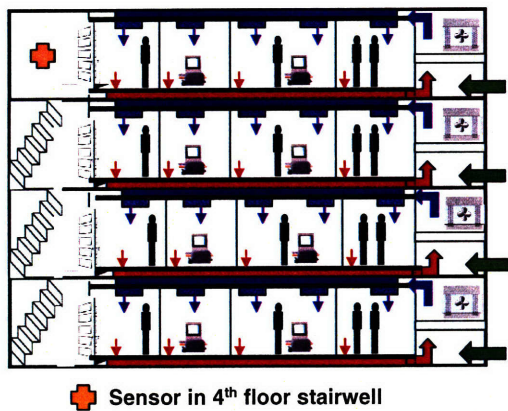
Goal : To quickly determine the sensing needs in large buildings

1. Number and placement of sensors to detect a given release mass
2. Placement and mass that would go undetected for a given number of sensors
3. Understand how building conditions affect sensing requirements

Assume : Dose dependant sensors

🔴 Sensor in 4th floor stairwell

Figure 1-1 Research goals

The first step is to break large building into zones consisting of air handling unit (AHU) zones and transport zones. AHU zones are collections of rooms that are supplied by a single air-conditioning fan, and thus share the same supply air. Transport zones are areas within a building that provide a high degree of airflow between multiple AHU zones and where the primary airflow is not from the HVAC system. They are referred to as

"transport zones" due to the key role they play in the movement of contaminants around buildings. Examples of common transport zones include stairwells and hallways.

Once the building is subdivided, the interfaces between the zones are defined. The zone interfaces describe both what zones are connected to each other and the effective flow-rate between any interconnected zones. The effective airflow rate takes into account both the dominant airflow between zones and the additional airflow needed to account for the diffusion of contaminants against the primary airflow gradient. Intra-zonal airflows can be calculated using analytical models taking into account the performance of the HVAC system and natural ventilation due to temperature and wind. One of the strengths of the reduced-order model is that the important airflow parameters are direct inputs making it easy to run simulations with a range of different airflows. Section 3.0 describes the methods for estimating intra-zonal transport in more detail.

Once the intra-zonal airflow rates are defined, a network model can be constructed that describes the reduction in contamination dosage between any two interconnected zones. In the network model the nodes are potential sensor locations and the path lengths between nodes is the reduction in dose as contamination travels between sensor locations. The contamination transport equations used to construct the network model are derived in detail in Section 4.0. These equations take into account the amount of airflow that is exchanged between two zones and the dilution of contamination as it passes through one zone into the next. The dilution for a given zone is a function of AHU parameters including air exchange rate, outside air fraction, and supply air filter efficiency.
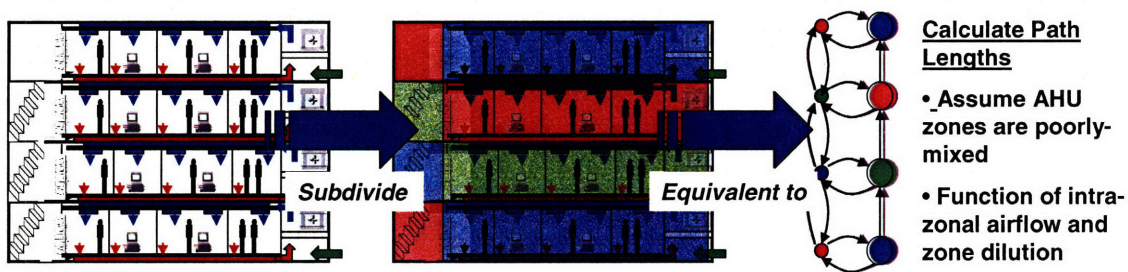
Figure 1-2 Analysis plan: Forming the network model

Utilizing the network model, the dosage that would result at a potential sensor location given a release in any building zone can be determined. This is analogous to determining the shortest path between any two points in a network. In keeping with the shortest path structure, a dynamic programming algorithm is described that takes the

network model and produces a matrix where the dosage at each sensor location is computed for a release in every possible zone. The problem of optimizing sensor layout then reduces to a set coverage problem, a common class of problems in network theory. The goal is to minimize the cost of the sensors required to provide full coverage, to guarantee a sensor alarm no matter what the release location.

	S1	S2	S3 ...,
S1	0	.65	1E-3
S2	.01	0	.1
S3	0	.10	0
4	0	.10	.65

Calculate distances

	S1	S2	S3 ...,
Z1	.02	.013	1E-5
Z2	.008	.80	.08
Z3	2E-5	.02	.22
Z4	1E-8	.003	

Minimum cost covering set

S1 → Z1
S2 → Z2
S3 → Z3
S4 → Z4

Represented as

Dosage is reduced (1/.01) = 100X from sensor location 2 to location 1

A release in Zone 2 leads to a dose of .8 at S2 and a dose of .8*.01 = .008 at S1

Sensor 3 covers zones {2,3,4}
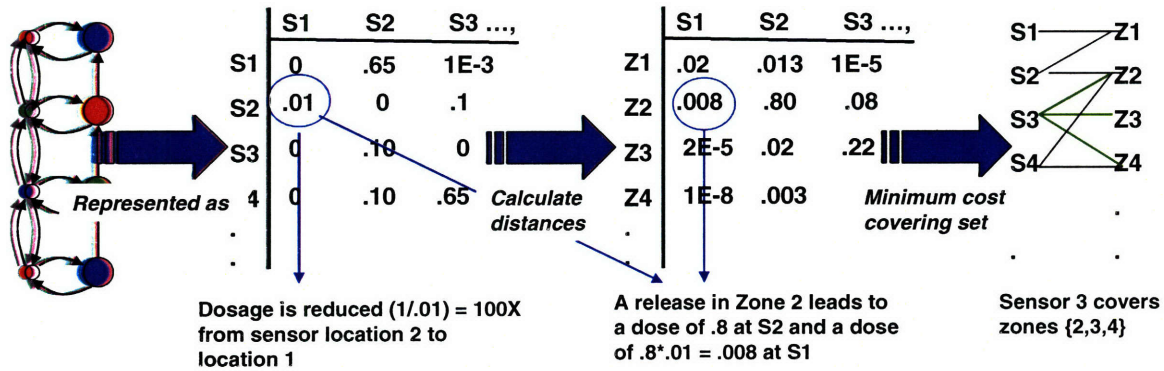
Figure 1-3 Analysis plan: Analyzing the network model

Binary integer programming is efficient for solving relatively modest set coverage problems and is sufficiently fast and accurate for this application. In the integer programming algorithm, the constraint is providing full building coverage and the cost of the sensors is to be minimized. Section 5.0 discusses the formulation and implementation of this model.

Section 6 explores applications of this methodology to three different building types and Section 7 utilizes the three models to understand some of the important tradeoffs in sensor selection. The relative importance of sensor cost and sensitivity is examined by simulating a large number of building conditions and then analyzing how different factors influence the optimal sensing solution. The problem of deploying a limited set of sensors is examined and a methodology is developed to guide the allocation of limited resources.

Determine the General Building Characteristics
- HVAC airflows
- HVAC layout
- Intra-zonal airflows

Chapter 3

Subdivide the Building into Zones
- HVAC zones
- Transport zones

Chapter 4

Create the Network Model
- Sensor positions
- Calculate path lengths

Chapter 5

Analyze the Network Model
- Set coverage problem
- How building properties affect the optimal sensing solution

Chapters 6-8

Figure 1-4 Chapter guide

2. LITERATURE REVIEW

Current methods for modeling the flow of contamination within buildings are time intensive and analyze only a single set of building conditions. This thesis moves away from the detailed analysis of large spaces and towards considering how the gross properties of a building influence the placement of sensors. Section 2.1 reviews some of the current approaches to understanding contamination transport and the placement of sensors inside buildings. Section 2.2 discusses concepts that were employed, or helped to inspire, the development of the reduced-order model discussed in the remainder of this document.

2.1. CURRENT METHODS

Numerous studies have been conducted on the methods to model the transportation of pollutants in the indoor environment. Both Computational Fluid Dynamics (CFD) and simpler multi-zone models have been used to address this problem. Common classes of problems include the location of sources within buildings based upon sensor data, and the appropriate placement of sensors within buildings.

Liu and Zhai (Liu, 2007a) and Zhang and Chen (Zhang, 2007) examine methods of solving inverse contamination transport models to determine contamination source locations based on sensor data in interior spaces. The inverse CFD approach is applied to an aircraft cabin in both studies, and (Liu, 2007a) also examines a single office space. Both techniques require that a detailed CFD model be created of the facility to determine airflow patterns which is then used to determine contamination transport dynamics. (Zhang, 2007) reports over 70 hours of simulation time was required for 20 minutes of real-time simulation for the 3-D CFD aircraft cabin model.

Multi-zone models represent rooms of buildings as zones with homogeneous pressure, temperatures, and contamination concentrations. The zones are connected by user-defined leakage paths and the airflow rates and contamination flow between zones is calculated by mass-balance. Due to there relative simplicity, multi-zone models can be applied to larger buildings than is feasible with CFD. The most popular multi-zone models are CONTAM (Walton, 2006) developed at the National Institute of Standards and Technology and COMIS (Feustel, 1997) developed largely at the Lawrence Berkley

12

National Laboratory. The models have been experimentally validated on a multi-zone single-family home (Haghighat, 1996) and commercial buildings (Upham, 1997).

Liu and Zhai (Liu, 2007b) conducted a broad overview of inverse modeling methods for indoor contaminant tracking and recommended a two-stage approach utilizing both CFD and multi-zone models. In their approach, the multi-zone model is used to approximate the source location within the building. A CFD-based inverse model is then used to provide greater fidelity near the source location. Wang and Chen (Wang, 2007) validated a coupled CFD / multi-zone model for a four room building and found better agreement with experimental data than using a purely multi-zone approach.

2.2. RELEVANT THEORY TO THE REDUCED-ORDER MODEL

This research proposes subdividing large buildings into even larger zones than is common with multi-zone models and formulating the model as a network diagram. Techniques taken from network theory are then used to analyze the efficient placement of sensors within the building.

The reduced order approach is similar in many ways to the multi-zone models. The concept of sub-dividing buildings into large zones with uniform properties is borrowed from multi-zone models. The major differences in the reduced-order approach are that intra-zonal airflow rates are input as opposed to calculated by the model and large AHU zones are assumed to be poorly-mixed as opposed to well-mixed.

Multi-zone models incorporate many factors in their airflow calculations making it time consuming to understand the influence of each parameter. Rao (Rao, 1993) recommends using sensitivity analysis for analyzing airflow sensitivities with respect to input parameter variation. The reduced-order model inputs the intra-zonal airflows directly making it much easier to parametrically study the influence of airflow rates on a building's sensing requirements.

Multi-zone models must be defined at a fine enough granularity so that the well-mixed assumption holds true. It is particularly difficult to accurately predict the contamination profile near the source location where small variations in airflow parameters can have a significant affect (Schaelin, 1994). The reduced-order model attempts to avoid these challenges by defining zones at an even coarser level, ignoring the localized

contamination "hot-spots", and calculating the lower bounds of contamination dosage within the zone.

Determining the minimum number of sensors needed to provide full building coverage is a common problem in network theory known as a set coverage problem. Set coverage problems are an example of a combinatorial optimization problem and are generally NP-complete. Binary integer programming is a common approach to finding an approximate solution to these problems. Chakrabaty et al. (Chakrabaty, 2002) describe an integer programming method to optimize sensor coverage area on a grid for sensors with varying detection ranges and costs. Altmael et al. (Altmael, 2006) solves a similar problem considering both perfect and imperfect sensors using binary integer programming with greedy and Lagrangean heuristics.

The idea of conceptualizing buildings as two dimensional networks is borrowed from the field of space syntax theory. Space syntax theory is a set of theories and techniques that help architects simulate the likely social effects of their designs. Buildings are represented as maps or graphs and the relationship between the structural form and the function of the built environment are explored (Hiller, 1984).

This thesis describes a new technique for conceptualizing indoor spaces and understanding the effect of their structure and HVAC characteristics on the transport of contaminants. A modified multi-zone approach is used to formulate a building as a two-dimensional network or graph and then methods borrowed from network theory are used to determine the optimal placement of sensors. By focusing on the properties of the space itself and not on the fine-grained airflow phenomena, very large buildings can be analyzed much faster than with more traditional time intensive methods.

3. CONTAMINATION TRANSPORT IN INTERIOR SPACES

Understanding the spread of contamination in an interior space is an important step in the design of bio-defense systems. The reduced order model does not calculate building airflows directly but instead takes intra-zonal airflows as input parameters. As explained in this section, airflow conditions in buildings depend on wide range of parameters. By treating intra-zonal airflows as input parameters it becomes easy to parametrically vary the airflow rates and understand the effect on sensing requirements.

This chapter describes the dominant factors affecting airflows, and thus contamination transport, around large buildings. It is meant only as a guideline for creating a first approximation of the airflow rates between different sections of a building. In addition, methods for modeling contamination propagation in buildings are discussed. A range of models are available with varying levels of granularity.

3.1. TRANSPORT MECHANISMS

Contamination can either propagate through a building's Heating, Ventilation, and Air-Conditioning (HVAC) system or it can be spread through direct contamination flows between neighboring rooms. Contamination flows between sections of a building supplied by different air-handling units (AHUs) occurs due to room-to-room airflows, whereas contamination spread within a single air-handling unit zone is the result of both direct airflows and HVAC transport.

3.1.1. FORCED VENTILATION

Forced ventilation systems use fans or blowers to provide fresh air to, control temperature and humidity in, and remove contaminants from buildings. Large buildings are typically sub-divided into groups of neighboring indoor spaces that share the same thermal requirements and thus are supplied by a single air-handling unit (AHU). These building sections will be referred throughout this thesis as "AHU zones", "HVAC zones", or simply "zones".
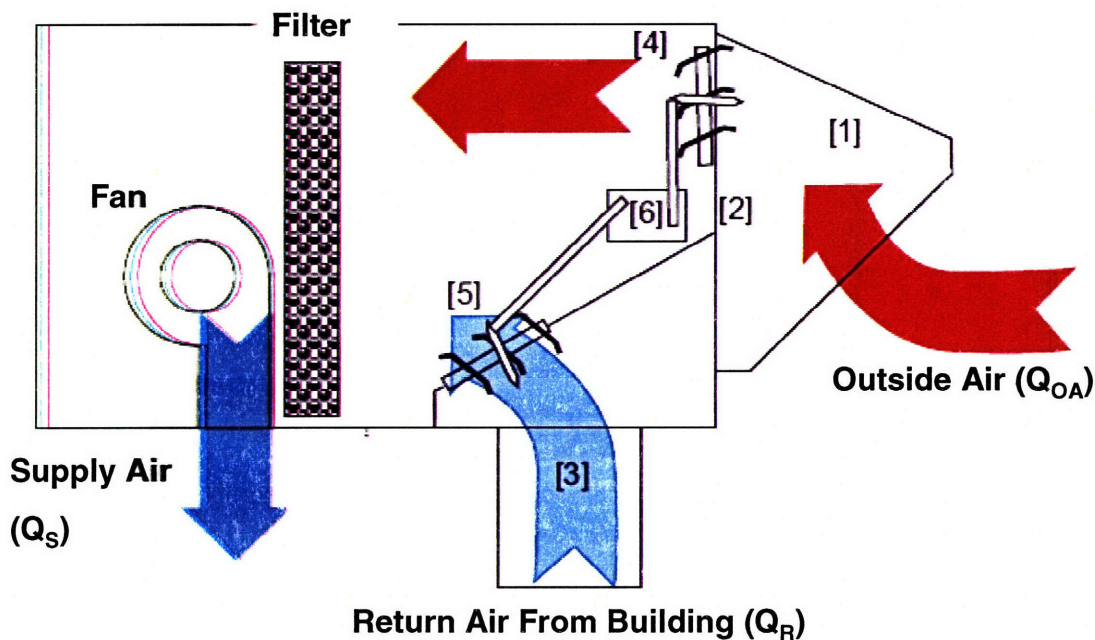
Figure 3-1 A typical air-handling unit

In Figure 3-1 the parameters of an AHU unit that affect the transport of contaminants are shown. A fan or blower draws in air from both outside the building and interior spaces. The relative proportion of outside air to return air is determined by a control system and controlled by dampers. The control system monitors the air temperature outdoors and indoors and then adjusts the outside air fraction to minimize the heating and cooling loads placed on the HVAC system. Typically as the outdoor air temperature approaches the set point for the supply air temperature the fraction of outside air will increase. If, however, the outside air is either very warm or very cold then the outside air fraction will approach a minimum value. The minimum outside air rate is defined in ASHRAE standard 62.1 and is the amount of fresh air needed to dilute building contaminants such as carbon dioxide (ASHRAE, 2004). Because buildings are always drawing some

16

amount of fresh air they are naturally over-pressurized relative to the outdoors. Typical building overpressure is around 5-10 Pa.

After the outside air and return air mixes it passes through a series of filters and heating and cooling coils. The heating and cooling coils bring the mixed air stream to the temperature needed maintain the building temperature. The filters remove contaminants from the air stream both to extend the lifetime of the AHU components and improve the breathing air for building occupants. The filter efficiency for AHU filters can vary considerably and the choice of filters depends on the use of the building. Hospitals and medical facilities oftentimes have filters that are at least 90% efficient and micro-electronic laboratories will have filters with efficiencies approaching 99.999%. ASHRAE standard 62.1 recommends office buildings have MERV 6 filters or better, filters that are only about 40% efficient in the size range of biological particles as specified by ASHRAE standard 52.2 (ASHRAE, 1999).

Standard 52.2 Minimum Efficiency Reporting Value (MERV)	Composite Average Particle Size Efficiency, % in Size Range,um		
	Range 1 0.30 - 1.0	Range 2 1.0 - 3.0	Range 3 3.0 - 10.0
1	n/a	n/a	E3 < 20
2	n/a	n/a	E3 < 20
3	n/a	n/a	E3 < 20
4	n/a	n/a	E3 < 20
5	n/a	n/a	20 $\leq$ E3 < 35
6	n/a	n/a	35 $\leq$ E3 < 50
7	n/a	n/a	50 $\leq$ E3 < 70
8	n/a	n/a	70 $\leq$ E3
9	n/a	E2 < 50	85 $\leq$ E3
10	n/a	50 $\leq$ E2 < 65	85 $\leq$ E3
11	n/a	65 $\leq$ E2 < 80	85 $\leq$ E3
12	n/a	80 $\leq$ E2	90 $\leq$ E3
13	E1 < 75	90 $\leq$ E2	90 $\leq$ E3
14	75 $\leq$ E1 < 85	90 $\leq$ E2	90 $\leq$ E3
15	85 $\leq$ E1 < 95	90 $\leq$ E2	90 $\leq$ E3
16	95 $\leq$ E1	95 $\leq$ E2	95 $\leq$ E3

Figure 3-2 Filter efficiencies for MERV filter ratings

Building owners can choose to install higher efficiency filters that may improve occupant health, but higher efficiency filters have a higher flow resistance and therefore increase the power draw of the fans and blowers.

17

The air handling unit characteristics that determine how rapidly contaminated air is removed from a zone are the outside air rate and the return air rate multiplied by the filter efficiency. The supply air filters scrub the recirculated air removing indoor contaminants. Increasing levels of fresh air causes exfiltration through the building envelope to increase in proportion, purging the building of contamination.

3.1.2. TURBULENT DIFFUSION

A number of studies have examined the diffusion of contaminants in the indoor environment. Most have focused on single rooms and employ computational fluid dynamics and / or detailed experimentation involving a full-scale climate room (Beghein, 2005), (Richmond-Bryant, 2006), (Yamamoto, 1994). The turbulent diffusion of contaminants is a complex problem that depends on many factors including room geometry, supply air diffuser locations and properties, furniture, and source location and properties. In the reduced-order model developed in this analysis, single rooms are grouped into larger AHU zones and are defined by a single concentration. In-room or even in-zone diffusion are not relevant, only the transport of contaminants between AHU zones must be estimated.

The rate of contamination diffusion is defined by Fick's 1st law of diffusion:

$$J = -D\frac{dC}{dX}$$

(3-1)

where:

J = contamination flux (g/(min*m^2))

D = diffusion coefficient (m^2/min)

dC/dX = the concentration gradient

At the supply diffuser location the room concentration should be close to the concentration in the remaining rooms in the zone with the exception of those rooms in the immediate vicinity of the source. A reasonable approximation for the concentration gradient might be the difference in concentrations between two zones divided by the shortest distance between their nearest supply air diffusers.

Once the contamination mass flow is determined the airflow between the two zones is calculated that would result in the equivalent mass flow.

18

$$Qx_{AB} = A\frac{J_{AB}}{C_A}$$

(3-2)

where:

Qx_{AB} = the airflow from **Zone A** to **Zone B** (m^3/min)

C_A = the concentration in **Zone A** (g/m^3)

A = cross sectional area of the opening btw A and B

The challenge becomes calculating the diffusion coefficient. A simplified form was suggested by Drivas etc. al. for contamination diffusion in large rooms (Drivas, 1994).

$$\left(\frac{1}{k^2 H^4}\right)D^3 + \left(g * \frac{dT}{HT}\right)D = \frac{au_0^2}{2}$$

(3-3)

where:

k = von Karman's constant (.4)

H = representative length scale (m)

g = gravitational constant (m^2/s)

dT = temperature difference between the ceiling and floor (K)

T = room temperature (K)

a = room air exchange rate (1/s)

u_0 = diffuser exit velocity (m/s)

 For example, two large zones that are each 80 m X 30 m with 10 m ceiling heights, a 5 deg K temperature gradient, 293 deg K room air temperature, and a diffuser exit velocity of 10 m/s would yield a diffusion coefficient of about 2. With reasonable parameters for the zone concentrations, and a very large opening between the zones an equivalent airflow of several hundred m^3/min is possible. This might be representative of the type of mixing that occurs between non-partitioned convention center halls as discussed in Chapter 6. Because of the strong dependence on room height and the area of the opening between zones, turbulent diffusion of contaminants will likely be a strong effect for very large zones with minimal restriction to intra-zonal airflows.

3.1.3. PEOPLE TRAFFIC

The movement of people in buildings influences the dispersion of contaminants through the shedding of particulates that have settled on peoples clothing and the entrainment of particulates in a person's turbulent wake as they move between zones. Weapons-grade material, like the anthrax used in the 2001 attack on the Hart Senate Office Building, is likely to consist of small uniform particles that are electrostatically treated to prevent clumping and remain aerosolized over long time periods (JAMA, 2002). Small particulates settle slowly and have low resuspension rates (Thatcher, 1995), (Ferro, 2004), and are considered only in their aerosolized form during this analysis. The entrainment of particle in a person's wake is more likely to occur with small particulates which will follow the local streamlines and could make an important contribution to transport dynamics in buildings.

While the quantity of contaminant transported through the movement of people is small relative to the other mechanisms considered in this chapter, it remains important because it occurs independently of the primary airflow gradient. This can lead to contamination dispersion into areas of buildings that normally would not be reachable from the source location.

Computational Fluid Dynamics (CFD) was used to investigate the amount of contamination that follows in a person's turbulent wake. A three-dimensional model was constructed using Fluent version 6.1, a commercial CFD code. In the model, a six foot tall person walks at 4.4 feet per second (3 miles/hour) down a long hallway. When the simulation begins the person is completely surrounded by a contaminant. The person walks through an uncontaminated area with clean air blowing on the person at varying rates. The amount of contamination in 100 ft^3 volume surrounding the person is recorded while he walks the thirty foot hallway length. Figure 3-3 shows a top view of the CFD model at two different time steps (Van Broekhoven, 2002).

Top View t = .5 s **Flow direction**   **Top View t = 2 s**

Results Domain ~ 100 ft³
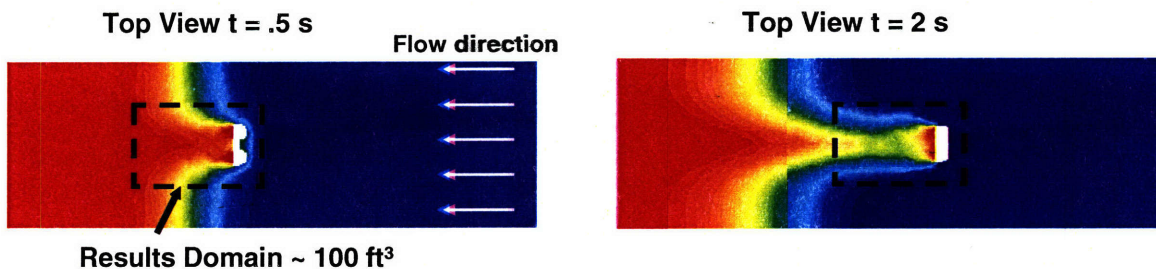
Figure 3-3 CFD simulation of contamination in turbulent wakes

The amount of contamination in the 100 ft³ volume surrounding the figure in the CFD model can be used to approximate the contamination that would result as a person walks through a doorway separating contaminated and uncontaminated building zones. Figure 3-4 shows that the contamination level in the results domain is reduced by one order of magnitude after the person exits the contaminated space. With a results domain equal to 100 ft³ this is the equivalent to the person dragging 10 ft³ of contaminated air into the clean zone.
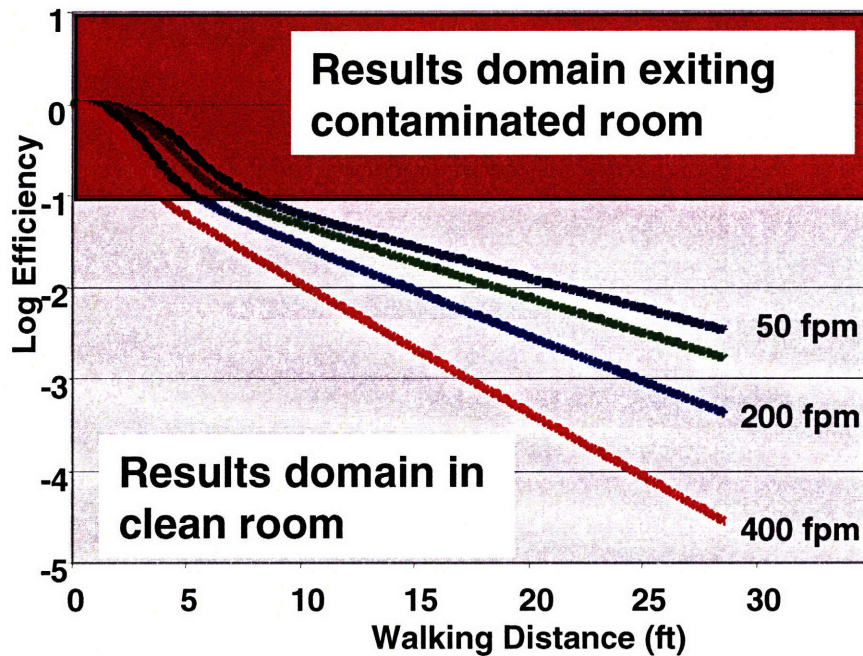
Figure 3-4 Concentration is reduced by 10X upon exiting the contaminated room

If each person transports 10 ft³ of contaminated air between zones the airflow rate providing the equivalent level of contamination transport equals the people movement rate (people / min) * 10 (ft³/person).

3.1.4. TEMPERATURE AND WIND

The air exchange rate between AHU zones in a building are oftentimes strongly influenced by the outside air temperature and wind. Outdoor conditions vary considerably from season to season or even from day-to-day, making it difficult to predict the internal airflow conditions at any single point in time.

Wind against a building leads to higher pressures on the windward side of the building and low pressures on the leeward side.
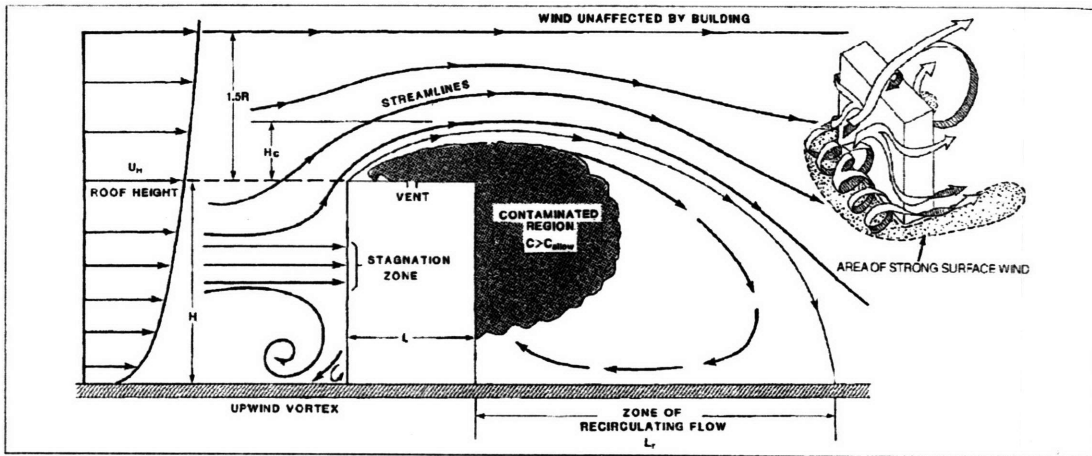
Figure 3-5 Flow patterns around rectangular buildings (ASHRAE, 2001)

The time averaged surface pressures are proportional to the wind velocity pressure p_V given by Bernoulli's equation:

$$p_V = \frac{\rho_a U_H^2}{2 g_c} \qquad (3-4)$$

where:

ρ_A = outdoor air density

g_C = gravitational constant

U_H = approach wind speed at wall height H

For high wind speeds the wind velocity pressure can exceed the design building overpressure. This will lead to air infiltration on the windward side and exfiltration on the leeward side. Intra-zonal airflows will follow the wind pressure profile with air flowing from the zones on the windward side to zones on the leeward side of the building.

In addition to wind, temperature difference between the outdoors and indoors can have a significant effect on the indoor airflow distribution. Temperature induced flows are most prominent in tall buildings with limited interior partitions.

The stack pressure is the hydrostatic pressure caused by the weight of a column of air. Temperature differences between outdoors and indoors cause stack pressure differences across the building envelope that drive airflows. If the indoor temperature is considered constant throughout the building then the stack pressure p_S across an opening is given by (ASHRAE, 2001):

$$\Delta p_S = \rho_A (\frac{T_O - T_i}{T_i}) g (H_{NPL} - H) \qquad (3\text{-}5)$$

where:

ρ_A = outdoor air density

T_O = outside air temperature (K)

T_i = indoor air temperature (K)

g = gravitational constant (m^2/s)

H = height of the opening (m)

H_{NPL} = height of the neutral pressure level across a reference plane (m)

The neutral pressure level (NPL) is the height at which there is no pressure difference between the outdoors and indoors. The NPL depends on internal partitions, vertical shafts such as stairwells and elevators, the location of openings in the buildings envelope, and the performance of the HVAC system. Figure 3-6 shows the qualitative variation in the NPL for buildings with uniform openings above and below the mid-height and no significant internal resistance.
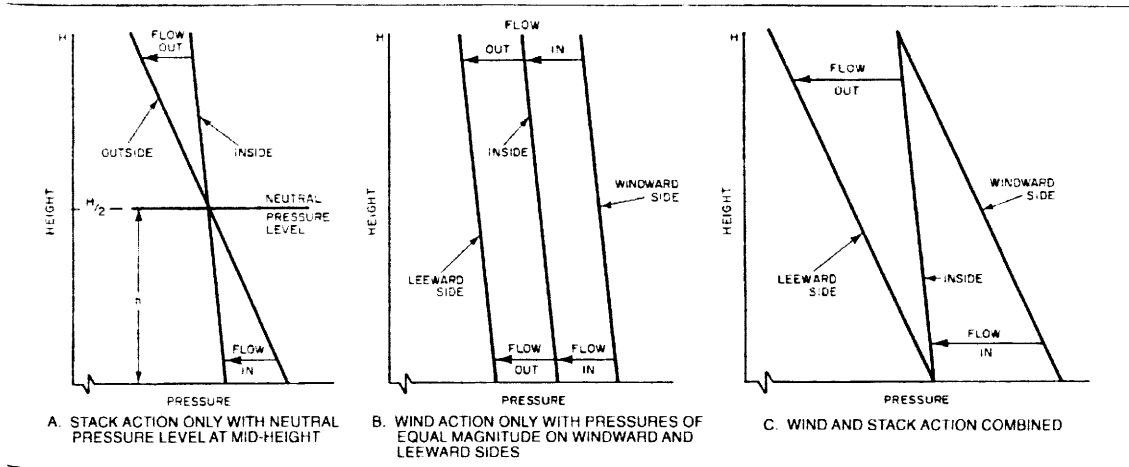
Figure 3-6 Distribution of inside and outside pressures over the building height (ASHRAE, 2001)

With an internal temperature greater than the external temperature the stack pressure difference is positive for openings above the neutral pressure line and air will flow out from the building. If, however, the opening is below the neutral pressure line the stack pressure is negative and air will flow into the building. In this situation the general intra-zonal airflows in the building will be from the bottom floors to the top floors. With a warmer outdoor temperature the airflow patterns reverse. Figure 3-7 shows the airflow pattern for a building with the inside warmer then the outdoors.
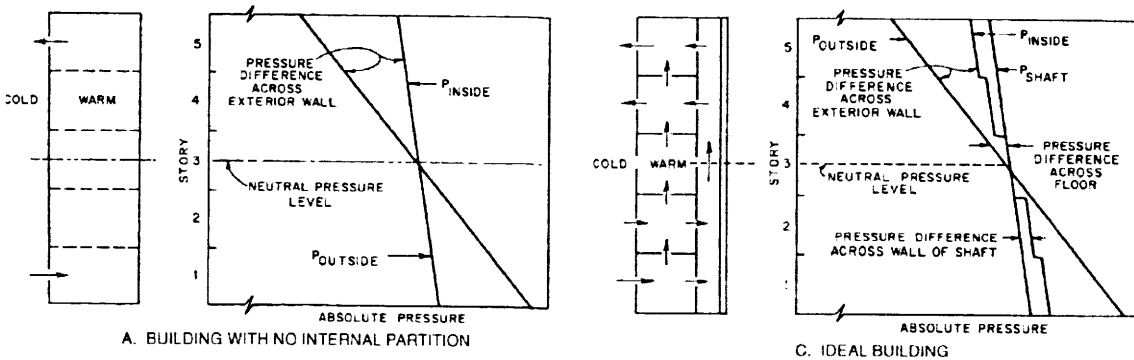
Figure 3-7 Stack effect flows (ASHRAE, 2001)

Considering the case of a 100 m tall office building with negligible internal flow resistance, a neutral pressure level at the buildings mid-level, and a 20 deg C temperature difference, an opening at the top of the building would experience a

24

pressure difference of 40 Pa. This is well above the 5-10 Pa overpressure common for buildings and would lead to considerable internal airflows.

3.2. MODELING THE TRANSPORT OF CONTAMINANTS

The development of an airflow and contamination transport model is a critical component for determining how best to protect a building from a biological attack. Understanding the distribution of contaminants inside buildings informs sensor placement decisions and overall sensing requirements. The information required to construct these models depend on the scope and specificity of the analysis, but typically require at minimum information about the building's architectural layout and HVAC system. The models themselves have varying levels of granularity, from detailed computational fluid dynamics (CFD) models to more simplified nodal models. The choice of computational model is dictated by the type of problem being addressed.

Computational fluid dynamics uses numerical methods to approximate the interactions between fluids and gasses. The basis of any CFD problem is the Navier-Stokes equations which describe the changes in momentum for an infinitesimal volume of fluid based on the sum of the various force acting upon that volume. CFD discretizes a volume of fluid into a fine three dimensional mesh and then applies an algorithm to approximate the Navier-Stokes equations. This process is computationally complex and can require hours of simulation time just to determine the airflow properties in a modest sized room under a single set of boundary conditions (Zhang, 2007). Because of its computational complexity CFD is good tool for exploring the airflow characteristics in small buildings or in sections of large buildings but it is not a reasonable approach to simulating contamination transport in large spaces.

An alternative to CFD are nodal models such as CONTAM and COMIS that subdivide a building into well-mixed zones (or nodes) and then solve for the airflow and contamination transport rates between the zones. CONTAM was developed by the Building and Fire Research Laboratory at the National Institute of Standards (NIST) to model smoke propagation through buildings for fire protection (Walton, 2006). COMIS was developed by the Lawrence Berkley National Laboratory to study indoor air quality and thermal space conditioning (Feustel, 1997). Both programs have been adopted in recent years to model contamination flow for bio-defense related research.

25

Zones in these nodal models are defined at each time step by a single temperature, pressure, and contamination concentration. The definition of what constitutes a zone is left to the user and can be rooms, groups of rooms, AHU zones, or even entire buildings. The user defines leakage paths between zones, HVAC parameters, exterior conditions (wind and temperature), and the time step, and the program calculates the intra-zonal airflow rates based on pressure differences between zones and leakage parameters. The contaminant concentration in each zone is formulated into a set of linear equations based on the conservation of contaminant mass and can be solved through a variety of methods.

While the nodal models are far less computationally complex than CFD, they still can require a considerable effort in constructing the model depending on its level of specificity. For instance, large office buildings can have thousands of rooms and tens of thousands of possible leakage paths (doorways, windows etc.). A model that incorporates all of these characteristics can take months to build and a similar allotment of time to debug and run simulations. The extra detail does not, however, necessarily produce a more accurate analysis. Small changes in building characteristics such as the opening and closing of doors and windows can significantly affect intra-zonal airflows and with a model consisting of thousands of leakage paths understanding the influence of particular variables becomes extremely challenging.

An approach, which more closely approximates the method suggested in this thesis, is to create a coarser model where the zones in the nodal model are defined to coincide with the building's AHU zones. But, by assuming that even very large zones are well-mixed, the nodal models over approximate the contamination spread and thus under approximate the building's sensing requirements. The difference between well-mixed and poorly-mixed zones is discussed in greater detail in Chapter 4.

3.3. SUMMARY

There are many factors that influence the intra-zonal airflows and contamination dispersion in buildings. In all buildings airflow conditions are strongly influenced by the operation of the HVAC system, the leakage rates between zones, and exterior wind pressures. Stack effect induced flows in tall buildings and turbulent diffusion in buildings with open floor plans can also strongly affect contamination movement. Additionally, people traffic further disperses contaminants without much regard to airflow direction.

Computational fluid dynamics and multi-zone models are the two methods typically used to examine airflows inside buildings. CFD is considered the most accurate tool for understanding detailed flow characteristics, but is too time intensive to be used for full-building simulations. Multi-zone models are more similar to the reduced-order model but differ in that the multi-zone models solve for airflows based on user defined leakage paths and assume all zones are well-mixed. These differences lead to multi-zone models that are more complex and less flexible then the equivalent reduced-order model.

Because so many factors affect indoor airflows and these factors are continually changing it does not make sense to base a building's sensing requirements on a single snapshot of building conditions. An advantage of the reduced-order model is its ability to directly vary the intra-zonal airflows. The building analysis codes discussed in Section 3.2 solve for the intra-zonal airflows as a function of a large number of parameters making it difficult to explore a wide range of building conditions quickly and efficiently.

4. ANALYTICAL APPROXIMATIONS

This chapter develops the equations to describe the transport of contamination in buildings. Buildings are subdivided into air handling zones and transport zones such as stairwells and hallways. The equations are derived first for single zones and then for the propagation of contaminants between zones. The intra-zonal contamination transport equations will then be combined to form a full-building model using the method described in Chapter 5.

4.1. ZONE DEFENITION

Two types of zones are considered in this analysis. The first type consists of sections of buildings supplied by a single air-handling unit (AHU). These zones generally are quite large and can consist of groups of offices, multiple gate areas in an airport terminal, or even large convention halls or auditoriums. Large buildings, like those examined here, can have anywhere from several AHU zones to several hundred. The second type of zone considered in this analysis is building areas that interconnect multiple AHU zones. These zones, such as stairwells and hallways, are typically small and their intra-zonal airflows are oftentimes of greater magnitude then their HVAC supply rates. This class of zone is referred to as transport zones due to the important role they play in the transport of contaminants through buildings.

Two possible assumptions when calculating the contamination spread within AHU zones are based on the relative importance of contamination spread through the HVAC system versus inter-zonal airflows. The first approach is to assume the entire zone is well-mixed (equal concentration) immediately following the introduction of contamination. This is the assumption made in the various nodal models that were touched upon in Section 3.2. The second possible assumption, and the one employed in the reduced-order model, is to assume that the zone is poorly-mixed. Poorly-mixed indicates that contamination is only spread through the zone's HVAC system and is not spread by airflow between rooms within the zone. The difference between these two assumptions is illustrated in Figure 4-1.

Poorly-Mixed Zone   **Well-Mixed Zone**
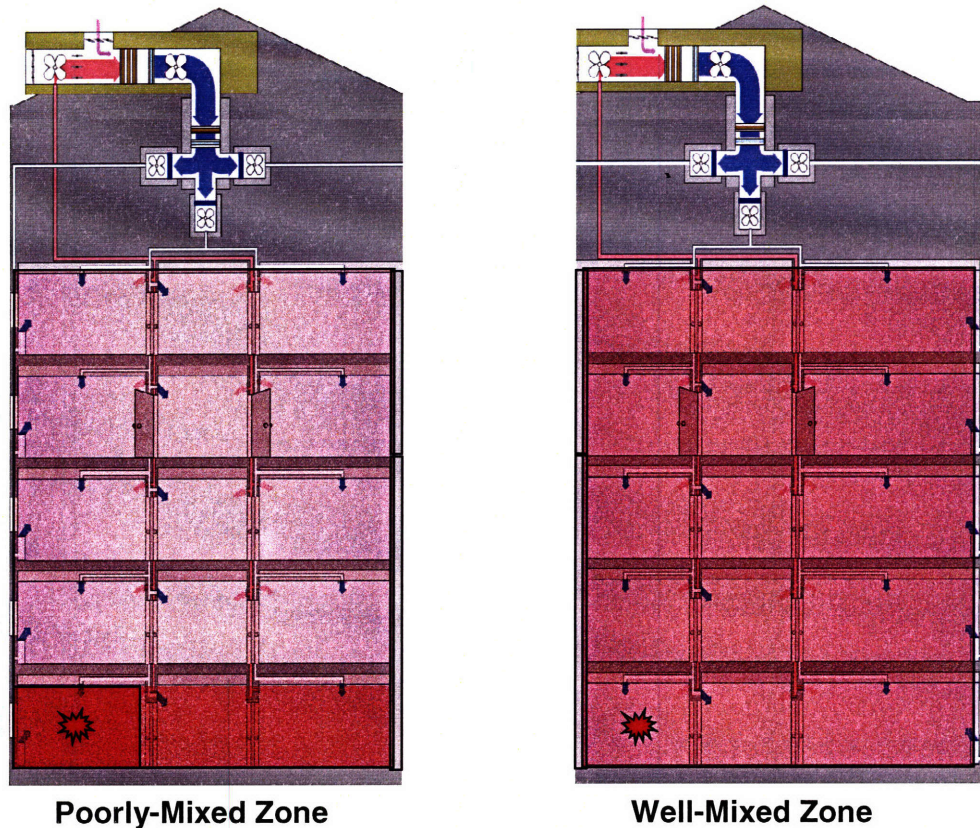
Figure 4-1 The difference between well-mixed and poorly-mixed zones

In Figure 4-1 the poorly-mixed zone is characterized by a high concentration in rooms neighboring the release and lower concentrations in rooms further from the release. In the well-mixed zone the contaminant is instantaneously spread throughout the zone at a uniform concentration, there are no "hot spots." The poorly-mixed zone is a more realistic representation of the actual concentration distribution in large AHU zones. Finer grained contamination transport models attempt to capture the full distribution of contaminants throughout the zone whereas the reduced-order model ignores the area immediate to the release and instead focuses on the remainder of the zone.

In the reduced-order model the dosage in each AHU zone is represented as a single value. If a priori knowledge existed as to the release location the sensor would be placed nearby, ensuring that it captures the maximum amount of contaminant. No such knowledge exists, however, and the sensor is assumed to be placed at random within the zone. A lower bound for the dosage that a sensor would experience is if the sensor is far away from the contamination release point. In this situation the only contamination that would be transported to the sensor would be through the HVAC system and not

through inter-zonal airflows. It is this lower bound for a poorly-mixed zone that is used throughout the analysis.

4.1.1. WELL MIXED AHU ZONES
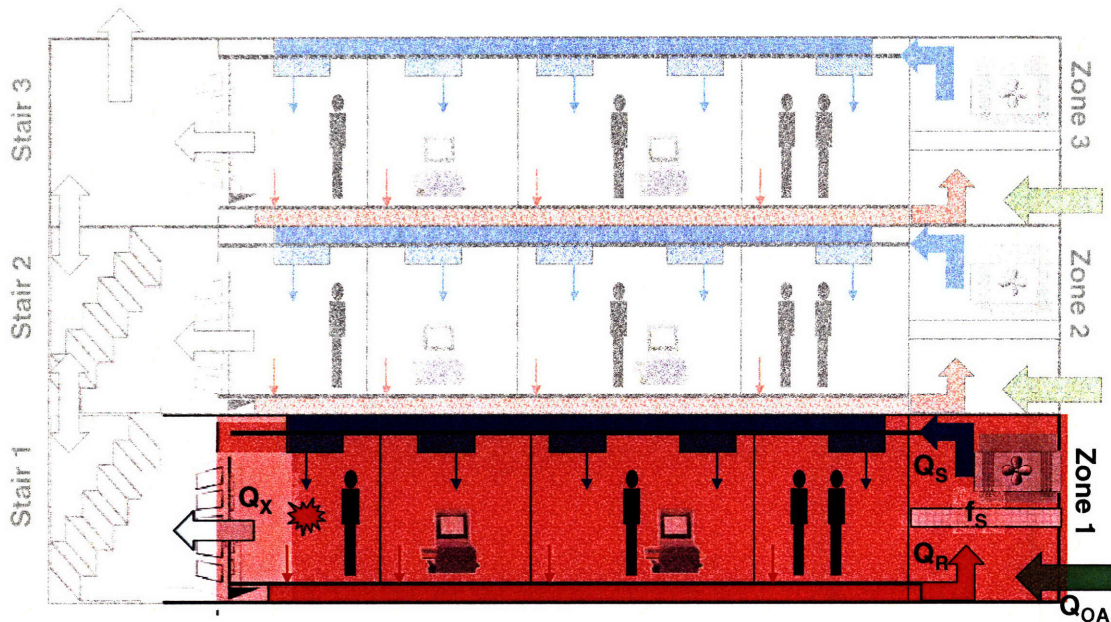
Figure 4-2 Block diagram of one zone model

The single AHU zone depicted in Figure 4-2 consists of multiple rooms all sharing a single air-handling system. In Equation (4-1) the dose in this well mixed zone is solved for as a function of the zone airflow parameters.

$$V\frac{dC}{dt} = f_s C_{OA} Q_{OA} - C(t)Q_X - C(t)Q_R + C(t)Q_R(1 - f_s) + mgen \qquad (4\text{-}1)$$

$$\frac{dC}{dt} = (-C(t)Q_X - C(t)Q_R f_s + mgen)/V$$

$$Q_x = Q_{OA}$$

$$C(t) = mgen/(f_S Q_R + Q_{OA}) - mgen/(f_S Q_R + Q_{OA}) * \exp(((-f_S Q_R - Q_{OA})/V)*t)$$

$$Dose = (\int mgen)/(f_S Q_R + Q_{OA}) - mgen * V +$$

$$\int \frac{dmgen}{dt} \frac{1}{(f_S Q_R + Q_{OA})} * \exp(((-f_S Q_R - Q_{OA})/V)*t)dt$$

$$Dose \sim (\int mgen)/(f_S Q_R + Q_{OA})$$

30

where

$V =$ Zone volume (m^3)

$f_s =$ Supply air filter efficiency (dmnl)

$C(t)=$ Zone concentration (g/m^3)

$Q_{OA}=$ Outside air rate (m^3/min)

$Q_X=$ Intra-zonal exchange rate (m^3/min)

$Q_R=$ Recirculation rate (m^3/min)

mgen= Contamination generation rate (g/min)

In Equation (4-1) the dose in a single zone is calculated to be a function of the amount of contamination released in the zone and the rate at which contaminant is removed from the zone. The filter efficiency multiplied by recirculation rate is the rate at which the supply air filters remove contaminants, and the outside airflow rate is the rate at which uncontaminated air is introduced into the zone and thus the rate at which contaminated air is removed. The filter efficiency times the recirculation rate added to the fresh air rate will be an important term and will be referred to as the zone's well-mixed dilution throughout this text.

Equation (4-1) assumes that the dominant method for removing contaminants is through HVAC airflows, not through intra-zonal (Qx) transport. In Section 4.1.3 the dose is derived for zones where intra-zonal airflows are large compared to the HVAC supply rate.

The well-mixed zone is the assumption made in the nodal analysis software discussed in Section 3.2. Therefore, the dosage term derived analytically should match the output from CONTAM for a one zone model. Figure 4-3 shows that the analytical and CONTAM results are equivalent for a 1 gram release in a 100 m^3 zone.

31
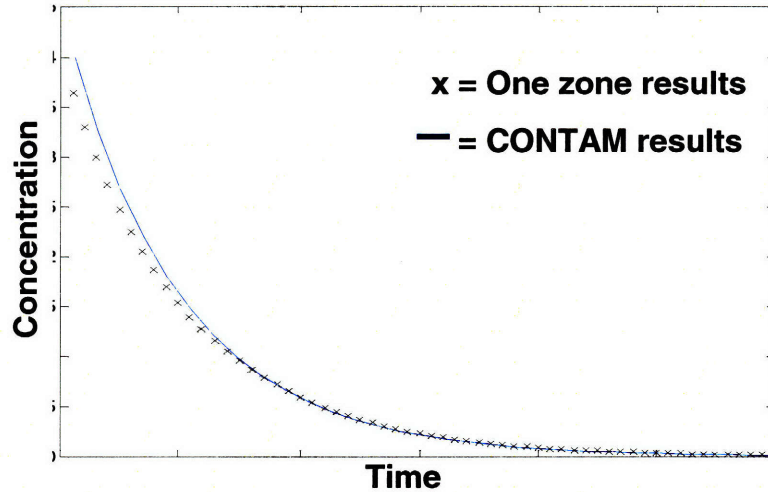
Figure 4-3 Comparison of CONTAM model with analytical results

4.1.2. A POORLY MIXED ZONE

As described in Section 4.1, the poorly-mixed assumption means that if contamination is released within an AHU zone the primary means for contamination transport within that zone is through the HVAC system and not through direct room-to-room airflows. The poorly-mixed assumption provides a lower bound to the dosage level a sensor will experience.
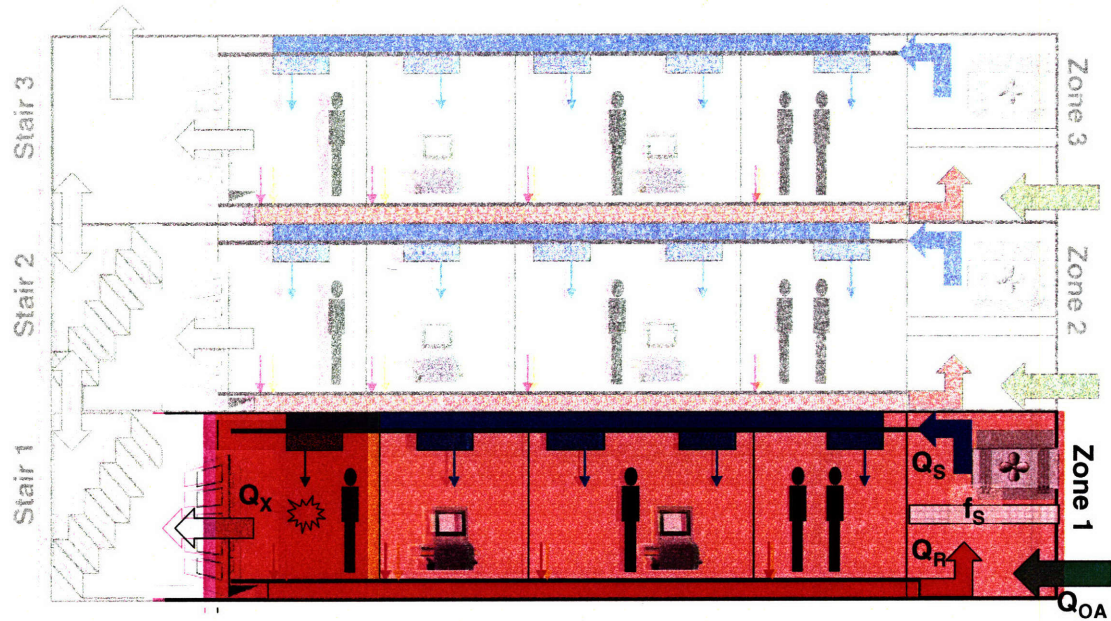
Figure 4-4 Block diagram of isolated release in a single zone

In buildings with large HVAC zones it is likely that only a small portion of the zone is directly exposed to a contaminant release and the poorly-mixed zone is a reasonable assumption. The expected dose in a poorly-mixed zone is derived in Equation (4-2).

$$\frac{dm}{dt} = m(t)\frac{-Q_R f_S - Q_{OA}}{V_1 + V_2}$$

(4-2)

$$m(t) = m_i \exp(-(\frac{Q_R f_S + Q_{OA}}{V_1 + V_2})t$$

$$V_2 \frac{dC_2}{dt} = \frac{m(t)}{V_1 + V_2} Q_R(1 - f_S) - C(t)_2 Q_{S2}$$

$$\frac{dC_2}{dt} + \frac{C(t)_2 Q_{S2}}{V_2} = \frac{m(t)}{(V_1 + V_2)*V_2} Q_R(1 - f_S)$$

$$\frac{dC_2}{dt} + \frac{C(t)_2 Q_{S2}}{V_2} = \frac{m_i Q_R(1 - f_S)}{(V_1 + V_2)*V} \exp(-(\frac{Q_R f_S + Q_{OA}}{V_1 + V_2})t$$

$$\text{integrating factor} = \frac{Q_{S2}}{V_2}$$

$$\frac{dC_2}{dt} e^{\frac{Q_S}{V_2}t} + \frac{C(t)_2 Q_{S2}}{V_2} e^{\frac{Q_S}{V_2}t} = \frac{m_i Q_R(1 - f_S)}{(V_1 + V_2)*V} e^{\frac{Q_S}{V_2}t} \exp(\frac{Q_{S2}}{V_2} - (\frac{Q_R f_S + Q_{OA}}{V_1 + V_2})t$$

$$C(t)_2 e^{\frac{Q_S}{V_2}t} = \int \frac{m_i Q_R(1 - f_S)}{(V_1 + V_2)*V} \exp(\frac{Q_{S2}}{V_2} - (\frac{Q_R f_S + Q_{OA}}{V_1 + V_2})t * dt$$

$$C(t)_2 = \frac{m_i}{V_1 + V_2} \exp(-(\frac{Q_R f_S + Q_{OA}}{V_1 + V_2})t - \frac{m_i}{V_1 + V_2} \exp(-\frac{Q_{S2}}{V_2}t)$$

$$Dose = m_i(\frac{1}{Q_R f_S + Q_{OA}} - \frac{1}{Q_S})$$

where

$m(t)$ = Total mass of contaminant in the entire zone (g)

Q_S= Supply airflow rate (m^3/min)

Subscript 1 = release room

Subscript 2 = rooms in zone not the release room

Comparing Equation (4-1) to Equation (4-2), the difference between the dose in well-mixed and poorly-mixed zones is that in poorly-mixed zones m/Q_S must be subtracted from the m/dilution term. Because Q_S equals $Q_{OA}+Q_R$ and the supply air filter efficiency

34

(f_S) is always less than one, the dose in a poorly mixed zone can never be negative. Figure 4-5 shows that the dose in a poorly-mixed zone can be considerably lower then the well-mixed dose depending on the percent fresh air and supply air filter efficiency.
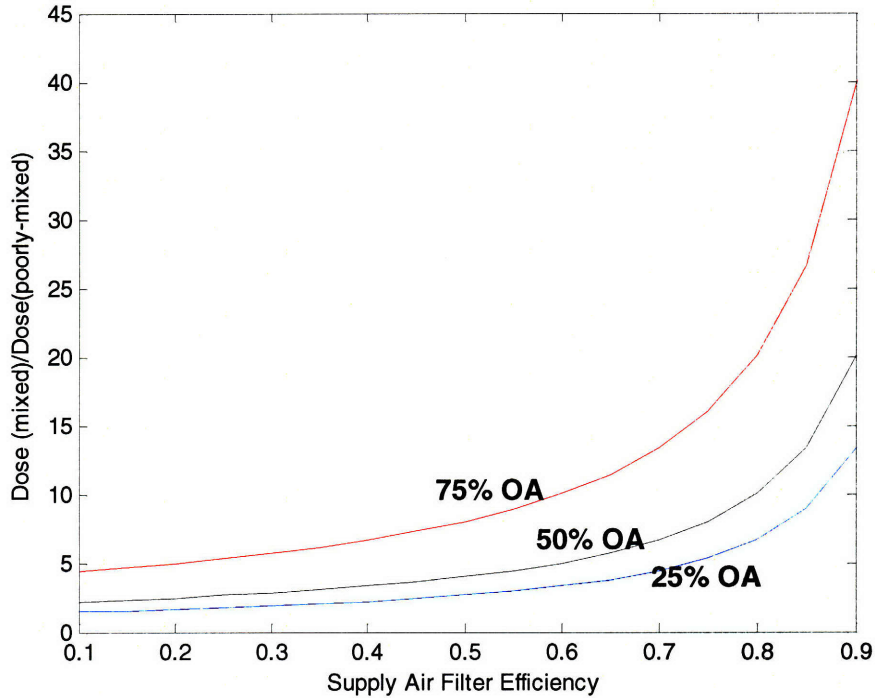
Figure 4-5 Effects of filter efficiency and OA% on mixed and poorly-mixed dilution

It is not surprising that filter efficiency and outside air percentage strongly affects poorly-mixed dilution. In a poorly-mixed zone the only way for contaminant to reach the rooms far from the release is through the HVAC system. If filter efficiency is high, or if the recirculation airflow is low, then the amount of contamination that travels from the release point to the rest of the zone will be low as well.

4.1.3. TRANSPORT ZONES

While stairwells, hallways, and similar zones make up a relatively small percentage of the total floor area for buildings, they are crucial in terms of contamination transport because they interconnect many different AHU zones. Because transport zones interconnect multiple AHU zones that might be at slightly different pressures and typically have small restrictions to airflow, it is common for transport zones to have substantial intra-zonal airflow rates. It is the intra-zonal airflow rates that determine the dilution levels for a transport zone.
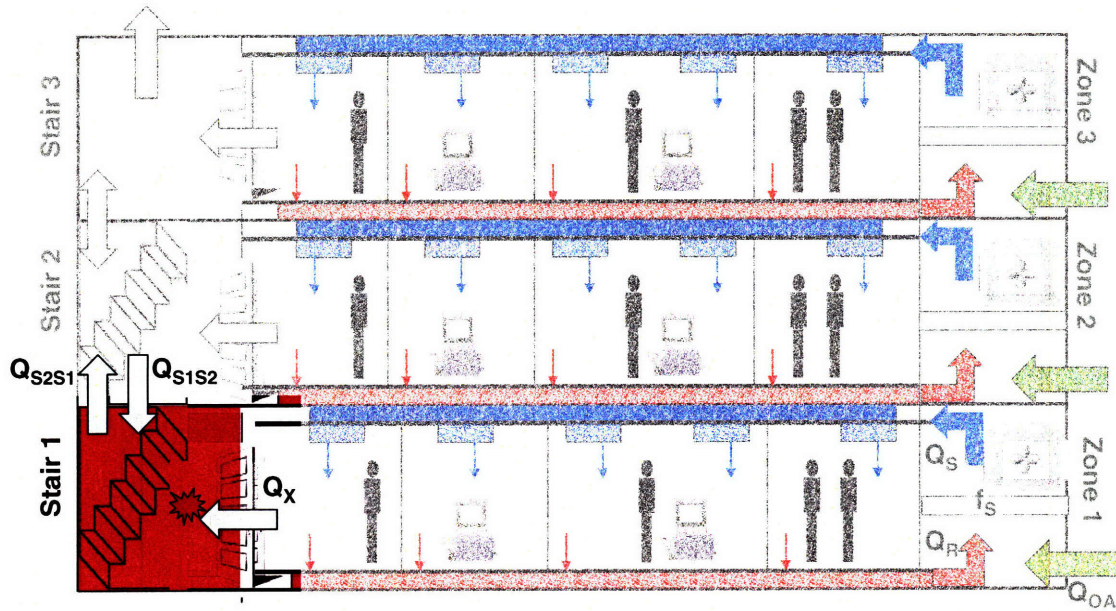
Figure 4-6 Stairwell airflows

$$V \frac{dC}{dt} = mgen - C(t)Q_{S1S2}$$

(4-3)

$$\frac{dC}{dt} = (mgen - C(t)Q_{S1S2})/V$$

$$C(t) = \frac{mgen}{Q_{S1S2}} - \frac{mgen}{Q_{S1S2}} \exp(-\frac{Q_{S1S2}}{V}t)$$

$$Dose = \frac{\int mgen}{Q_{S1S2}}$$

The dose in a transport zone is simply the amount of mass released in the zone divided by airflow rate out of the zone.

4.2. INTRA-ZONAL TRANSPORT

Intra-zonal transport refers to airflow between different zones including AHU zones (both mixed and poorly-mixed) and transport zones. This section determines how dosage levels change as a contaminant propagates throughout a building.

36

4.2.1. MULTIPLE WELL-MIXED ZONES

Figure 4-7 depicts the transport of contaminants between multiple well-mixed zones. Despite all three AHU zones having internal partitions, the contamination is instantaneously spread evenly throughout the zone once it is introduced.
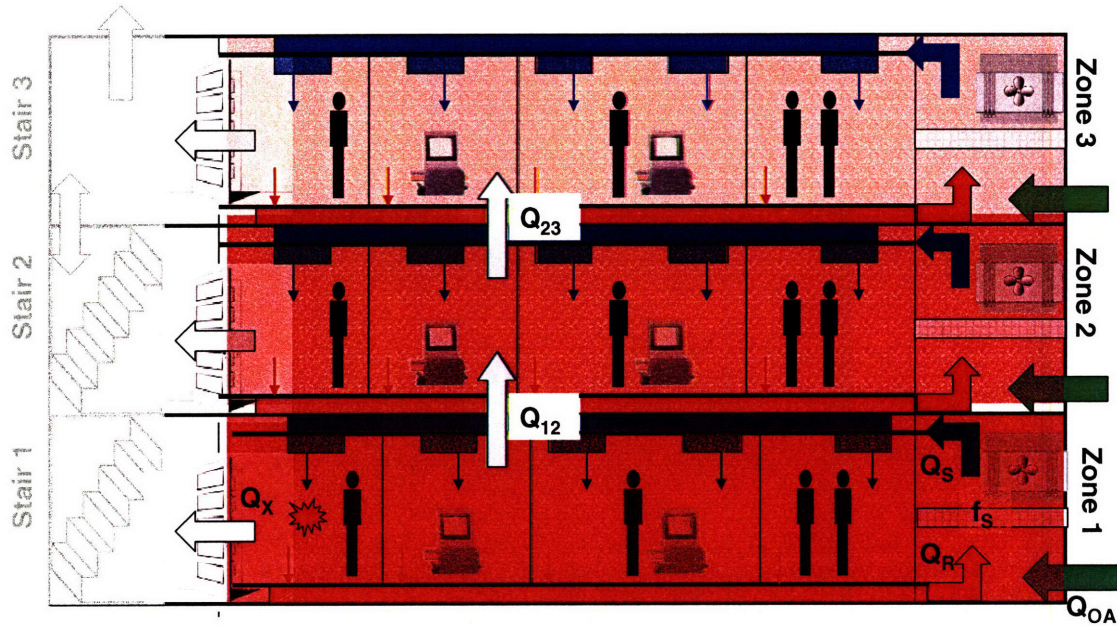
Figure 4-7 Block diagram of contamination flow between well mixed zones

The dose in a single well mixed zone was found previously.

$$Dose \sim (\int mgen)/(f_S Q_R + Q_{OA}) \qquad (4\text{-}4)$$

It is possible to extrapolate from the single zone analysis to the multi-zone case. In the single zone analysis the dosage in a given zone can be approximated from the integration of the mass flow rate into the zone divided by the zone's dilution.

The equivalent term to the generation rate for the multi-zone case is the concentration in the upstream zone multiplied by the air exchange rate between the two zones. In Figure 4-7 the equivalent to mgen for Zone (2) would be the concentration in Zone (1) multiplied by the exchange rate between Zones (1) and (2), $C(t)_1 {}^* Q_X$. The dosage in Zone (2) can therefore be calculated as a function of the dose in the upstream zone.

$$Dose_1 \sim (\int mgen)/(f_s Q_R + Q_{OA}) \qquad (4\text{-}5)$$

$$Dose_2 \sim (\int C(t)_1 Q_X)/(f_s Q_R + Q_{OA}) \qquad (4\text{-}6)$$

$$Dose_2 \sim (\int C(t)_1) * \frac{Q_X}{(f_s Q_R + Q_{OA})}$$

$$Dose_2 \sim Dose_1 * \frac{Q_X}{(f_s Q_R + Q_{OA})}$$

The dosage in Zone (2) is the dose in Zone (1) multiplied by the intra-zonal exchange rate from Zone (1) to Zone (2) divided by the dilution in Zone (2). The intra-zonal airflow rate (Q_X) is assumed to be constant throughout the simulation and thus can be removed from the integral. This assumption is discussed further in Section 4.4. The relationship derived in Equation (4-6) can be further extrapolated to Zone (3) and beyond.

$$Dose_n \sim Dose_1 * (\frac{Q_X}{(f_s Q_R + Q_{OA})})^{n-1} \qquad (4\text{-}7)$$

Equation (4-7) assumes that the intra-zonal exchange rate and the zone dilution are constant over all of the zones. If this is not the case then the (Q_X/dilution) terms for each of the (n) zones are multiplied together to determine the dose in Zone (n). It is useful to note that both the numerator and divisor in the above equation have units of airflow (m^3/min), therefore the dose in Zone (n) has the same units as the dose in the release zone (g-min/m^3).

4.2.2. MULTIPLE POORLY MIXED ZONES

In multiple poorly mixed zones both the release zone and all subsequent zones are considered poorly-mixed. Localized areas of high concentration exist in the release zone near the release and in subsequent zones where the air exchange with the higher concentration zones occurs.
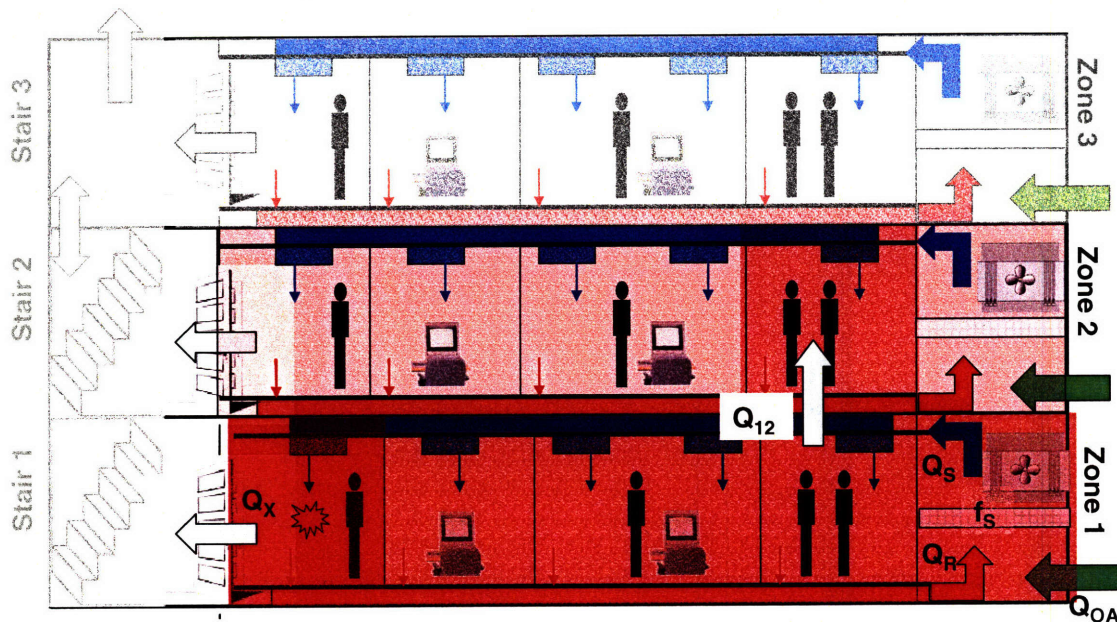
Figure 4-8 Block diagram of contamination transfer between two poorly mixed HVAC zones

In Figure 4-8 the release occurs in the room on the far left of Zone (1). Contamination flows through the HVAC system from the source location to the rest of the rooms in Zone (1). Then, through airflow path Q_{12}, the contaminant spreads directly to a room in Zone (2). From that room the contamination further spreads through the Zone (2) HVAC system to the remainder of Zone (2).

The equation describing the contamination transport in this system can be deduced using the same logic used in Section 4.2.1 to determine the transport equation for well mixed HVAC zones. The dosage for a single poorly mixed zone was found previously.

$$Dose \sim m_i \left(\frac{1}{Q_R f_S + Q_{OA}} - \frac{1}{Q_S} \right)$$

(4-8)

For transport between multiple HVAC zones the mass term (m_i) is replaced with the mass flow rate between the two zones, $C(t)Q_X$. This term is then integrated to find the

dosage in the downstream zone as a function of the dosage in the upstream zone. Again, the assumption is made that Q_X is constant throughout the simulation.

$$Dose_2 \sim Dose_1 * Q_X \left(\frac{1}{Q_R + Q_{OA}} - \frac{1}{Q_S}\right) \tag{4-9}$$

Like the well-mixed model the dose in Zone (n) can be extrapolated as shown below.

$$Dose_n \sim Dose_1 * \left(Q_X \left(\frac{1}{Q_R + Q_{OA}} - \frac{1}{Q_S}\right)\right)^{n-1} \tag{4-10}$$

The ratio of intra-zonal airflow rate (Q_X) to the zonal dilution (mixed or poorly-mixed) will be a critical parameter in the development of the full building model.

4.2.3. INTRA-ZONAL AIRFLOWS, TRANSPORT ZONES

The reduction in dosage as a contaminant travels through transport zones is analogous to the unmixed and mixed AHU zone cases. From Section 4.1.3 the dose in a transport zone is given by:

$$Dose = \frac{\int mgen}{Q_{S1S2}} \tag{4-11}$$

For multiple transport zones the mass generation term, mgen, can be replaced with the airflow into the zone from the contaminated zone. The dose in a zone neighboring the source zone is:

$$Dose_2 = Dose_1 * \frac{Qin_{source}}{Qout_{total}} \tag{4-12}$$

The dose reduction from Zone (1) to Zone (2) is determined by the airflows into the zone from the higher concentration zone divided by the total outflows from the zone. Because the total air inflows into a zone must equal the total outflows, the ratio of inflows from any particular zone to the total outflows must be less than one. This relationship can be extended to (n) additional zones in the same manner as it was for AHU zones.

40

4.3. COMPARISON OF ANALYTICAL RESULTS TO CONTAM RESULTS

To verify that the analytical results derived in the previous sections were accurate, they were compared to the results obtained by exercising a detailed CONTAM model of a five story office building. A simplified CONTAM model was also created of the same building and a simulated release was conducted using this simplified model. The results show that the analytical solution using the poorly-mixed zone assumptions more closely approximated the detailed CONTAM model than the simplified CONTAM model with well-mixed zone assumption.

The five-story office building CONTAM model consists of 12 levels; five occupied floors, a return plenum above each occupied floor, a basement level, and a roof. The building has 22,500 ft^2 of floor area per level and a floor height of approximately 11.5 ft. (including the return plenum). The detailed CONTAM model consists of 1,031 different zones and 4,536 different airflow paths and required several weeks to create and debug.
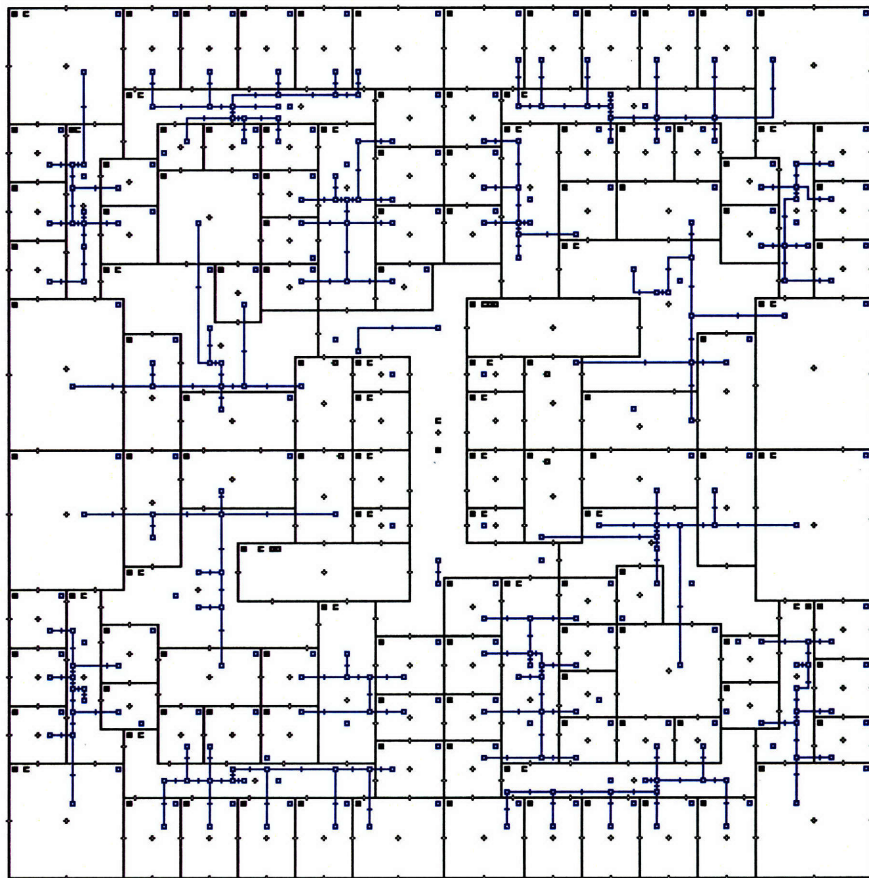
Figure 4-9 An occupied floor in the detailed CONTAM model

Each occupied floor is serviced by its own dedicated air handling unit for a total of five AHUs in the building. The return air from the occupied space travels through an open plenum above the ceiling to a mixing box in the return plenum. In the mixing box the return air is mixed with outside air ducted in from the outdoors and is then filtered and resupplied to the occupied space. The supply air rate is 24,000 cfm per floor of which 6,000 cfm is fresh air.

The interior space in the building is set to 20 degrees C and the ambient conditions are set to 0 degrees C. This temperature difference induces stack-effect flows that cause the major airflow direction in the building to be upwards. The vertical airflow is most prominent in the stairwells and escalator shafts which are the primary means for contamination transport between floors. In order to account for the contamination diffusion against the dominant flow direction due to people traffic small bi-directional fans have been modeled in one stairwell. These fans push contamination downwards against the upwards stack-effect flows.

The simplified CONTAM model has seven floors; five occupied floors, a basement, and a roof. It utilizes the simplified AHU model available in CONTAM and therefore does not require ductwork or special levels for return plenums. Like the detailed model, the simplified model consists of 22,500 ft^2 floors with 11.5 ft ceiling heights. Five separate AHU systems, one per floor, supply 24,000 cfm of air per floor with 6,000 cfm of that total as fresh air. Filters in the AHUs' supply air are modeled to have an efficiency of .4, matching the efficiency in the detailed model.

The simplified CONTAM model includes two stairwells, one with mixing fans and one without. The intra-zonal airflow rates in the simplified CONTAM model and the poorly-mixed analytical model are set to equal the airflow rates in the detailed CONTAM model.
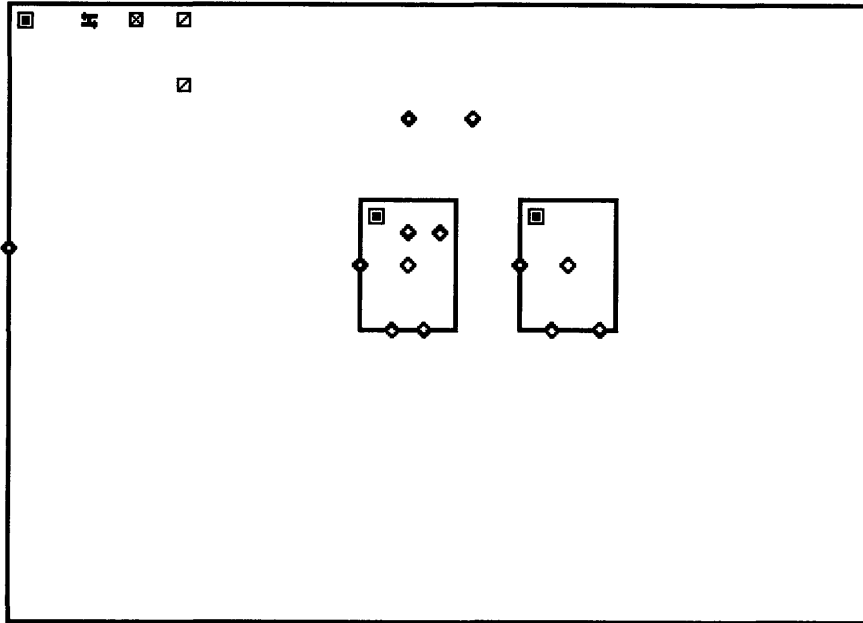
Figure 4-10 Simplified CONTAM model

Ten minutes after the simulated release of the contamination, the concentration distribution calculated by the CONTAM detailed model is shown in Figure 4-11.
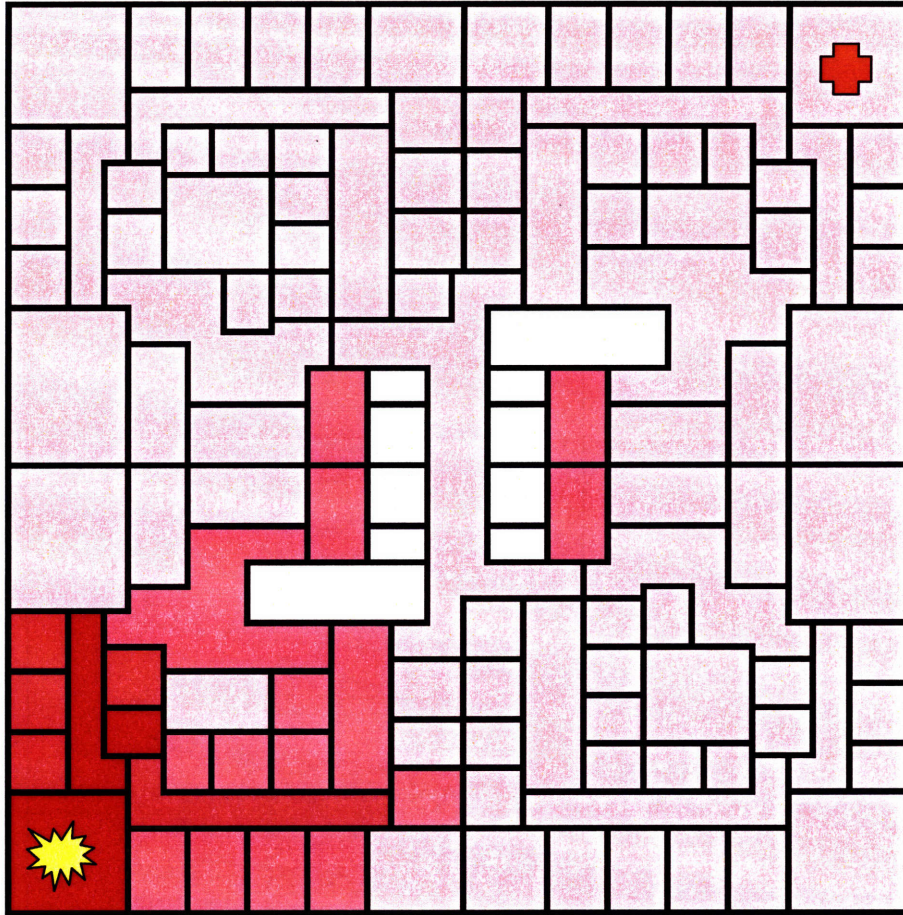
Figure 4-11 The high contamination concentration remains fairly localized

The CONTAM concentration contours in Figure 4-11 seem to indicate that the poorly-mixed zone assumption is reasonable for this set of simulation parameters. Over ¾ of the zones on the release level exhibit concentrations consistent with contamination transport solely through the air handling system. Only those zones in close proximity to the release zone have high concentrations due to direct zone-to-zone airflows. For a sensor placed at random, a reasonable lower bound for the sensor sensitivity required to detect the release is the poorly-mixed dosage that was calculated in Section 4.1.2.

To compare the poorly-mixed and well-mixed zone assumptions, the five floor office building simulation is run and the contamination dosage is recorded on each of the occupied levels in the office space in the upper right-hand corner of Figure 4-11. The results from the detailed CONTAM model are compared to the results from running the simplified CONTAM model and the analytical approximation. The analytical analysis uses the equations for multiple poorly-mixed zones that were derived in Section 4.2.2,

44

whereas the simplified CONTAM model employs the **well-mixed zone assumption.** The comparison between the three methods is given in Figure 4-12.
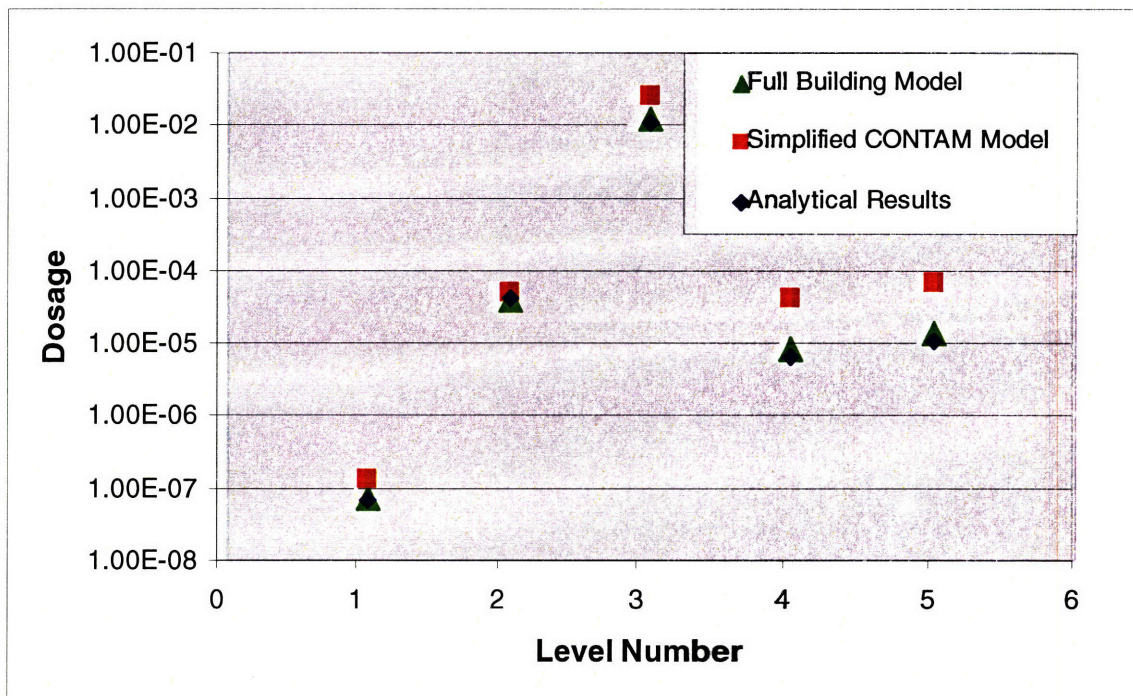
Figure 4-12 Analytical results compare favorably with the detailed CONTAM model

The analytical results based upon the poorly-mixed zone assumption closely approximate the detailed CONTAM model while the dose computed by the simplified CONTAM model is off by as much as a factor of 10X. The reason for this discrepancy is that the simplified model assumes that the contamination is instantaneously mixed throughout the entire zone. Instead of a localized hot-spot near the release as shown in Figure 4-11 the contamination is evenly distributed throughout the entire level with the well-mixed assumption. This over approximates the contamination level in areas far from the release while under approximating the contamination level near the release. The poorly-mixed zone approach ignores the areas near the release assuming a worst-case scenario for the sensor. Figure 4-12 shows that this approach approximates the sensor dosage in areas far from the sensor release much better then the well-mixed zone approach. In the large buildings considered in this analysis, it is likely that the poorly-mixed assumption provides a reasonable lower bound on the dose that a sensor would experience and thus an upper bound on the sensor sensitivity requirement.

4.4. LIMITATIONS OF THE MODEL

The poorly-mixed contamination transport model assumes; that contamination transport through the HVAC system is the principle means of contamination spread within AHU zones; that the sensitivity of a sensor is sufficient to detect releases in the sensor zone; that the geometry of the building is such that a contamination introduced into a zone is diluted before passing into the next zone; and that the intra-zonal airflow rates can be represented by a single time-averaged number for each flow path. The first of these assumptions is unique to the poorly-mixed building model whereas the remaining three are common with other multi-zone transport models.

The poorly-mixed model assumes that the HVAC transport of contaminants is paramount. However, if the building's zones are small, or if contamination transport through the HVAC system is significantly reduced, this assumption may not hold. In small AHU zones a release in one part of the zone is much more likely to spread to the remaining areas through simple diffusion and inter-zonal mixing. To test whether the poorly-mixed assumption is appropriate a detailed model could be constructed of the buildings smallest AHU zone. Either a multi-zone model or a CFD model could be used to construct the detailed model. If contamination release simulations show that the majority of the zone remains poorly-mixed then the poorly-mixed assumption can be used, otherwise the well-mixed assumption should be applied.

The factors that would reduce the contamination transport through the HVAC system are more efficient supply air filters and a higher percentage of fresh air. Increasing the filter efficiency traps more particulates and lowers the amount of contamination transported from the release point to the rest of the AHU zone. Increasing the outside air percentage has the dual effect of decreasing the amount of contamination transported through the HVAC system and increasing the inter-zonal and intra-zonal airflows. The relative importance of HVAC contamination transport within a zone in comparison to direct zone-to-zone contamination transport depends on both the recirculation rate and the level of inter-zonal airflows. If the outside air percentage is set too high, then the zone will become too well-mixed and the poorly-mixed zone assumption will no longer hold.

A sensor must be able to detect the smallest relevant release within the largest of the AHU zones in the model, otherwise the AHU zones would need to be subdivided and

46

sensors would need to be placed within the zone. This is a potential problem with concentration dependant sensors but is much less likely with the more sensitive dosage dependant sensors. As discussed in Section 6, even a low quality dose detecting sensor should have a minimum detection threshold of 10,000 spores. For a 100,000 ft^2 zone with a 20 ft ceiling height, an air exchange rate of 5 ACH, 90% filter efficiency, and 75% outside air, a sensor in the return air could detect a perfectly aerosolized release of .08 grams in the AHU zone. Equivalently, the same sensor could detect a 1 gram release in a similar zone with a floor space of 1.2 mil ft^2.

The coarser nodal models, including the poorly-mixed model, assume that as a contaminant passes through a zone it is dispersed throughout the zone. This assumption can create inaccuracies under certain building configurations as shown in Figure 4-13.

Contamination is fully diluted in Zone (2) before passing into Zone (3)

A transport zone between (1) and (3) allows the user to control the path of contamination flow
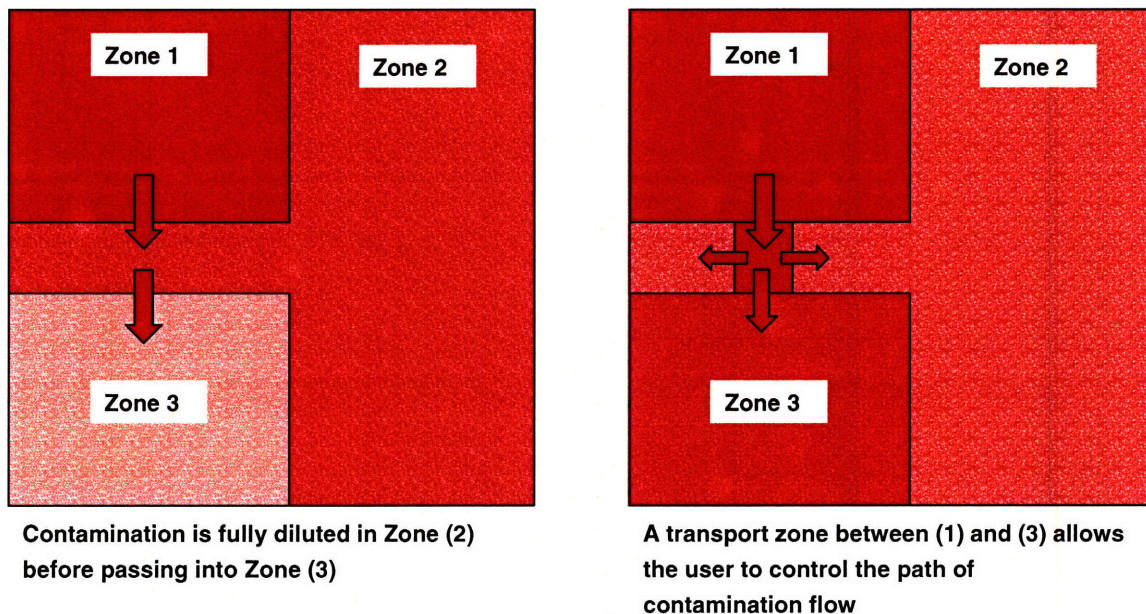
Figure 4-13 The geometry of a zone can determine zone partitioning

In the building from Figure 4-13 a contaminant passes through only a sliver of Zone (2) on its path between Zones (1) and (3). In a multi-zone model, however, the contaminant is fully diluted in the large Zone (2) before ever reaching Zone (3), likely under predicting the dose in Zone (3). This conflict can be remedied by inserting a transport zone between Zones (1) and (3). The airflows into and out from the transport zone then determines the amount of contamination that makes it into Zone (3) without first being completely diluted in Zone (2).

The models presented in this chapter all assume a constant value for the intra-zonal exchange rate between any two zones (Q_X). If Q_X varies during the release then it could significantly impact the amount of contamination transported between zones. For example, if a stairwell door is propped open only during lunch break and the airflow through that door is 200 cfm during that time and 0 cfm otherwise the model designer must choose what exchange rate to use in the model. If the release occurs at the beginning of the lunch hour then 200 cfm might be an appropriate number, if the release occurs after lunch then zero would be appropriate. But what if the release occurs in the middle of the lunch hour? One of the advantages of the reduced order model is the ability to run a large number of simulations easily while varying the important input parameters such as the intra-zonal exchange rate and building dilution. This allows the user to understand the effect of different building states on the optimal sensing solution.

4.5. SUMMARY

The contamination properties in a zone can be calculated by assuming the zone is either well-mixed or poorly-mixed. A well-mixed zone assumes that contamination is instantaneously spread throughout the zone at a uniform concentration immediately following a release. A poorly-mixed zone assumes that there is a localized "hot-spot" neighboring the release, but that the remainder of the zone only sees the contamination that is spread through the zone's HVAC system. The reduced-order model employs the poorly-mixed assumption, while multi-zone models such as CONTAM assume zones are well-mixed. The analysis in Section 4.3 appears to indicate that for large AHU zones the poorly-mixed assumption may provide more accurate results then the well-mixed assumption for coarse models.

The equations for calculating the dose in well-mixed and poorly-mixed zones were derived in Sections 4.1.1 and 4.1.2. The dose in a well-mixed zone is approximately the mass of contaminant released within the zone divided by the rate at which contaminated air is removed from the zone. The rate at which contaminated air is removed from a zone was defined as a zone's well-mixed dilution. The dose in a poorly-mixed zone is approximately the release mass divided by the total air supply rate then subtracted from the well-mixed dose. The dose in a poorly-mixed zone is always less than or equal to the dose in a well-mixed zone and defines the lower bound of the dose a sensor is expected to experience.

The equations for calculating the dose multiplier as contamination is transported between neighboring zones was calculated in Section 4.2.1 for a well-mixed zone and in Section 4.2.2 for a poorly-mixed zone. In both cases the multiplier is equivalent to the intra-zonal air exchange rate divided by the dilution rate (either poorly-mixed or well-mixed) in the inflow zone. In Sections 4.1.3 and 4.2.3 the dose equations were also derived for transports zones, a special case of a well-mixed zone where the intra-zonal airflow rates dominant the HVAC supply rates.

Section 4.4 discussed some of the limitations of the reduced-order model. Many of these limitations are also common with traditional well-mixed multi-zone models. Further research is needed to fully understand the bounds of the reduced-order model.

5. CREATING A FULL-BUILDING MODEL

By incorporating the contamination transport equations derived in Section 4 into a framework that examines an entire building, the problem of optimizing the placement of sensors can be addressed. The first step in creating a full-building model involves defining the building itself, particularly the building layout and airflow characteristics. Once the layout is defined, the potential sensor locations are determined using a criteria discussed in Section 5.1.

The potential sensor locations become the nodes in a network model representation of the building with the path lengths of the network model defined by the dosage multiplier between any two sensing locations. Using the network model, the dose at any sensor location that would result from a release in any zone is then determined. The zones that a sensor covers are defined as those zones where a release of a certain size would result in a dosage at the sensor's location exceeding the sensor's detection threshold. The optimal set of sensors is the set that provides full coverage (covers all of the building's zones) while minimizing the cost of the set of sensors. The set coverage problem is solved by binary integer programming. All the modeling and simulations utilize Matlab and the Matlab optimization toolbox.

5.1. SENSOR PLACEMENT OPTIONS

Defining a building's zones and zone interfaces are the first step in constructing the model. Zones are defined by their size, type (AHU vs. transport zone), and their HVAC properties including air supply rate, outside air fraction, and supply air filter efficiency. For simplicity, in this analysis the zone airflow parameters were defined globally as a function of their size and type, although this need not be the case.

Zone interfaces are the connection between any two zones with a direct and significant airflow pathway between them. A Matlab function defines the zone interfaces including what zones are interconnected, the principle air exchange between them (magnitude and direction), and whether there are two-way mixing airflows between the two zones. The capability to modify the dominant airflows and mixing airflows globally using multipliers is designed into the Matlab functions.

After the zones and interfaces are defined the potential sensor locations can be deduced. For AHU zones there are two potential sensor locations. The first is in the

occupied space of the zone ideally near the location of the release. However, because we have no a priori knowledge of the release location the highest dosage that the sensor will be guaranteed to detect is defined by the poorly-mixed zone equations. The second potential sensor location in an AHU zone is in the return air of the HVAC system immediately upstream of where the return air mixes with the outside air. The return air has the advantage of being the combination of airflows from the entire zone and thus has the same concentration that a well-mixed zone would experience.
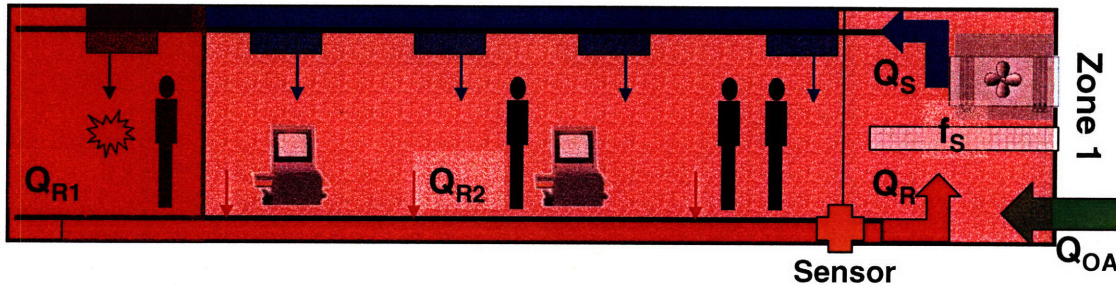
Figure 5-1 A sensor located in the return air experiences a well-mixed zone

$$C_R Q_R = C_1 Q_{R1} + C_2 Q_{R2} \qquad (5\text{-}1)$$

$$Q_R = Q_{R1} + Q_{R2}$$

$$C_R = C_1 \frac{Q_{R1}}{Q_{R1} + Q_{R2}} + C_2 \frac{Q_{R2}}{Q_{R1} + Q_{R2}}$$

where:

C_R = concentration in the return air

Q_R = total return airflow rate

Subscript 1 = Properties in release room

Subscript 2 = Properties in the remainder of the AHU zone

If the return air rate is proportional to the volume of the space being conditioned then the above relation shows that the concentration in the return air is in fact the average concentration across the entire zone. A return air sensor is therefore exposed to contamination levels consistent with a well-mixed zone which are always higher then the contamination levels in a poorly-mixed zone not near the release location.

$$\frac{mass}{dilution} > mass(\frac{1}{dilution} - \frac{1}{Q_s}) \qquad (5\text{-}2)$$

Because in-zone sensors are dominated by sensors in the return air, only the return air sensors are considered.

The one time when in-zone sensors are considered for AHU zones are when two AHU zones share a common interface. By placing a sensor at the interface between the AHU zones the sensor is modeled as being able to detect the poorly-mixed dosage level in both of the interface zones. This interface sensor is not as good as a return air sensor for either of the two zones individually, but might be a better choice for covering both zones.

Transport zones are considered to be well-mixed zones due to their small size and therefore the only possible sensor location for a transport zone is in the zone itself. Because transport zones are well-mixed and generally have a fairly low dilution level, sensors at the interfaces between transport zones and other types of zones are not considered. In total, there are three possible sensor locations, in the return air for AHU zones, at the interface of multiple AHU zones, and within a transport zone.

5.2. A NETWORK MODEL IMPLEMENTATION

Once the building layout and potential sensor locations are known it is possible to define a network model that describes the transport of a contaminant through a building. In Section 4 the analytical approximation for the change in contaminant dosage as a contaminant spreads between different zone types was derived. The equations are reproduced below.

$$Dose_n \sim Dose_1 * (\frac{Q_X}{(f_s Q_R + Q_{OA})})^{n-1} \quad \text{(well-mixed)} \qquad (5\text{-}3)$$

$$Dose_n \sim Dose_1 * (Q_X (\frac{1}{Q_R + Q_{OA}} - \frac{1}{Q_S}))^{n-1} \quad \text{(poorly-mixed)}$$

$$Dose_2 = Dose_1 * \frac{Qin_{source}}{Qout_{total}} \quad \text{(transport zones)}$$

52

As an example we consider the building in Figure 5-2.
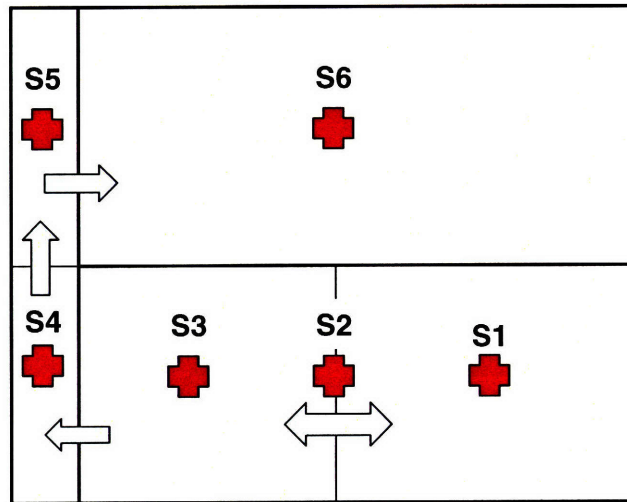
Figure 5-2 Simple building for network example

The building represents a two-story office building and has three AHU zones and two transport zones. Using the sensor placement criteria defined in Section 5.1 there are six possible locations for sensors (S1-S6). For simplicity the sensors in the AHU returns {S1, S3, S6} are depicted in the zones. The corresponding network model is shown in Figure 5-3.
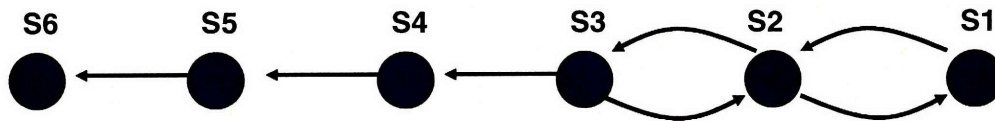
Figure 5-3 Network model for simple building

Due to the bidirectional airflow across the interface for the lower level AHU zones there are bidirectional paths between Sensors (1) and (2) and Sensors (2) and (3). The remaining paths are all unidirectional. To calculate the path length from Sensor (1) to Sensor (2) we consider a contamination release in the first AHU zone. Sensor (1) would experience a dosage equivalent to the mixed zone dosage.

$$Dose_{S1} = \frac{mass}{dilution_{Zone1}}$$

(5-3)

The sensor S2 located at the interface between Zones (1) and (2) would experience the poorly-mixed zone dosage.

53

$$Dose_{S2} = mass(\frac{1}{dilution_{Zone1}} - \frac{1}{Q_{S1}}) \qquad (5\text{-}4)$$

The dose at sensor location (2) divided by the dose at location (1) is the path length between Sensors (1) and (2).

$$Pathlength_{12} = \frac{mass(\frac{1}{dilution_{Zone1}} - \frac{1}{Q_{S1}})}{\frac{mass}{dilution_{Zone1}}} \qquad (5\text{-}5)$$

$$Pathlength_{12} = (1 - \frac{dilution_{Zone1}}{Q_{S1}})$$

To determine the path length between Sensors (2) and (3) we consider again a release in the first AHU zone. The dose at sensor S2 is given in Equation (5-5) and the dose at sensor S3 is:

$$Dose_{S3} = mass(\frac{1}{dilution_{Zone1}} - \frac{1}{Q_{S1}}) * \frac{Q_{Z1Z2}}{dilution_{Zone2}} \qquad (5\text{-}6)$$

The path length from sensor (2) to sensor (3) is given by dividing the dose at S3 by the dose at S2.

$$Pathlength_{23} = \frac{Q_{Z1Z2}}{dilution_{Zone2}} \qquad (5\text{-}7)$$

There are four additional potential types of paths in addition to the two path types already discussed. The formulas for these path lengths are:

$$Pathlength = \frac{Q_X}{dilution_{ZoneB}} (transport\ zone \rightarrow transport\ zone) \qquad (5\text{-}8)$$

$$Pathlength = \frac{Q_X}{dilution_{ZoneB}} * (1 - \frac{dilution_{ZoneA}}{Qs_A}) \ (AHU \rightarrow AHU)$$

$$Pathlength = \frac{Q_X}{dilution_{ZoneB}} * (1 - \frac{dilution_{ZoneA}}{Qs_A}) \quad (AHU \rightarrow transport)$$

$$Pathlength = \frac{Q_X}{dilution_{ZoneB}} \quad (AHU \rightarrow transport)$$

where Zone A is the outflow zone and Zone B is the inflow zone.

Once the path lengths are determined the network from Figure 5-3 can be presented in a matrix form.

	To					
	S1	**S2**	**S3**	**S4**	**S5**	**S6**
S1		P12				
S2	P21		P23			
S3		P32		P34		
S4					P45	
S5						P56
S6						

Figure 5-4 Matrix representation of the network model

In Figure 5-4 PAB is the path length from A to B as computed previously.

Once the network model is created, the next step is to determine the distance between any zone in the building and each of the sensor locations. The final output is the n X m matrix *zonedose* which describes the dose at sensor location (m) for a release of a given size in each of the (n) zones. The algorithm that constructs this matrix utilizes a dynamic programming approach.

First, for a release in Zone (1) the sensor located within Zone (1) (for a transport zone) or in the AHS return of Zone (1) (for an AHS zone) is set to a dose of (mass/dilution). This is the dosage for a sensor located in a well-mixed release zone.

	S1	S2	S3	S4	S5	S6
Z1	(m/d1)					
Z2						
Z3						
Z4						
Z5						

Next, all of the outflows from Zone (1), which are all the entries in row 1 of the matrix representation of the network model, are multiplied by the dose at sensor location 1. The resulting value is the dose at each of the outflow endpoints. These doses are entered in row 1 (the release was in Zone 1), and the column of the endpoint of the outflow.

	S1	S2	S3	S4	S5	S6
S1		P12				
S2	P21		P23			
S3		P32		P34		
S4					P45	
S5						P56
S6						

Update zonedose w/ path lengths from Z1

	S1	S2	S3	S4	S5	S6
Z1	(m/d1)→	(m/d1)*P12				
Z2						
Z3						
Z4						
Z5						

The endpoints of the outflows then become the new starting locations for the algorithm. The process is repeated and the outflows from the starting points are multiplied by the dose at each starting point and then the appropriate columns in row 1 are updated.

	S1	S2	S3	S4	S5	S6			S1	S2	S3	S4	S5	S6
S1		P12					Update zonedose w/ path lengths from Z2		$(m/d1)+$ $(m/d1)$					
→ S2	(P21)		(P23)					Z1	$*P12*P21$	$(m/d1)*P12$	$(m/d1)*$ $P12*P23$			
S3		P32		P34				Z2						
S4					P45			Z3						
S5						P56		Z4						
S6								Z5						
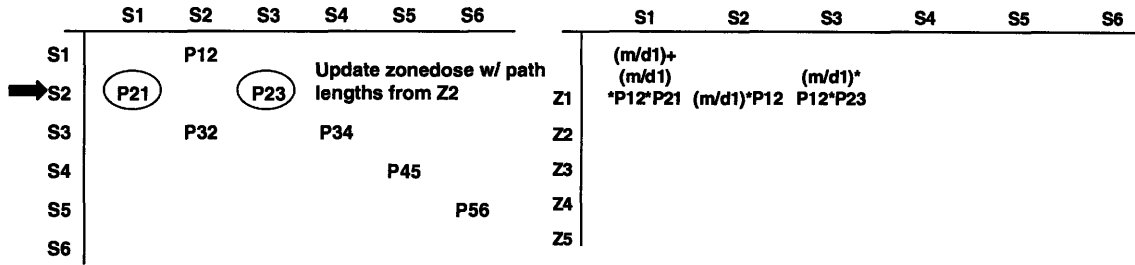
The algorithm truncates a branch of the analysis if it revisits a sensor location that has already been visited. In the above example, contamination from sensor location 2 flows back to Sensor (1), but in the next program iteration the outflows from 1 will not be recomputed because Sensor (1) was previously visited. The algorithm continues until all of the sensor locations have been visited or all the branches are truncated. The process then begins anew from the next zone and the columns in the next row are filled out in the same manner. The final result is the matrix *zonedose* that describes the dose at every sensor location for a release of a given size in any zone.

5.3. OPTIMIZING SENSOR PLACEMENT

Using the *zonedose* matrix, the zones covered by each sensor is determined and the minimum cost set of sensors that provide full coverage is estimated using binary integer programming. This minimum cost set of sensors is considered the optimal sensing solution.

For each column in the *zonedose* matrix the dose level is compared to the sensor's threshold. If the sensor's threshold is below the dose it would experience, then the sensor would alarm and the sensor is considered to cover that release zone. Each zone can be listed with the sensors that cover that zone as shown in Figure 5-5.

Zone	Covered by Sensor
1	S1, S2
2	S2, S3, S4, S5
3	S4 ,S5, S6
4	S5, S6
5	S6
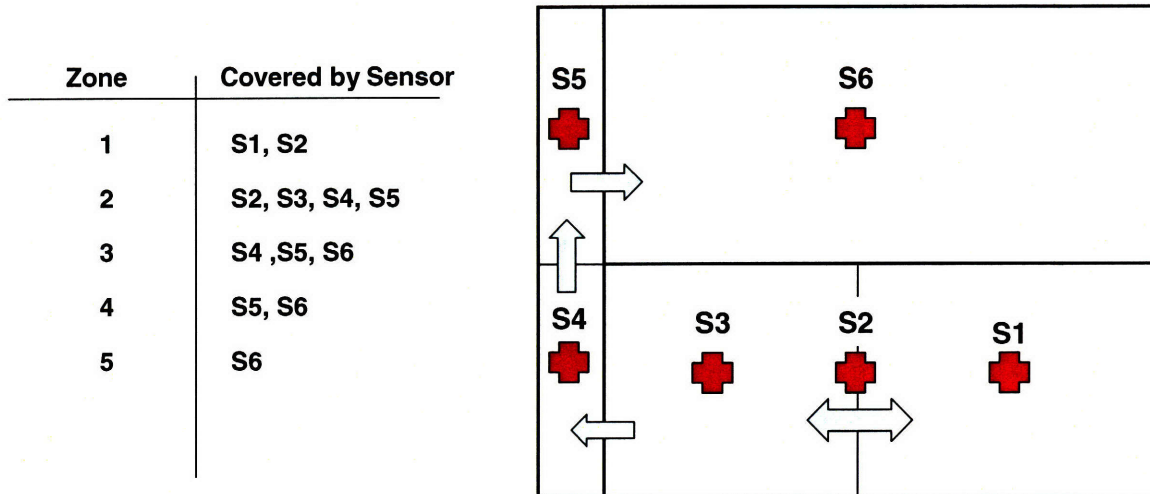
Figure 5-5 The zones covered by each sensor are calculated from the matrix zonedose

The problem is to determine what set of sensors covers the full set of zones while minimizing costs. This class of problem is fairly common and is referred to as a set coverage problem. Binary integer programming is a common approach to solving set coverage problems and is the approach used in this analysis. The objective function is the minimization of sensor cost. Assuming the all the sensors cost $100 the objective function would be:

$$\min(100S1 + 100S2 + 100S3 + 100S4 + 100S5 + 100S6)$$

with the constraints of full coverage

$$S1 + S2 \geq 1$$

$$S2 + S3 + S4 + S5 \geq 1$$

$$S4 + S5 + S6 \geq 1$$

$$S5 + S6 \geq 1$$

$$S6 \geq 1$$

and the integer constraint.

$$\text{int}\{S1, S2, S3, S4, S5, S6\}$$

Through inspection it is possible to see that the optimal sensing solution for the example problem is a combination of Sensor 6 and Sensor 2.

58

The optimal solution can also determined using the Matlab function bintprog. The function bintprog employs a linear programming (LP) branch-and-bound method. The branching technique repeatedly adds constraints (new branches) and solves an LP-relaxation problem given the constraints at that node. Depending upon the solution of the LP-relaxation problem the algorithm then chooses whether to branch or to move to another node. The algorithm continues until an optimal solution is found or a maximum number of iterations are reached. The branch-and-bound technique dose not necessarily produce a global optimum, but is likely sufficient for this type of problem.

If multiple sensor types with different sensitivities and costs are available then each sensor would be compared against the values in *zonedose* and the zone coverage relationships would be determined for each type. If, in the previous example, there were two different types of sensors available there would be 12 sensors in the constraint and optimization equations (six locations X two sensor types).

5.4. SUMMARY

Chapter 5 discussed how the equations derived in Chapter 4 could be formulated into a full-building network model and then used to determine the optimal sensing solution. The network model is defined such that each node represents a possible sensor location. The path length between each sensing location is determined using the intra-zonal transport equations derived in Section 4.2 and the sensor placement criteria described in Section 5.1. The distance between each zone and every sensing location is calculated using a dynamic programming algorithm described in Section 5.2. Distance is defined as the reduction in dose between a release point and a sensor location.

The problem is then formulated as a set coverage problem and solved using binary integer programming. A sensor is said to "cover" a zone if the release mass divided by the distance between the zone and the sensor is greater then the detection threshold of the sensor. The goal is then to determine the minimum cost set of sensors that "covers" every zone in the building.

6. EXAMPLE CASES

This chapter describes the application of the contamination transport model to three different building types. A single baseline case is simulated for each model and the optimal sensing solution is computed. The underlying network models for the three cases are presented and the implications for sensor placement are discussed.

Three different types of dosage dependant sensors are considered. In reality the "sensor" in all three cases is likely a particle collector which could be a filter or a more complex particle impaction and collection devise. The difference in sensor cost and sensitivity is due to the type of analysis performed after the particulates are collected. Three methods are considered; color based hand-held assays (HHA's), fluorescent HHAs requiring a reader, and polymerase chain reaction (PCR). The actual techniques themselves are not critical for this analysis, like the building models the sensors are chosen to be representative of what might be available but do not necessary correspond to a specific product. The cost and sensitivities used for the three sensors are given in Figure 6-1.

Sensor Type	Detection Threshold	Cost
Color HHAs	10,000 spores	$100
Fluorescent HHAs	1,000 spores	$150
PCR	100 spores	$225

Figure 6-1 Properties of bio-defense sensors

The costs are an estimate based on the overhead cost of purchasing the equipment and the variable cost of performing the analysis spread over several hundred applications. The detection threshold is converted from spores to g-min/m^3 by assuming a particle size of 3 microns, a particle density equivalent to water, and a sample rate of 10 liters/min. An example calculation for the inexpensive sensor is given in Equation (6-1).

$$V_p = \frac{4}{3}\pi(1.5E-6)^3 = 1.4E-17 \qquad (6\text{-}1)$$

$$M_p = V_P * \rho = 1.4E-17 * 1.2E6 = 1.7E-11$$

$$Dose = N * M_P * 1/SR = 10,000 * 1.7E-11 * 1/.01 = 1.7E-5$$

where:

V_P = Particle volume (m^3)

M_p = Particle mass (g)

ρ = Particle density (g/m^3)

N = Number of particles needed for detection

SR = Sampling rate (m^3/min)

6.1. BUILDING MODELS

Three examples of the network model are presented including an office building, airport, and convention center. These buildings were chosen as example cases due to their unique network structure, their high population densities, and their perceived vulnerability to attack. For each of the three buildings a brief description is given about the structure and assumptions in each baseline model and a single sensor optimization case is simulated. All three of the baseline models are loosely based on existing buildings of their type. The focus, however, is not on defending specific buildings, but on how the analysis methodology might be applied to various classes of buildings.

6.1.1. OFFICE BUILDINGS

Multi-story office buildings such as skyscrapers are fairly common in layout. The stairwells, elevators, and utilities are typically located at the central core of the building with office spaces or living areas located around the periphery. The square footage per floor can vary considerably between buildings with the largest skyscrapers exceeding an average of 40,000 ft^2 per floor and 4 million ft^2 in total. The office building model constructed for this analysis is relatively modest in size at 22,500 ft^2 per floor with five occupied levels, and closely resembles the office building considered in Section 4.3.

61

System Design Concept
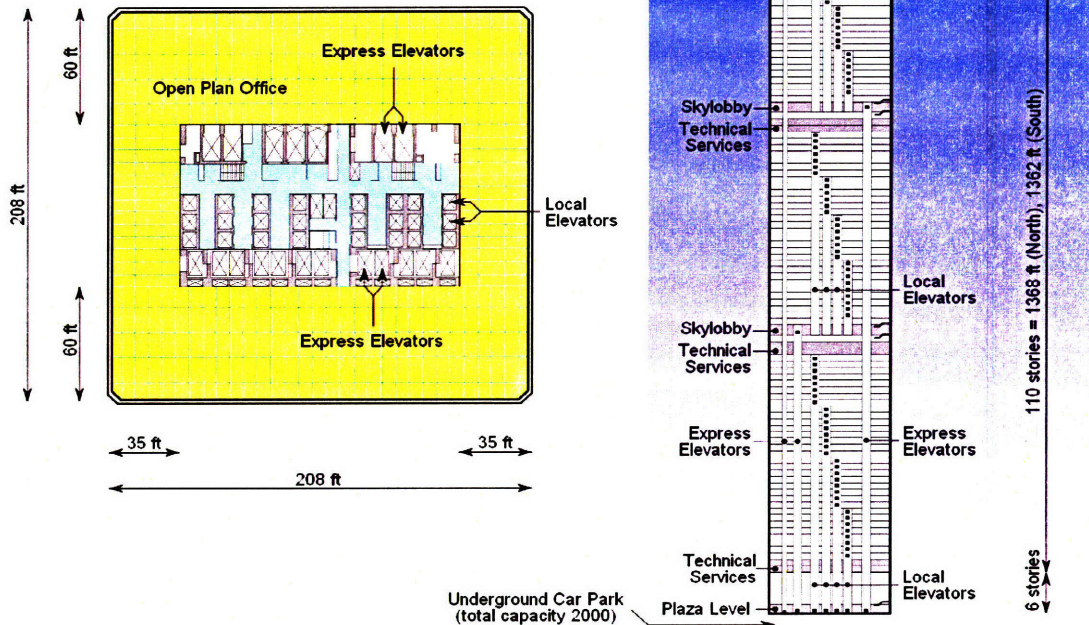
Figure 6-2 A common skyscraper floor plan (Wikipedia, 2008)

Each floor is either serviced by its own dedicated air-handling unit (AHU), or multiple floors can be grouped together and supplied by a single unit. The baseline office building model assumes a separate AHU per floor for a total of five air-handling systems. The return air to the HVAC system is taken from the floors supplied by that same AHU either through ducted returns or, more commonly, through an open plenum return.

Fresh air is supplied to the AHU through common chases that run the height of the building and connect to vents on the top or bottom floors. The minimum fresh air requirements for the populated building areas are specified in ASHRAE standard 62.1, Ventilation for Acceptable Indoor Air Quality (ASHRAE, 2004). The standard specifies 5 cfm/person as a minimum outdoor air rate for office spaces and an occupant density of 5 people / 1000 ft^2 if the occupant density is not known. The office building model assumes an air supply rate exceeding the minimum requirement and equivalent to roughly 1.5 air changes per hour.

Filters in the air-handling system remove particulates from the room air improving occupant health and reducing wear on the AHU components. ASHRAE standard 62.1

identifies MERV 6 filters as the minimum filter efficiency for achieving acceptable indoor air quality in office buildings whereas both DOE and LEED building standards recommend MERV 13 filters. A MERV 6 rated filter only removes roughly 40% of the particulates in the 1-10 micron range typical of biological particles. The baseline office building simulation assumes filter efficiencies consistent with MERV 6 filters. In Section 7.1 the effect of higher efficiency filters is examined.

A dominant airflow characteristic in tall office buildings is temperature induced stack effect flows. The stack effect occurs when warm air rises in buildings causing the higher floors to become positively pressurized relative to the outdoors and the lower floors to become negatively pressurized. The opposite occurs during the summer months when the cold building air falls to the lower floors causing outflows from the lower levels and inflows on the higher floors. Stack effect flows are discussed in more detail in Section 3.1.4. The office building model uses intra-zonal airflow rates consistent for a five floor building at 20 deg C above ambient temperature with two open stairwells connecting all five floors.

Figure 6-3 shows the zone layout in the five floor office building model. There are a total of 16 zones; five office floors each with 22,500 ft^2 of floor area, two stairwells of five zones apiece (transport zones), and a single ambient (outdoor) zone.
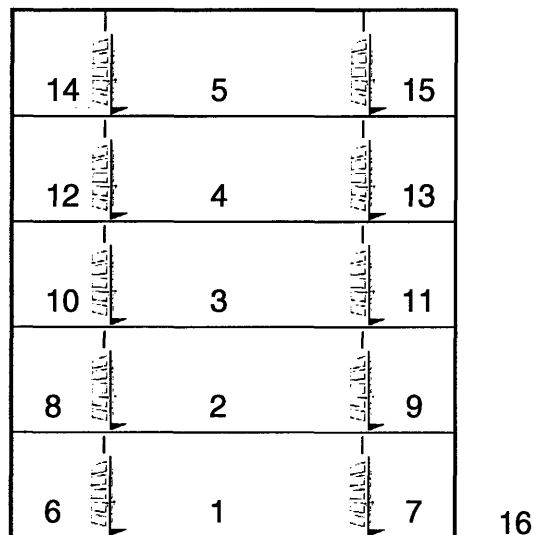
Figure 6-3 Layout of the office building model

Figure 6-4 shows the airflow paths modeled in the five floor office building model. The major airflows are dominated by the stack effect leading to a strong vertical airflow in

63

both stairwells. Lesser airflows are modeled between the stairwells and office areas on each floor and between one set of stairwell zones to simulate the mixing that occurs due to people traffic. These mixing airflows have the effect of transporting contamination against the primary flow gradient. The mixing flow rate was set in the baseline model to .5 m^3/min, which is approximately equivalent 90 people per hour crossing over the mixing interfaces in each direction.

Dominant Airflow Paths   **Mixing Between Zones**
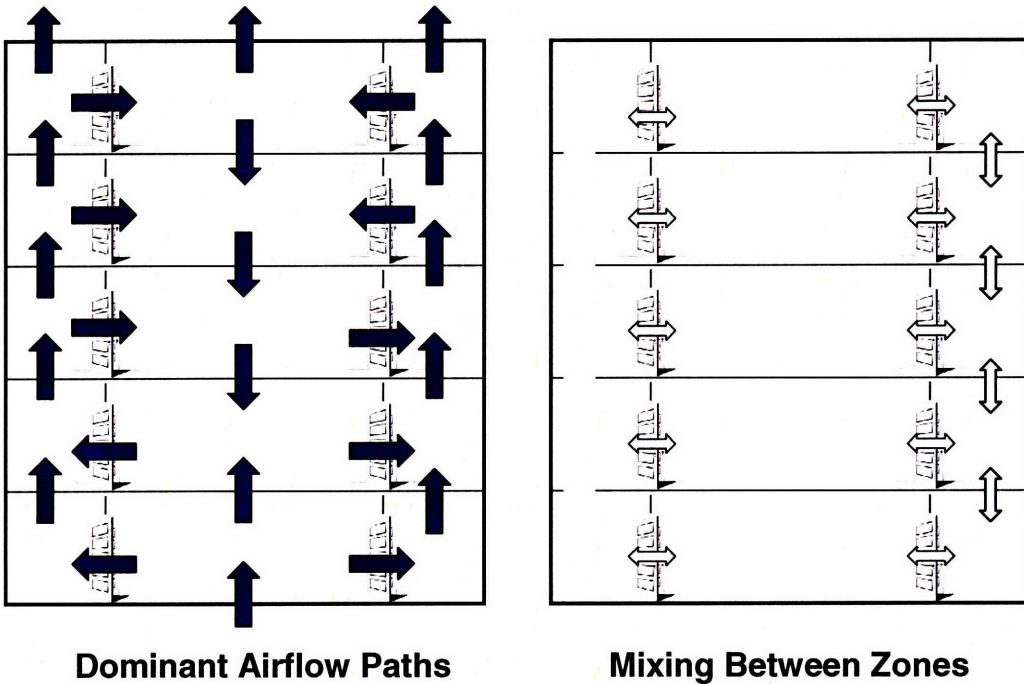
Figure 6-4 Airflow pattern in office building model

The network analysis code was run to determine the path lengths between each of the fifteen interior zones and then the shortest path algorithm was used to determine the dosage each zone would see as a result of a release in any other zone. The zone doses that result from a 10 gram release in each of the five office areas is shown below.
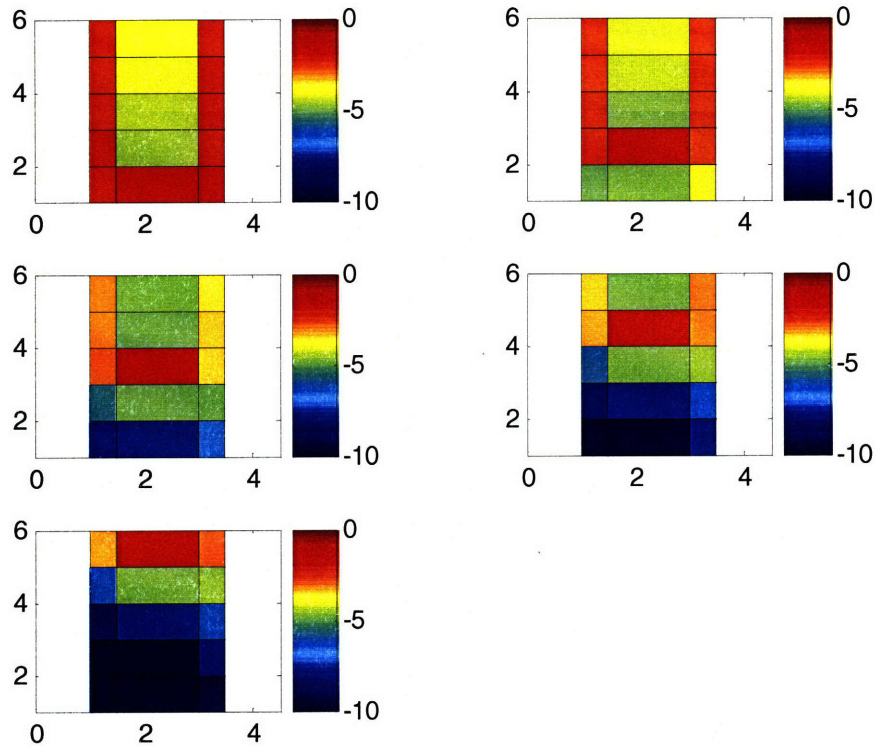
Figure 6-5 Log$_{10}$ (g-min/m^3) for a release in each office area

Figure 6-5 shows that a release in the lower office area spreads efficiently to the higher zones of the building, but a release in an upper zone spreads poorly to the lower office areas. This is not surprising when one considers the dominant airflow pattern in the building given in Figure 6-4. Contamination from the lower levels is forced upwards due to stack effect induced flows, whereas contamination is transported downwards principally through mixing airflows due to people traffic, a much weaker phenomena.

The optimal sensor layout for the office building was calculated by solving the set coverage problem using binary integer programming as described in Section 5.3. The least cost sensing solution as calculated by the Matlab code involved placing a single inexpensive sensor in either the return air for top office floor, or in either stairwell on the top floor.

A single sensor solution is possible for the five story office building because there are sensor locations where the release mass divided by the minimum dilution from any zone to that sensor zone is greater than the sensor sensitivity. The maximum of the minimum dilution paths from any single sensing location is analogous to the concept of a vertices' eccentricity in network theory. The eccentricity of a vertex is the maximum distance from

any point to any other point in the network. In the context of this model the eccentricity would be the maximum dilution or the smallest dosage multiplier. The furthest point in the network from top floor office area is the fourth floor office area and the dilution multiplier is 4.7E-6. Therefore a sensor with a sensitivity greater than 10 (release mass in grams) * 4.7E-6 would be expected to detect a release in any other zone in the model. Figure 6-6 shows the "distance" from any sensing location in the office building model to any release zone.

Sensor Location

Release Zone	1	2	3	4	5	6	7	8	9	10	11	12	13	14	15
1	2.9E-03	6.3E-06	8.2E-06	2.6E-05	3.9E-05	9.0E-04	9.8E-04	6.7E-04	7.5E-04	6.1E-04	7.0E-04	5.9E-04	6.4E-04	5.6E-04	5.6E-04
2	4.2E-06	3.0E-03	3.7E-06	1.2E-05	1.8E-05	1.3E-06	9.6E-06	3.5E-04	3.0E-04	3.2E-04	2.8E-04	3.0E-04	2.5E-04	2.9E-04	2.2E-04
3	4.2E-09	2.9E-06	2.9E-03	3.0E-03	4.7E-06	1.3E-09	3.7E-08	3.3E-07	1.3E-06	1.1E-04	4.6E-05	1.0E-04	4.1E-05	9.9E-05	3.6E-05
4	7.5E-12	4.0E-09	4.0E-06	2.8E-06	4.7E-06	1.7E-12	1.3E-09	4.6E-10	4.7E-08	1.5E-07	2.1E-06	5.5E-05	9.7E-05	5.2E-05	8.4E-05
5	6.0E-14	7.1E-12	5.7E-09	3.8E-06	2.8E-03	2.3E-15	3.6E-11	6.1E-13	1.3E-09	2.0E-10	6.0E-08	7.2E-08	2.8E-06	5.9E-05	1.2E-04
6	5.1E-05	3.9E-05	1.5E-04	4.8E-04	7.6E-04	3.5E-02	1.7E-05	2.6E-02	1.7E-05	2.4E-02	1.9E-05	2.3E-02	3.3E-05	2.2E-02	6.1E-05
7	8.2E-05	6.4E-05	2.6E-04	7.7E-04	1.1E-03	2.6E-05	5.8E-02	2.6E-05	4.4E-02	3.4E-05	4.1E-02	4.7E-05	3.7E-02	6.9E-05	3.3E-02
8	5.7E-08	4.0E-05	1.5E-04	5.0E-04	7.8E-04	1.8E-08	1.3E-07	2.7E-02	4.1E-06	2.5E-02	6.5E-06	2.4E-02	2.3E-05	2.2E-02	5.2E-05
9	1.9E-06	6.5E-05	2.6E-04	7.9E-04	1.2E-03	5.9E-07	1.2E-03	8.0E-06	4.6E-02	1.7E-05	4.2E-02	3.1E-05	3.8E-02	5.4E-05	3.4E-02
10	2.2E-10	1.5E-07	1.6E-04	5.1E-04	8.0E-04	6.8E-11	2.0E-09	1.8E-08	6.8E-08	2.5E-02	2.8E-06	2.4E-02	2.0E-05	2.3E-02	5.1E-05
11	4.2E-08	1.7E-06	2.8E-04	8.3E-04	1.2E-03	1.3E-08	2.7E-05	2.1E-07	9.7E-04	1.0E-05	4.5E-02	2.6E-05	4.0E-02	5.0E-05	3.6E-02
12	1.4E-12	7.6E-10	7.7E-07	5.4E-04	8.5E-04	3.3E-13	2.5E-10	8.8E-11	9.0E-09	2.9E-08	4.1E-07	2.6E-02	1.9E-05	2.5E-02	5.2E-05
13	9.2E-10	3.8E-08	7.4E-06	9.3E-04	1.4E-03	2.9E-10	5.9E-07	4.7E-09	2.1E-05	2.8E-07	9.8E-04	1.8E-05	4.6E-02	4.6E-05	4.0E-02
14	2.3E-14	2.7E-12	2.2E-09	1.5E-06	1.1E-03	8.8E-16	1.4E-11	2.3E-13	5.0E-10	7.6E-11	2.3E-08	2.8E-08	1.0E-06	3.1E-02	4.5E-05
15	2.8E-11	1.2E-09	2.3E-07	3.1E-05	2.1E-03	8.7E-12	1.8E-08	1.4E-10	6.5E-07	8.7E-09	3.0E-05	6.1E-07	1.4E-03	4.5E-05	6.2E-02

Smallest multiplier for 5th floor AHU sensor is 4.7E-6, from 4th floor office space

Top two stairwell sensors have greater min multipliers

Figure 6-6 *Zonedose* matrix shows model eccentricities

The eccentricity for the two top floor stairwell zones are 4.5E-5 and 3.6E-5 indicating that they are more central then the office area and would detect an even smaller release.

6.1.2. CONVENTION CENTERS

Like office buildings, convention centers have a relatively consistent layout. Convention centers are typified by several large convention halls connected by movable partitions. These exhibit halls can vary considerably in size with the larger ones totaling well over 100,000 ft^2. Along the perimeter of the convention halls oftentimes are located smaller office areas for private meetings and a pre-function space or broad corridor that links the various exhibit halls. For the baseline analysis only the convention halls themselves were considered because they constitute a vast majority of the floor space and most likely contain most of the people. Also, making this assumption further distinguishes the convention center model from the office building model. Figure 6-7 shows an example layout for a convention space.
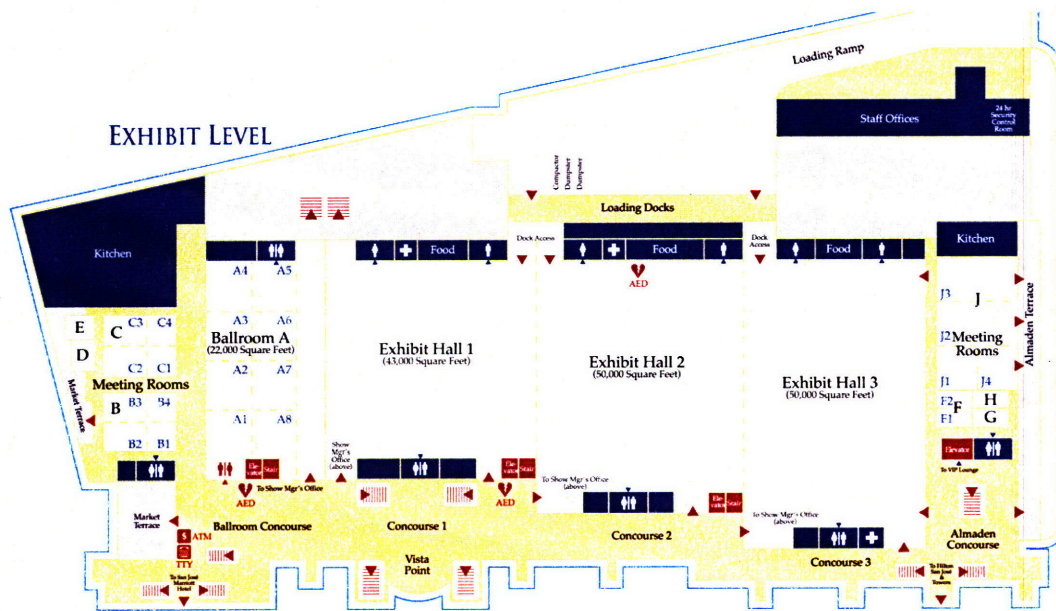
**Figure 6-7 Convention center floor plan (sanjose.org, 2007)**

The HVAC systems in convention centers are structured such that separate air-handling units supply each convention space. An exhibit hall is either supplied by a single AHU or by multiple smaller AHUs. Each hall has a separate system so that unused exhibit spaces do not need to be conditioned reducing energy costs. ASHRAE standard 62.1 recommends a minimum fresh air supply of 5 cfm / person which is consistent with the recommended level for office buildings. The default population density suggested for conference or meeting areas is 50 people per 1000 ft^2 10 times greater then the default density for office buildings (ASHRAE, 2004). For a 100,000 ft^2 convention space this translates into a minimum fresh air requirement of 25,000 cfm.

In convention centers the dominant contamination transport mechanism between occupied exhibit spaces is likely to be bi-directional turbulent diffusion. As discussed in Section 3.1.2, the rate of contamination diffusion between two spaces is directly related to the cross-sectional area in the direction of the diffusion. For large exhibit halls with the movable partitions pulled back this diffusion area can be on the order of several thousand square feet. In addition, with one exhibit sharing multiple halls, the traffic of people between the halls is expected to be quite large increasing the bi-directional nature of the airflow. The convention center simulation considers a scenario in which all the exhibit halls are occupied.

67

For the baseline convention center simulation a five exhibit hall convention center was considered. Each of the exhibit halls is roughly 100,000 ft² with a supply air rate equal to 5 ACH and an outside air ratio of 50%. The filter efficiency is set to 40% in the particle size range of interest and the mixing airflow rate between any two neighboring zones is equivalent to 3,500 cfm. The resulting dosages from releases in each exhibit hall are given in Figure 6-8.
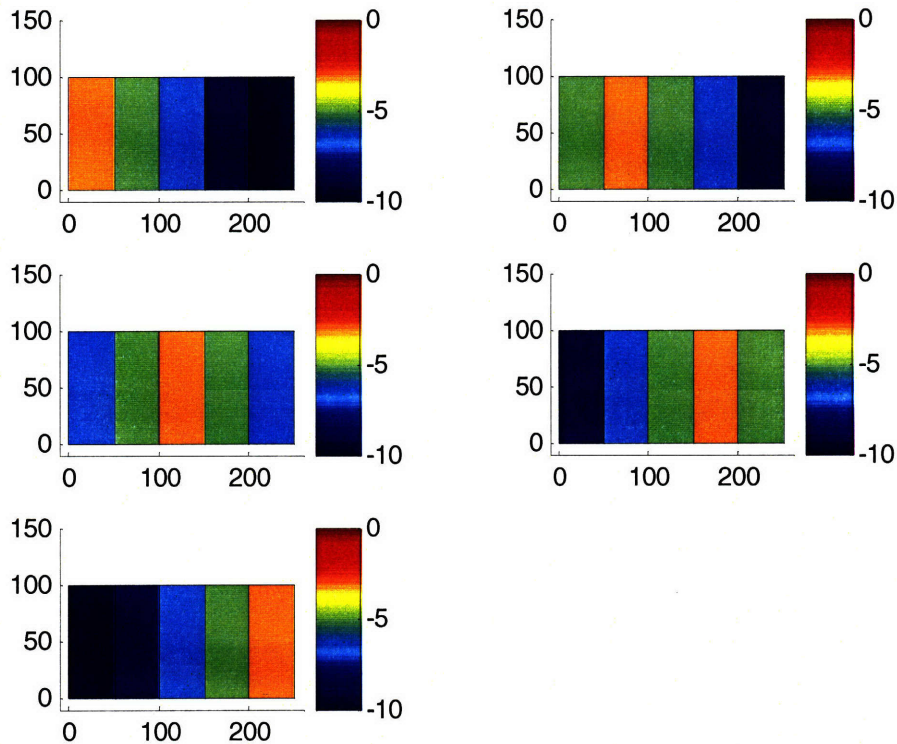
Figure 6-8 Log$_{10}$(dose) for a release in a convention center

When the optimization algorithm is run the recommended sensor allocation is to place a less expensive sensor in Zones (2) and (4). A single expensive sensor in Zone (3) would also supply full coverage, but the cost of the most expensive (PCR) sensing technique is modeled as more than twice the cost of the least expensive (color based HHAs) sensing method. The medium price sensor is not sensitive enough to provide full coverage with a single sensor in Zone (3). The tradeoff between sensitivity and sensor cost under different building conditions is considered in Section 7.1.

6.1.3. AIRPORTS

Unlike office buildings and convention centers, airports vary considerably in layout and AHU characteristics. Airport designers face the problem of trying to bring people together to facilitate check-in, baggage claim, and access to food and retail, while at the same time providing sufficient spacing for passengers to board their planes. This quandary has led airport designer towards five basic configurations for terminal design at major airports. These basic configurations are finger piers, satellites with or without finger piers, midfield – either X-shaped or linear, linear with one side devoted to aircraft, and transporters (de Neufville, 2003).

From an airflow and contamination transport perspective these five configurations could likely be reduced to two general classes. The first encompasses the finger pier and linear terminal designs which include the check-in and baggage claim areas within the same structure as the departure and arrival gates. Also included in this design class would be satellite terminals or midfield concourses that are connected to a main terminal by fingers. The connection between check-in and baggage areas to departure terminals is significant because the major leakage path to the outdoors occurs when people enter and exit the terminal building. This will tend to cause a dominant flow direction towards the main terminal from the finger piers. From a network model perspective, the finger piers will begin to resemble the office buildings with stack effect induced flows as described in Section 6.1.1 because of the highly directional nature of the airflow.

The second grouping of airport terminal classes includes the satellites, transporter, and midfield configurations (unconnected). All typically separate the check-in, security, and baggage claim areas from the gate areas. This may reduce the highly directional airflow nature that is common in finger pier and linear designs, especially if the entrance into the satellite terminals is by way of trams or people movers and do not involve direct flow paths to the outdoors or to the main terminal. Figure 6-9 depicts Chicago's O'Hare international airport, a hybrid of finger pier, linear, and satellite configurations. Figure 6-10 shows Denver's International Airport, an example of an unconnected satellite design.
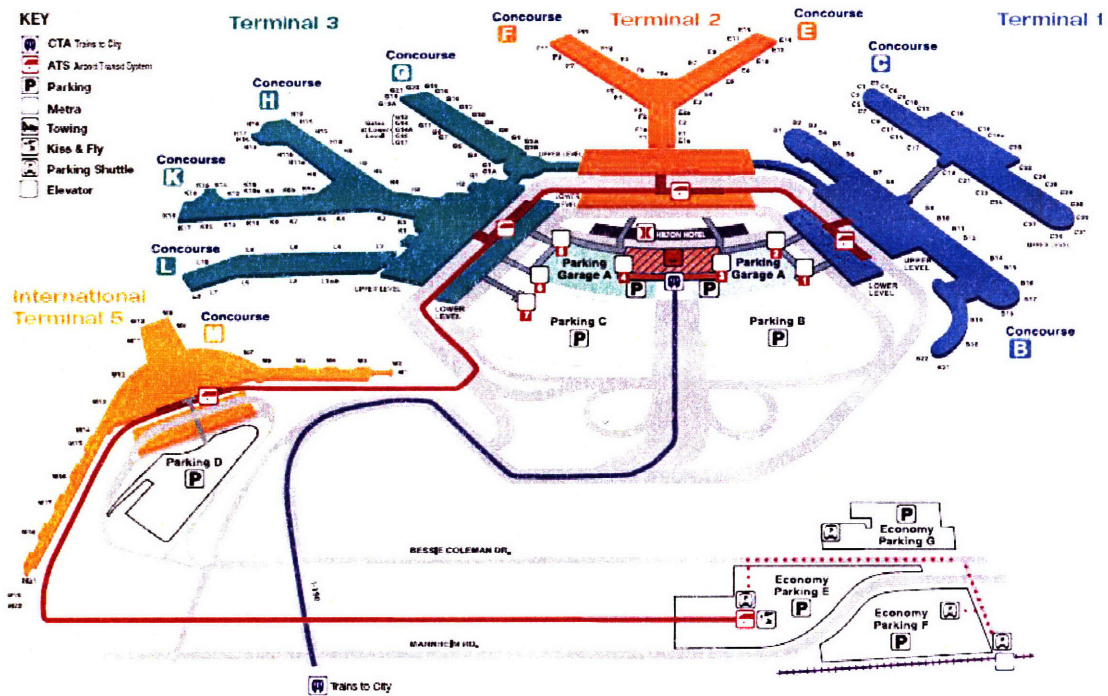
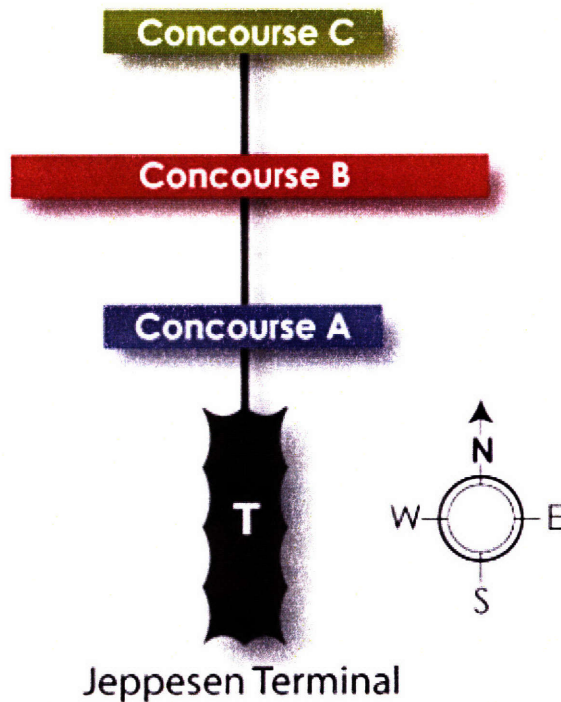**Figure 6-9 Layout of Chicago's O'Hare airport (flychicago.com, 2008)**

**Figure 6-10 Layout of Denver International Airport (flydenver.com, 2008)**

The airport terminal reduced-order model is an example of a finger pier design, and is based loosely on O'Hare airport's terminal three. The finger pier design is used as an

example airport case because it incorporates network characteristics similar to both the office building and convention center models. The finger or departure terminals in the airport model have a tree-like network structure similar to that of the office building model whereas the main terminal building is modeled similar to the convention center, albeit smaller in size.

The airport model consists of two piers projecting outwards from the main terminal. The first pier consists of four HVAC zones with a corridor running through the center. The second pier is larger and splits 1/3 of the distance down the pier. This second Y-shaped pier consists of a total of 10 HVAC zones and five corridor segments.

Separate HVAC zones supply either side of the corridor in the departure terminal due to the different thermal requirements placed on either side. Airport terminals oftentimes have large windows on both sides of departure terminals. Depending on solar angle the heat loading can vary considerably from either side of the departure terminals necessitating separate thermal control. Having either side of the terminal building supplied by different air-handling units (AHUs) is one possible solution to this problem. The design layout for the airport model is shown in Figure 6-11.
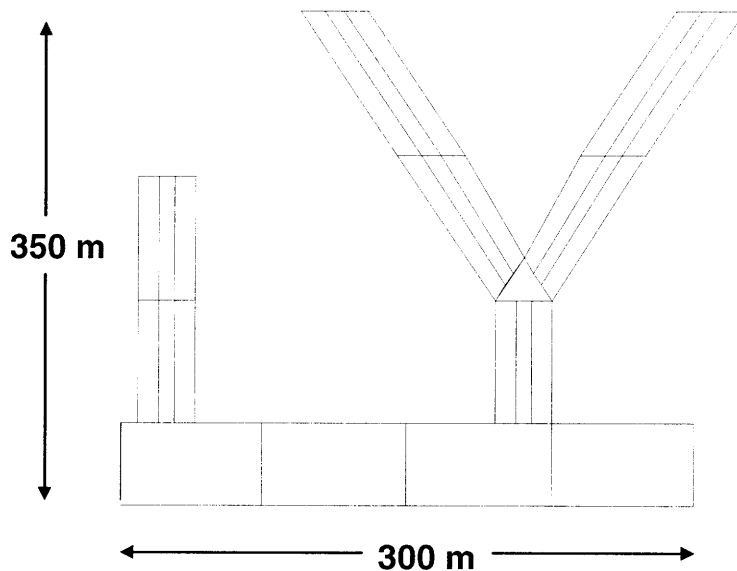
Figure 6-11 Layout of airport terminal model

As mentioned previously, it is common to have considerable directional airflows within airport terminals due to pressure imbalance between the departure terminals and the main terminals. Airports are also characterized by high levels of people traffic leading to

71

considerable spread of contamination even against the dominant flow gradient. The airport network model attempted to incorporate both the directional and mixing airflows.

Dominant Airflows   Mixing Airflows
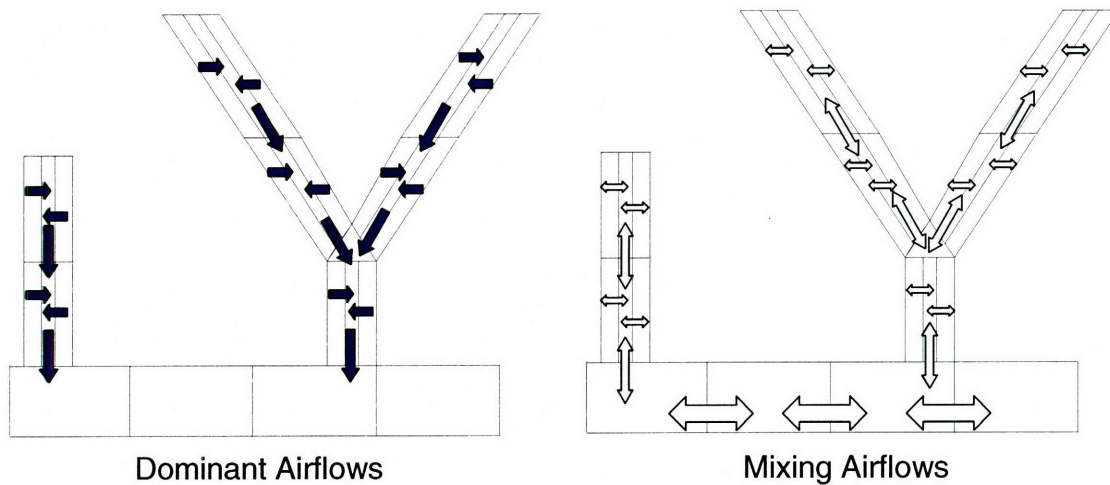
Figure 6-12 Airflow pattern in airport model

For the baseline airport simulation the air exchange rate was set to five air changes per hour and the outside air percentage equaled 25%. The mixing airflow rates are set in the baseline case to 10 m^3/min, approximately 300 cfm. The supply air filters were set to 70% efficient in the baseline simulation with the thought that airports may have better filters than the other facilities examined in order to remove the noxious combustion particulates created by the jet engines. The results for a 10 gram release in six selected zones are given in Figure 6-13. The release zone is the zone with the highest concentration levels.
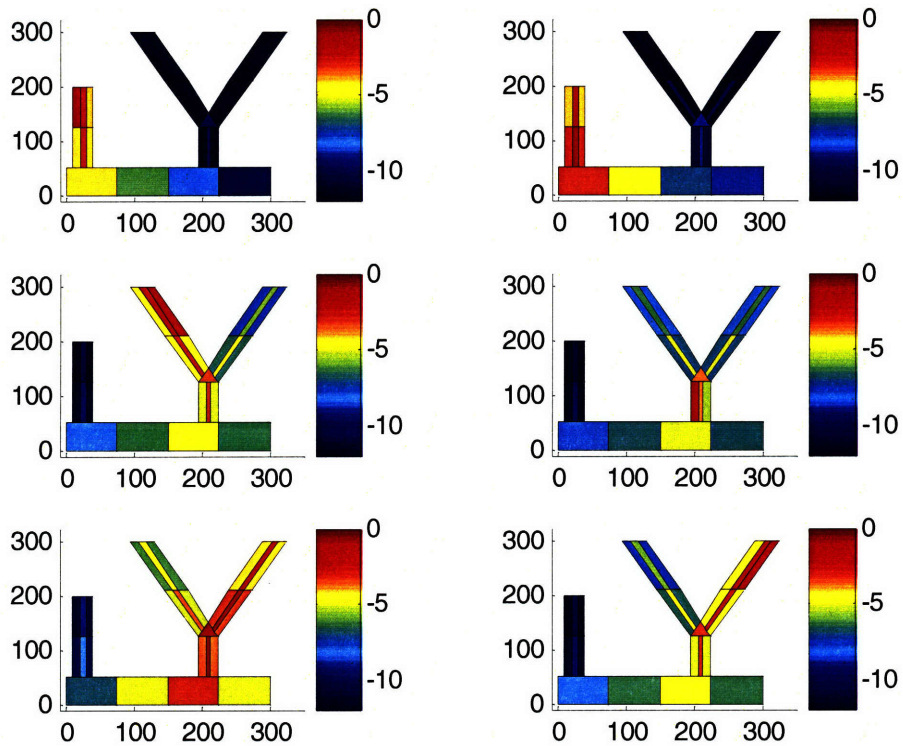
Figure 6-13 Log_{10}(dose) for release in six airport zones

Contamination efficiently travels down the finger piers towards the main terminal building, but does not travel in the opposite direction as efficiently. This is due to the highly directional pressure driven flows in the corridors and is similar to the stairwell airflows in the office building model. The path lengths between zones in the main terminal building appear quite large with over five orders of magnitude difference in dose levels between terminal zones in some cases. Longer path lengths indicate that the intra-zonal airflows in the main terminal are fairly small relative to the zone dilution levels.

The set coverage optimization routine determined that two inexpensive sensors located in the main terminal building would provide appropriate coverage for all possible releases. The sensors should be located in the two zones where the finger piers interface with the main terminal building. This orientation is shown in Figure 6-14.

73
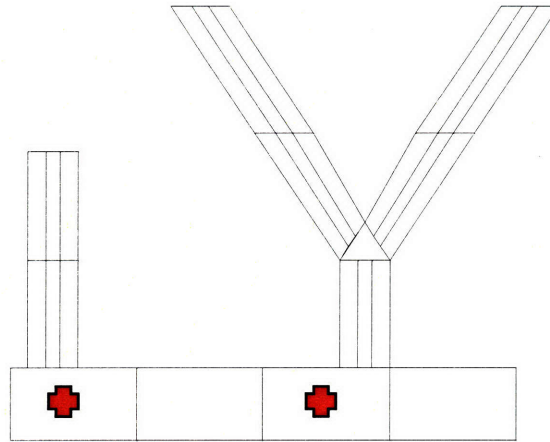
Figure 6-14 Airport sensor locations for baseline simulation

The optimal solution for the airport model is reminiscent of the optimal sensing solution in both the office building and convention center models. Like the office building model, the optimal sensors are placed at the end of a highly directional air flow paths; the end of corridors in the airport model and the top of stairwells in the office building model. And like the convention center, the sensors are placed in the main terminal such that they minimize the maximum distance from a sensor location to any other terminal zone.

6.2. SUMMARY

Three unique building models were created to explore the application of the reduced order contamination propagation model. An office building, convention center, and airport terminal were chosen due to their large size, high population density, and unique airflow characteristics.

The office building model is characterized by highly directional airflow among its vertical chases leading to very short unidirectional path lengths between the office areas and the stairwell zones on the upper floors. Because of its highly directional nature, the network representation of the office building resembles more of a tree structure. The direction of the stack effect flows determines the location of the leaves of the tree and thus the optimal sensor placement within office buildings.

The convention center model is a linear five zone model where the primary means of contamination transport is through mixing airflows between the large non-partitioned event spaces. This model is very different than the office building model due to the diffusive non-directional nature of the contamination transport. Optimal sensor

placement depends on finding the geographic center of the model, which corresponds to the network center. With multiple sensors available the sensors placement problem reduces to minimizing the maximum number of zones between any zone and a sensor location.

The airport building model has characteristics of both the convention center and office building models. The two finger piers have highly directional airflows through the corridors, resembling the airflows in the office building stairwells. The main terminal building is modeled as several large open zones that have characteristics similar to the convention center model. If the directional airflow in the transport zones of the finger piers is strong enough, the model can be reduced by grouping all of the zones as a single zone for each of the finger piers. The path length for the grouped zone would be equivalent to the longest path length of the finger pier zones.

In Figure 6-15 the underlying network diagrams for the three models are shown. The airport finger piers are each grouped as a single zone for added simplicity.
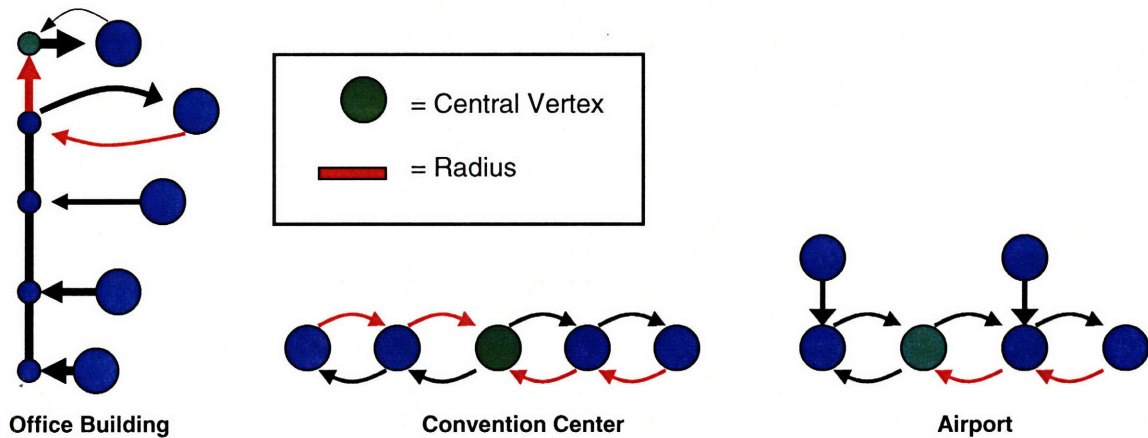
Figure 6-15 Network diagrams for the three example cases

The eccentricity of a vertex in a graph is the distance to the farthest vertex from that point. The central vertex in a graph is the vertex with the minimum eccentricity and is shown in green in Figure 6-15. A sensor positioned at the central vertex has the best chance of providing coverage for the all of the building's zones.

The radius of a graph is the minimum of the vertex eccentricities and is represented by the red arrows in Figure 6-15. It is the distance between the central vertex and the vertex furthest from that point (Gross, 2006). For a one sensor solution to cover all of the building zones the network's radius must shorter than the detection threshold of the

75

sensor. In the office building model the radius is such that a single sensor is sufficient, in both the baseline convention center model and the baseline airport model additional sensors are required.

7. APPLICATIONS

In this chapter the building models developed in Chapter 6 are used to understand some of the important tradeoffs in sensor selection. In Section 7.1 the tradeoff between sensor cost and sensitivity is examined by optimizing the sensing solution over a large number of building conditions. The problem of placing a limited number of sensors in a given building is examined in Section 7.2. The goal is to appreciate how building conditions influence sensor requirements in the general sense, not necessarily specific to the three case studies.

7.1. SENSOR COST VS. SENSITIVITY

In all three simulations conducted in Section 6 the optimal sensing solution consisted of only the least expensive sensors and none of the more expensive sensing options. This despite the fact that the sensitivity improved by an order of magnitude between each sensing option but the cost only increased by a factor of 1.5X. In this section the model input parameters are varied and the optimal sensing solutions are recalculated. By examining a larger set of potential building parameters we hope to determine if it is a characteristic of the models themselves that favor the low-cost, low-sensitivity sensors or if it is an artifact of the default parameters used in the three baseline simulations.

Simulations were conducted for the office building, convention center, and airport models varying the size of the zones (or the air exchange rate), the filter efficiency, the outside air fraction, and the mixing airflow rate. In addition the dominant airflows present in both the office building model and the airport model were varied. The convention center is modeled as having only bi-directional mixing airflows. The values used for the input parameters are given below.

	Office Building	Convention Center	Airport
Filter Efficiency	.4,.7,.9	.4,.7,.9	.4,.7,.9
Outside Air %	25,50,75%	25,50,75%	25,50,75%
Size	.5,1,2X	.5,1,2X	.5,1,2X
Mixing Airflow	.5,1,2X	.5,1,2X	.5,1,2X
Principal Airflow	.5,1,2X	-	.5,1,2X
Number of Sims	**243**	**81**	**243**

Figure 7-1 Variable values in sensitivity / cost simulations

A total of 243 simulations were initially run for both the airport and office building models and 81 simulations were run for the convention center model. For each model run, a ten gram release of contaminant was simulated. The lowest cost set of sensors required to detect a release in any zone was determined and the sensing cost and sensors required were recorded.

7.1.1. OFFICE BUILDING MODEL

The initial 243 simulations of the office building model results in 222 scenarios where full coverage only requires a single inexpensive sensor in one of the 5th floor stairwells. The remaining 21 simulations require a single moderately expensive sensor in the 5th floor stairwell.

Of the simulations requiring the more sensitive sensor, twelve have the highest dilution levels. These simulations include a supply air filter efficiency of .9, an outside air rate of 75%, and double the air exchange rate of the baseline simulation. The remaining nine simulations requiring the more sensitive sensor have the second highest dilution level. Figure 7-2 shows the influence of poorly-mixed dilution on sensing requirements.
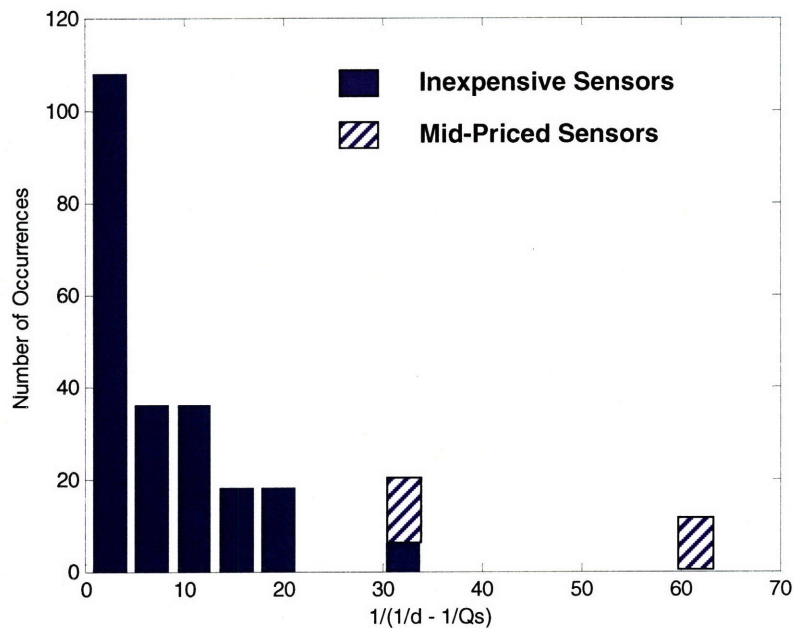
Figure 7-2 Affect of dilution on sensing requirements in office buildings

Examining the flow characteristics of the office building model it is evident why the poorly-mixed dilution in the office spaces is the most significant variable in determining sensor requirements. The zones that are the greatest distance from the 5th floor sensor location are the 4th floor office space and the opposing 4th floor stairwell zone. It seems counterintuitive at first that the 4th floor zones are a greater distance from the 5th floor sensing location when compared to lower level zones. However, due to the highly directional nature of the airflow in the stairwells, only minimal dilution occurs between stairwell zones along the principle transport direction. It is therefore the magnitude of the airflow from each office space into the stairwell that determines how closely connected a zone is to the sensor zone.

$$D_1 = mass * \left(\frac{1}{dilution_1} - \frac{1}{Q_S}\right)$$

$$D_2 = mass * \left(\frac{1}{dilution_1} - \frac{1}{Q_S}\right) * \frac{Q_{12}}{\sum Q_{out2}}$$

$$D_3 = mass * \left(\frac{1}{dilution_1} - \frac{1}{Q_S}\right) * \frac{Q_{12}}{\sum Q_{out2}} * \frac{Q_{23}}{\sum Q_{out3}}$$
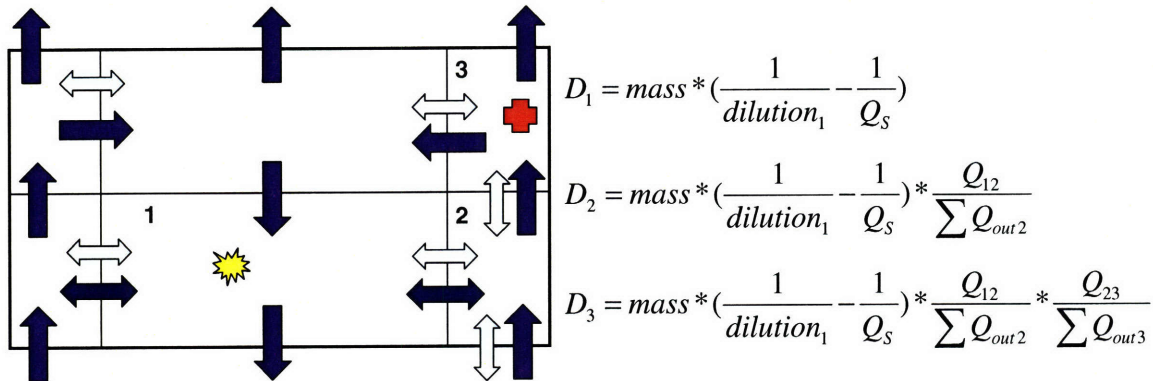
Figure 7-3 Dilution in office building transport

In Figure 7-3 Zone (1) represents the 4th floor office space and Zones (2) and (3) represent the 4th and 5th floor stairwells respectively. If a large percentage of the inflows to a transport zone are from a contaminated zone then the ratio of contamination inflow to total outflow, and thus the path length between zones, will be close to 1. With high vertical air exchange rates due to stack effect airflows, the dose reduction in the dominant airflow direction is small and significant dilution only occurs when the contaminant passes through an HVAC supplied zone.

As seen in Figure 7-2, with a dilution of approximately 30 there are situations where inexpensive sensors are adequate and other situations where a more expensive sensor is needed. The 18 simulations with a dilution of 30 and their corresponding parameters are given below.

Filter Eff	OA%	Size	Qmix	Qmult	Cost
0.9	0.5	2	0.25	0.5	150
0.9	0.5	2	0.25	1	150
0.9	0.5	2	0.25	2	150
0.9	0.5	2	0.5	0.5	100
0.9	0.5	2	0.5	1	150
0.9	0.5	2	0.5	2	150
0.9	0.5	2	1	0.5	100
0.9	0.5	2	1	1	100
0.9	0.5	2	1	2	150
0.9	0.75	1	0.25	0.5	150
0.9	0.75	1	0.25	1	150
0.9	0.75	1	0.25	2	150
0.9	0.75	1	0.5	0.5	100
0.9	0.75	1	0.5	1	150
0.9	0.75	1	0.5	2	150
0.9	0.75	1	1	0.5	100
0.9	0.75	1	1	1	100
0.9	0.75	1	1	2	150

Figure 7-4 Office building simulations with a dilution of 30

The scenarios requiring the less expensive sensor are highlighted in green. It appears that the simulations including greater mixing airflows (Qmix) and lower stack effect flows (Qmult) required the less sensitive sensor. In fact, all the scenarios listed in Figure 7-4 where the ratio of Qmix/Qmult < 1 require the $150 sensor and all the scenarios where Qmix/Qmult >= 1 only require the $100 sensor.

The relationship between Qmix and Qmult primarily influences the path length between the office areas and the stairwell zones. As shown in Figure 7-3, the dilution of contamination in the fourth floor stairwell zone is determined by the inflows to the stairwell from the fourth floor office space (both mixing and stack effect) divided by the outflows from that zone (primarily stack effect airflows). An increase in the mixing rate and a decrease in the stack effect multiplier would therefore be expected to shorten the path length between the AHU zone and the stairwell requiring a less sensitive sensor. If, however, the stack effect flows are reduced enough relative to the mixing flows the strong directional nature of the model will begin to disappear. The dilution between stairwell zones will become significant, and building will begin to behave more like the convention center discussed in following section.
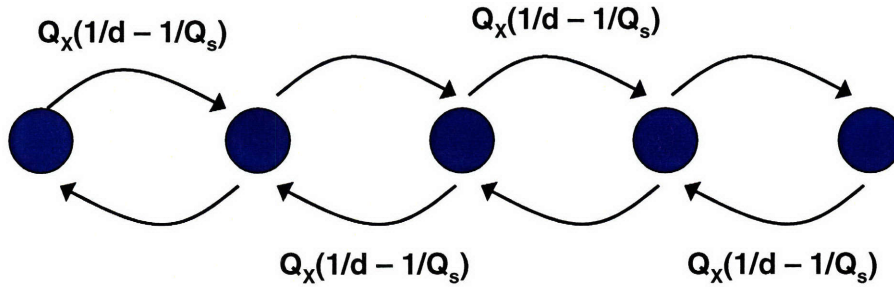
7.1.2. CONVENTION CENTER

Of the eighty-one simulations conducted for the convention center model the optimal sensing solution cost $200 (two inexpensive sensors) on three occasions, $250 (one inexpensive, one medium priced sensor) on thirty occasions, and $300 (three inexpensive sensors) for the remaining forty-eight simulations. There are no instances where a high-cost, high-sensitivity sensor is part of the optimal solution.

The underlying network model is simple for the convention center and by examining the model it is evident how the input parameters influence the sensing solution. The convention center network model consists of five zones, one for each of the convention halls, spaced linearly. In addition, the four hall interfaces are potential sensor locations bringing the total number of possible sensor locations to nine. The path lengths between any two neighboring zones are equal to the mixing flow-rate divided by the dilution (poorly mixed) for the inflow zone. The path length between an interface sensor and the AHU sensors in the two zones that compose the interface is 1-(dilution/Qs). Interface sensors always detect a lower dose then a sensor in the release zone's AHU return, but

detect a higher dose then a sensor in the neighboring zone's AHU return. The tradeoff between various sensor positioning strategies was discussed in detail in Section 5.1. All of the exhibit halls are modeled as having identical size and airflow parameters, the "distance" between any two neighboring zones or any zone and an interface sensor is approximately equal.

Figure 7-5 The path length between neighboring zones in the convention center model

If we make the assumption of equivalent path lengths between zones then the dilution from a zone to any sensor location in the return air is given by:

$$(\frac{mass}{dilution}) * (Q_X(\frac{1}{dilution} - \frac{1}{Q_S}))^N \qquad (7\text{-}1)$$

where N = the number of zones between the release zone and the sensing location. For sensor locations at the interfaces between zones the equation is modified slightly to:

$$(Q_X(\frac{1}{dilution} - \frac{1}{Q_S}))^N \qquad (7\text{-}2)$$

where N includes the zones on either side of the interface as well. The sensitivity and hence the cost of the sensing solution should be separable based upon the terms given above. Figure 7-6 shows good agreement with this assumption.
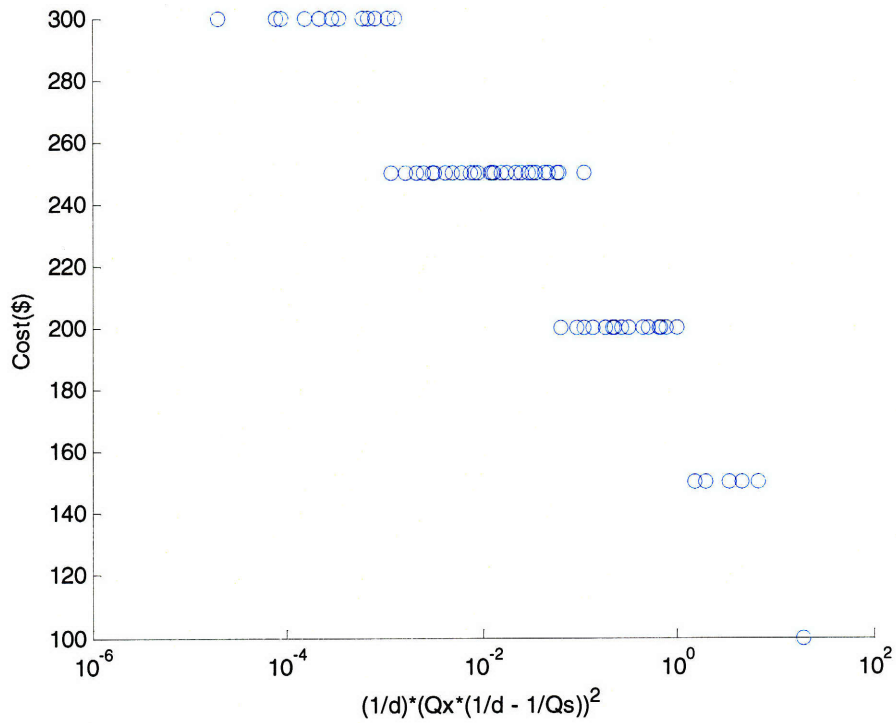
Figure 7-6 Sensing costs depend on dilution parameters

The sensor costs vary in a fairly linear manner with the log10 of the dilution parameters principally because sensor cost is a function of the log10 of sensor sensitivity. A different assumption for sensor cost vs. sensitivity would result in a different relationship for cost and dilution. In Section 7.1.4 the optimal tradeoff between sensor cost and sensitivity will be discussed in more detail.

7.1.3. ·AIRPORT

With the most complex underlying network model, the airport simulations possessed the most varied array of optimal sensing solutions based upon the model input parameters. In the 243 scenarios analyzed there were eight unique optimal sensing solutions at eight different cost points.
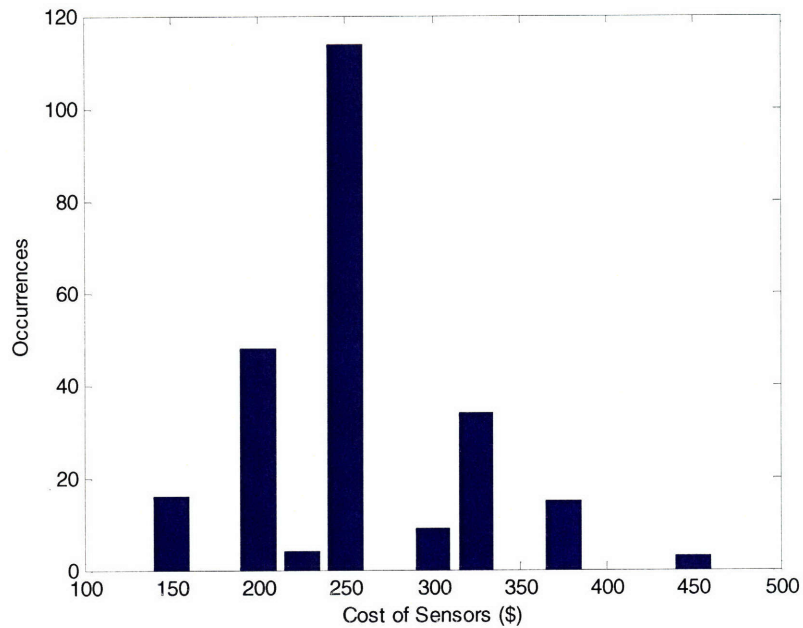
Figure 7-7 The distribution of optimal sensing solutions in the airport model

Of the eight unique sensing solutions five are combinations of two sensors, two are single sensor solutions, and one ($450) is a four sensor solution. The sensor layout within these classes is fairly consistent with the types of sensors changing but the positioning remaining essentially the same. The typical sensor positions for the one, two, and four sensor solutions are given in Figure 7-8.
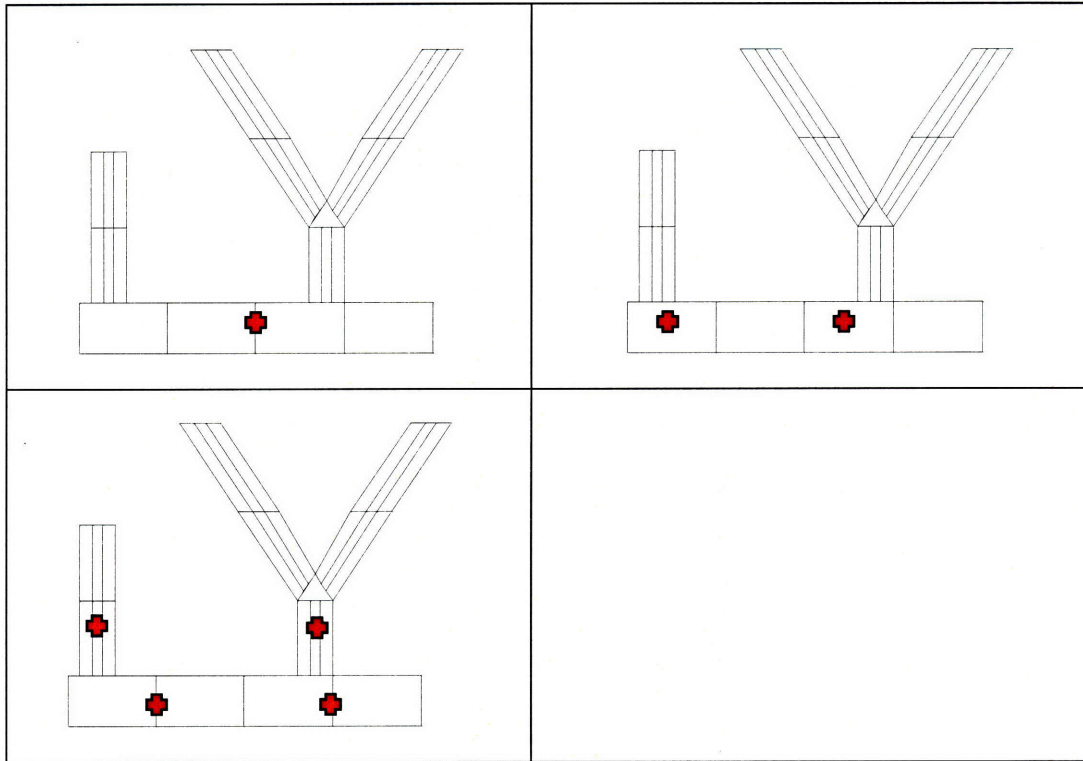
Figure 7-8 Sensor positioning for airport model

Like the convention center and high-rise models the sensing costs in the airport model are expected to be a strong function of the building's dilution parameter. It is a bit unclear, however, which power of the building's dilution parameter is the best determinant of sensing requirements. Sensing requirements depend upon (1 / unmixed dilution)^n, were n = number of zones between the release and the sensor location. The most common sensing solution involves two sensors. In these situations the shortest path between the release and the sensor passes through two AHU zones (the source zone and the sensor zone) along with multiple transport zones. Therefore $(1/d - 1/Qs)^2$ is expected to be a strong predictor of sensor requirements.
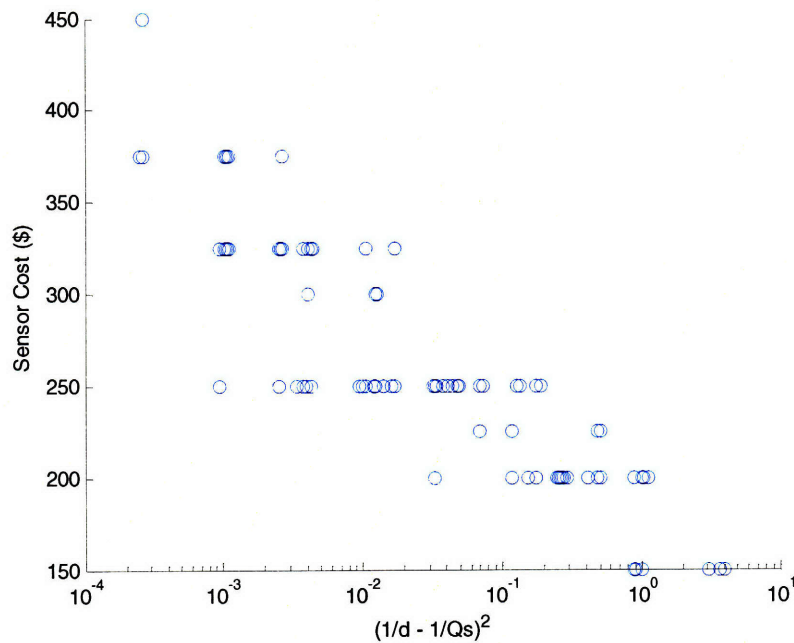
Figure 7-9 A good predictor of airport sensing requirements is (1/d - 1/Qs)^2

Figure 7-9 shows that $(1/\text{poorly-mixed dilution})^2$ is a good predictor of sensor costs, but that at certain levels of dilution there remain solutions at multiple price points. For example, at $(1/d - 1/Qs)\wedge2 = .01$ there are sensing solutions at \$250, \$300, and \$325. The additional factors that could influence the sensing requirements are the intra-zonal air exchange rates which vary due to different mixing rates and pressure driven airflows.

In the airport simulations both the mixing airflow rates and the dominant airflows were varied from the nominal conditions by multipliers of .5, 1, and 2. The 243 cases simulated were equally partitioned among the three multiplier levels and the effects of both Qmix and Qmult on the cost of the sensing solution are given in Figure 7-10.
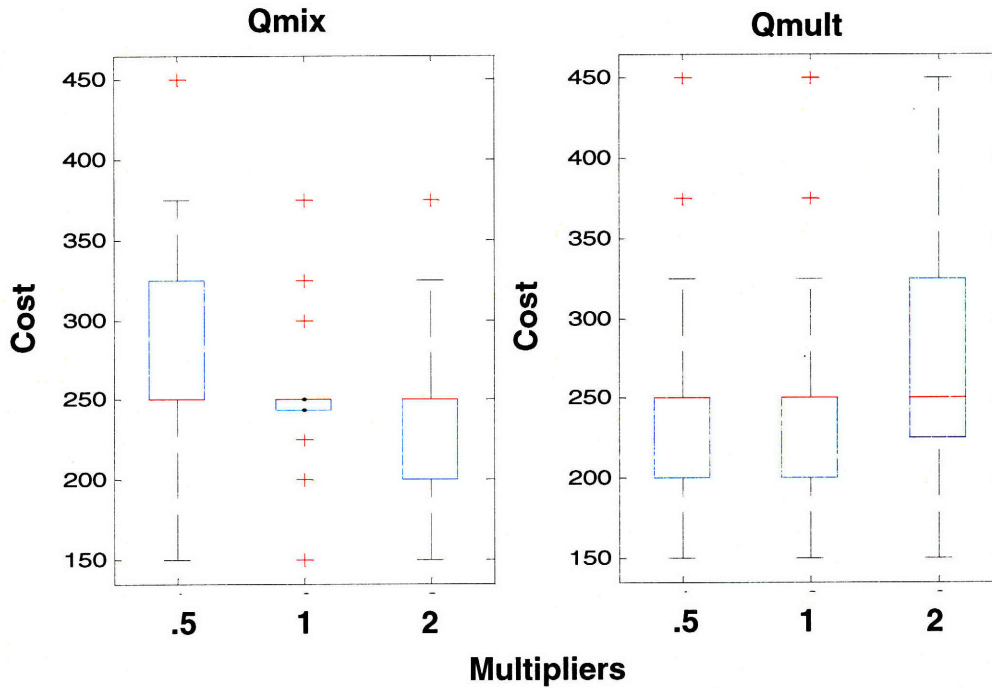
Figure 7-10 The effect of Qmix and Qmult on sensing costs

The mixing airflow rate appears to have an inverse relationship to the cost of the sensing solution. The higher the mixing airflow rate, the lower the cost of the system. Qmult, however, appears to have a small direct correlation with the cost of the sensing system. The box and whisker plot in Figure 7-10 shows almost no difference in sensing cost for the cases where Qmult equals .5 or 1 and a slight increase in sensing cost when the dominant airflows are doubled. The mean and standard deviation for all six cases are given below.

	Qx			Qmult		
	.5	1	2	.5	1	2
Mean	$273	$256	$239	$252	$255	$260
Std. Dev.	$64.8	$55.2	$52.2	$60.7	$59.2	$57.5

**Figure 7-11 Qmix has a stronger effect on the cost of the sensing solution**

Qmult has a minimal effect on the sensing requirements because the dominant airflows are high enough that only minor dose reductions occurs as the contaminant travels between transport zones. The path length from a hypothetical transport Zone A to another hypothetical Zone B equals the airflow rate from A to B divided by the airflow out

of Zone B. As long as the pressure induced airflows are high relative to the mixing airflows, the airflow into and out of zone B will be dominated by the pressure induced flows and the dose multiplier will be close to one. This type of situation was discussed in Section 6.1.1 relative to the airflows in office building stairwells.

Higher mixing rates tend to lead to less expensive sensing solutions mainly due to contamination transport in the main terminal building. The main terminal building is modeled similarly to the convention center with mixing between the large open spaces as the primary means of contamination transport between zones. In several instances it was the requirement to provide coverage for other main terminal zones that drove the increased sensor costs and not the finger piers.

Qx = 10 **Qx = 5**

Filter Eff = .9, OA % = .75, Size =2X, Qmult = 1
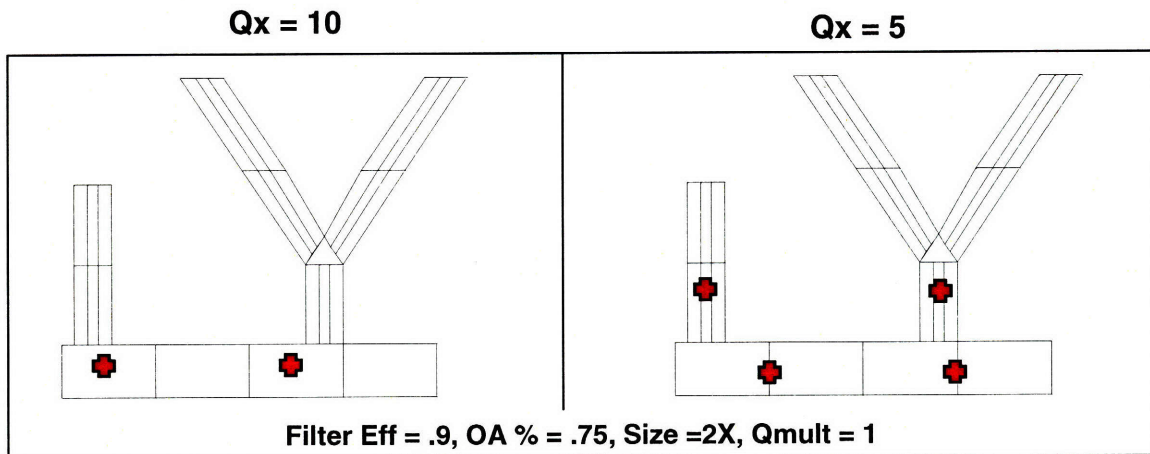
Figure 7-12 A decrease in mixing airflows leads to an increase in sensor cost

Figure 7-12 is an example of a situation where decreasing the mixing airflow rates led to more expensive sensing solution requiring a greater number of sensors. Figure 7-13 shows that main reason for the increased sensor costs is that the sensor at the base of the Y-shaped finger pier (finger pier 2) can no longer cover the neighboring terminal zones. Both sensors must then migrate to the interfaces between the main terminal zones requiring additional sensors to cover the finger piers.
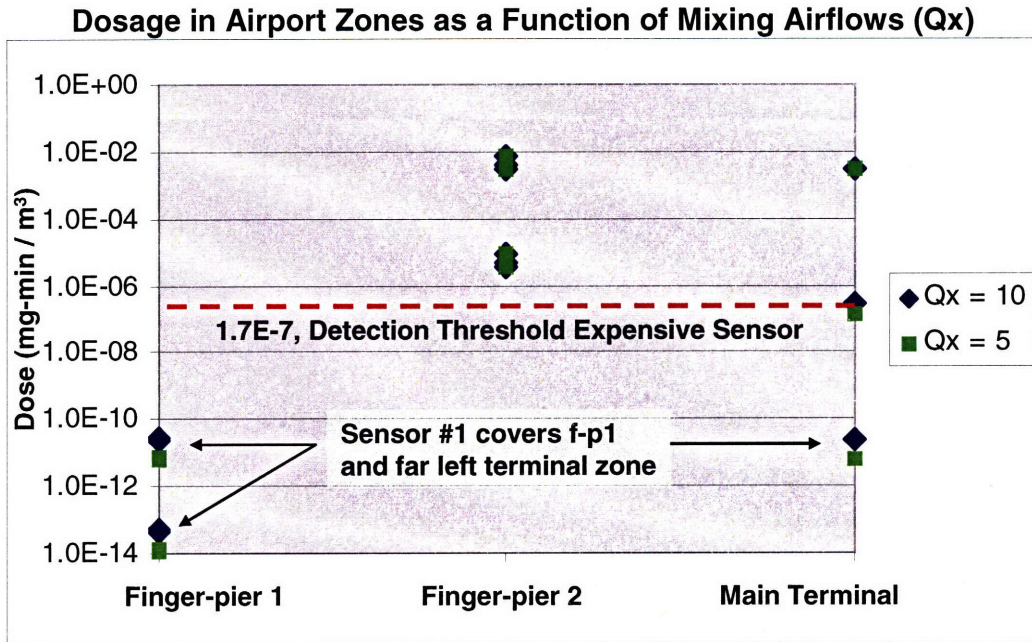
Figure 7-13 Two sensors can no longer cover the entire airport

Determining the sensing requirements in the main terminal building is analogous to the problem in the convention center. The dosage in the release zone is (m/d) and the path length to neighboring zones are $Qx*(1/d-1/Qs)$. The challenge is to determine the intra-zonal exchange rate which depends principally on turbulent diffusion and people movement. If the zone dilutions and supply rates are known, the required sensitivity of the sensor in a neighboring zone can be determined as a function of Qx.
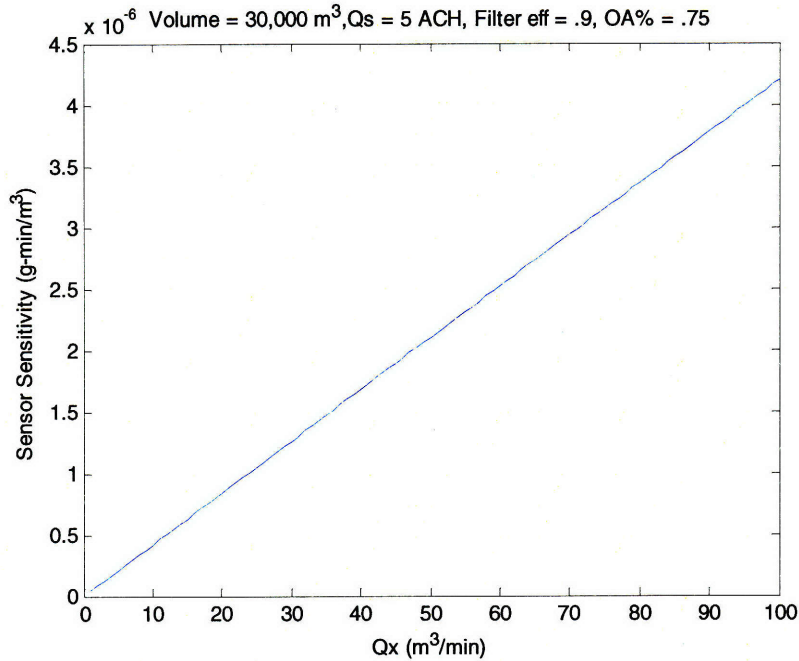
Figure 7-14 Required sensitivity as a function of Qx

Ignoring the relatively small contribution that Qx has on dilution, the sensor requirements for a sensor in a neighboring AHU return is linear function of Qx as shown in Figure 7-14. Because of the low dilution levels in the transport zones in the airport model, it can be considered as a similar case to the convention center model but with a bit more complex geometry.
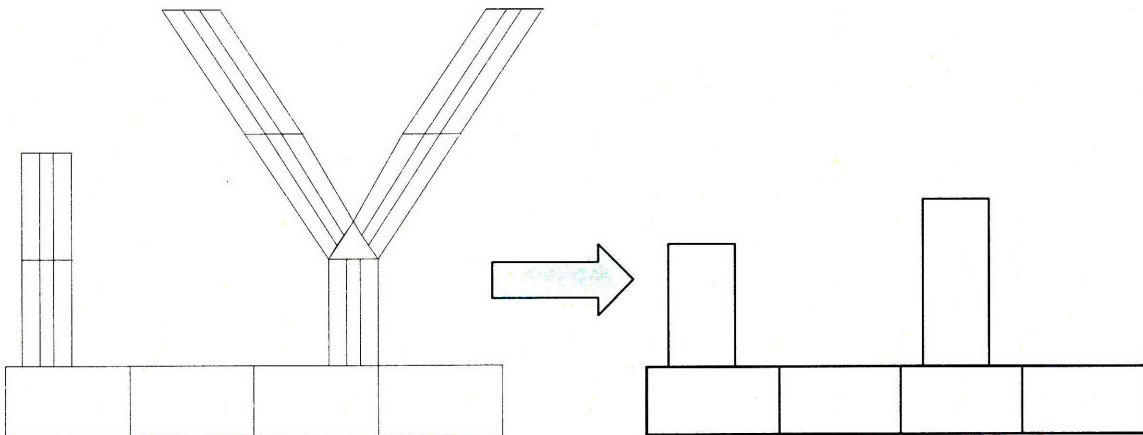
Figure 7-15 The more complex airport model can be represented in a simpler form

A more complex building geometry affects the optimal cost-sensitivity tradeoff as will be discussed in Section 7.1.4. In more complex geometries it is harder to position sensors

such that each sensor covers an equal section of the building. Subdividing a set of zones may require using more sensors than optimally would be the case, leading to more expensive sensors being included in the optimal coverage solution. More complex geometry may also restrict the spread of contamination throughout a facility leading to small pockets of high contamination concentration, favoring a greater number of less expensive sensors.

7.1.4. EFFECT OF BUILDING CONDITIONS

For the classes of buildings considered in this analysis, it appears that cheaper less sensitive sensors are favored over more costly higher performance sensors. This despite the sensor sensitivity varying by a factor of 10X between sensors and the cost only varying by 1.5X. The factors with the most influence on the sensing requirements in buildings include the intra-zonal air exchange rate (Q_X), the zone dilution for poorly-mixed zones, and the building geometry.

The preference for the cheaper less sensitive sensors can be better understood by examining the general case of contamination transport through a series of identical poorly mixed AHU zones. The sensitivity needed to detect a release in zone (n) was given in Section 4.2.1.

$$Sensitivity = \frac{mass}{dilution} * Q_X (\frac{1}{d} - \frac{1}{Q_S})^n \tag{7-3}$$

Rearranging the above equation to determine the number of zones covered (n) for a sensor with a given sensitivity:

$$A = Q_X (\frac{1}{dil} - \frac{1}{Q_S}) \tag{7-4}$$

$$Sensitivity = (\frac{mass}{dil})A^n$$

$$n = Log_A (sensitivity * \frac{dil}{mass})$$

For a one dimensional zone layout, like the convention center, the total number of zones covered is 2*n, not including the sensor zone. A sensor can not provide coverage for a

91

fraction of a zone so the number of zones covered must be rounded down. The total number of zones covered by a sensor in a convention center like building is:

$$Covered\ zones = 1 + 2 * floor(Log_A(sensitivity * \frac{dil}{mass})) \qquad (7\text{-}5)$$

The price of a sensor should be approximately proportional to the number of zones it covers. For example, if a building has fifteen zones then it would require three sensors capable of covering five zones to provide full coverage or alternatively one sensor that could cover all fifteen. The breakeven point would occur when the cost of the more sensitive sensor is three times that of the less sensitive sensors.

For the baseline convention center simulation Qx(1/d − 1/Qs)=.017 and d/m = 249. The number of zones covered as a function of sensitivity is shown in Figure 7-16.
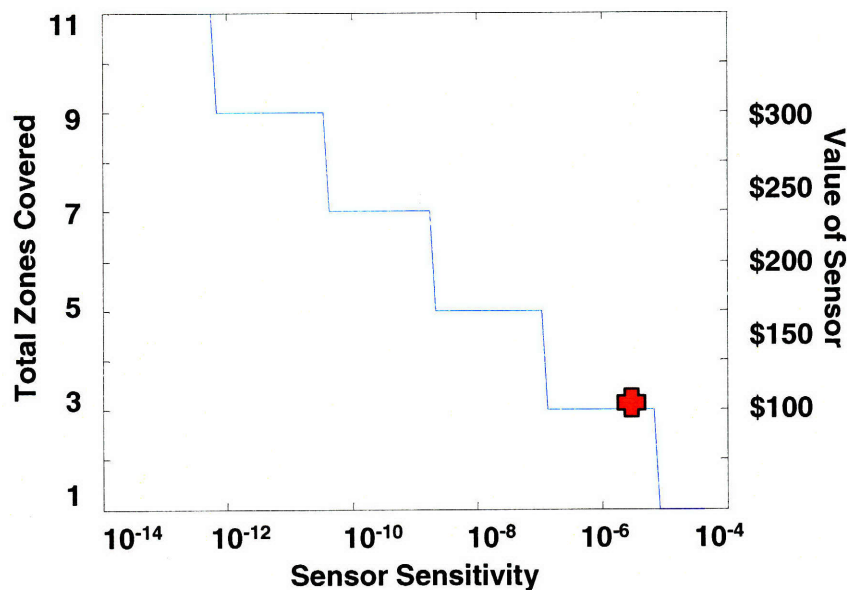
Figure 7-16 Sensitivity v. cost tradeoff in a series of poorly mixed zones

The color HHA sensor's sensitivity is equal to 1.7E-5, which according to Figure 7-16 is sufficient to cover three zones. This is consistent with the baseline analysis performed in Section 6.1.2 that suggested two inexpensive sensors are the optimal solution for the five zone convention center model. The value scale in the Figure 7-16 is scaled relative to the inexpensive sensor with a cost of $33 per zone covered. The fluorescent HHA sensor has a sensitivity of 1.7E-6 and the more sensitive PCR sensor is modeled as

having a sensitivity of 1.7E-7. According to Figure 7-16 the fluorescent HHA covers three zones, and the PCR sensor covers five zones. Both of these sensors are priced above $33 per zone covered and are therefore less efficient then the inexpensive sensor. This is the reason that the cheaper sensor is dominant choice for a majority of the convention center simulations.

The tradeoff between cost and sensor sensitivity in the optimal sensing solution is a function of the path lengths in the network model. The path length is equal to the ratio of mixing airflow rates to unmixed dilution.
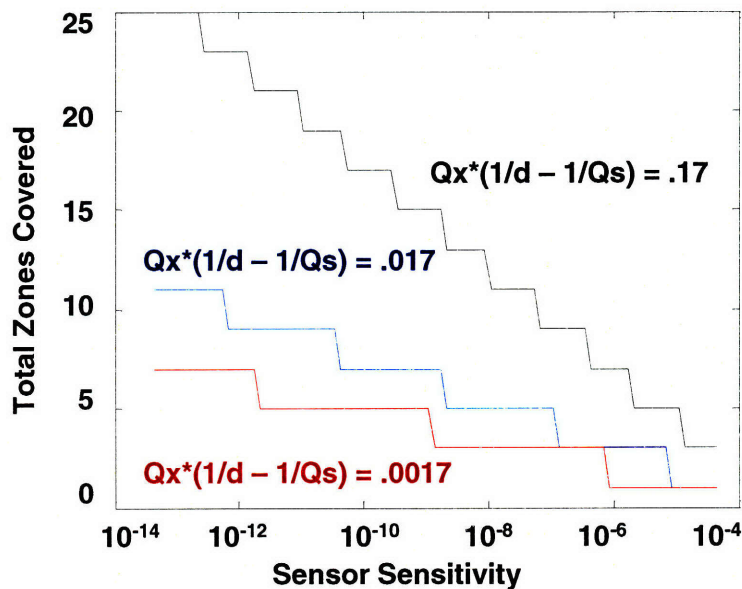
Figure 7-17 The effect of Qx and dilution on the cost-sensitivity tradeoff

Figure 7-17 shows that as Qx*(1/d-1/Qs) increases smaller changes in sensitivity leads to larger changes in the number of zones coverage. This indicates that in better mixed buildings higher sensitivity sensors would have greater value then in poorly-mixed spaces. Conceptually, if a building has many small pockets of high contaminant concentrations it is logical that multiple cheaper sensors would be more effective. If a low-level of contamination is evenly spread throughout the building fewer sensors with a higher sensitivity is a more effective solution.

The slope of the optimal tradeoff between sensitivity and cost also depends on the geometry of the network model. For a linear structure the total number of zones covered is a function of 2n, because the sensor covers zones on either side of the sensor zone.

In a more diffuse structure the multiplier for (n) might be higher because the sensor zone might have more pathways leading out from the zone. For example, the central node in a cross would cover 1+4n zones, approximately twice the number covered in a linear network.

N=1; Covers three zones

N=1; Covers five zones
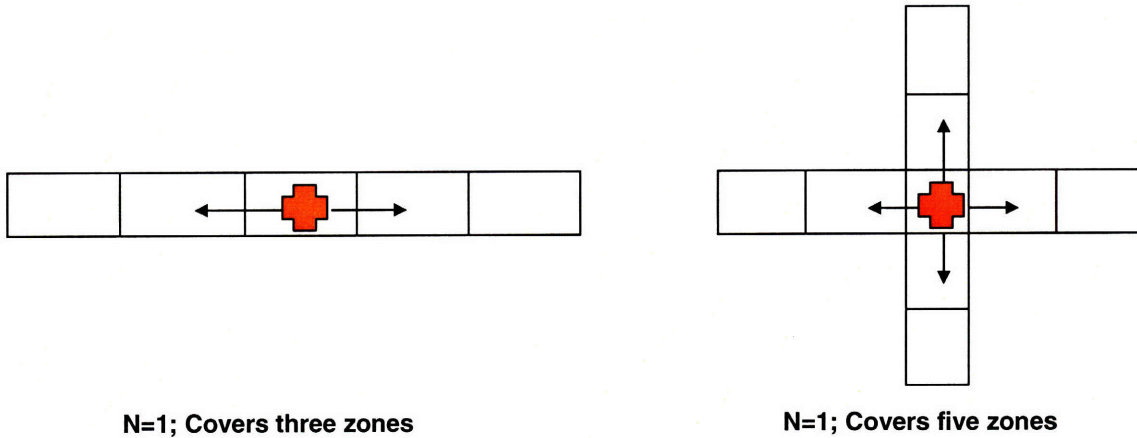
Figure 7-18 Influence of building geometry on zones covered

Qualitatively, the more connected a building's network model the more zones each sensor will be able to cover and the greater the preference for high sensitivity sensors. In graph theory, the concept of a minimum dominating set describes the minimum number of nodes in graph that must be occupied so that every other node is a maximum distance from an occupied node. Finding the minimum dominating set (MDS) has been shown to be an NP-complete problem for arbitrary graphs (Haynes, 1998). The binary integer program described in Section 5.3 approximates the solution to a type of MDS problem in order to determine the optimal sensor layout.

Although most of these subset problems are NP-complete, it is possible to bound the domination number based upon the number of nodes and the connectivity of the graph. For any graph G;

$$\left[\frac{n}{1+\Delta(G)}\right] \leq \gamma(G) \leq \frac{(n+1-(\delta(G)-1)\frac{\Delta(G}{\delta(G)})}{2}$$

(7-6)

where:

n = number of vertices in the graph

Δ(G) = maximum degree of any vertex

94

$\delta(G)$ = minimum degree of any vertex

$\gamma(G)$ = domination number (number of vertices needed to dominate)

From Equation (7-6) it is evident that the number of vertices needed to dominate a graph is inversely related to the maximum degree of that graph and directly related to the minimum degree. Additional more stringent bounds on a graph's domination number can be found by restricting the type of graphs analyzed (Haynes, 1998).

A full exploration of the concept of dominating sets is outside the scope of this analysis. The important point is that as graphs, and therefore the building network models they represent, become more interconnected the number of vertices needed to dominate the graph becomes fewer. Fewer dominant vertices indicate that each sensor is able to cover more zones with a given sensitivity and therefore the value placed on sensor sensitivity increases.

In addition to minimizing cost while providing full coverage there are additional metrics that would need to be considered in a deployed system and may affect the preference for different sensor types. The false alarm rate of the sensors is one of these metrics. It is probable that the higher sensitivity sensors would have a lower false alarm rate then the lower cost options. In addition, with fewer high-cost sensors needed to provide full coverage, the probability of false alarm might be considerably lower with the more expensive sensors. Conversely, if the false alarm rates of the less expensive sensors are uncorrelated it might be possible to build a more robust system by including many low-cost sensors and then requiring multiple sensor alarms before action is taken. These scenarios could be included in future analysis but are beyond the current scope of this effort.

7.2. SENSOR ALLOCATION WITH LIMITED SENSING RESOURCES

Up to this point we have attempted to determine the number of sensors needed to detect a release of a given size in a variety of buildings. It is oftentimes the case, however, that building owners are faced with limited resources and must determine the best way to utilize their limited assets. This section develops a methodology for determining the optimal placement of sensors based upon minimizing the worst-case undetectable release. The methodology is then applied to the three baseline models discussed in

Section 6. The optimal sensor placement is determined for situations where the building operator has only two inexpensive sensors available. The criterion used to optimize the placement of sensors is to minimize the worst-case attack that the sensors would not be able to detect. Worst-case is defined by the largest number of people that would receive a lethal dose of the contaminant.

7.2.1. EXAMPLE CASES

The convention center model is used as an example case because it is the simplest of the three models and has the fewest zones and potential sensor locations. A depiction of the convention center model is shown Figure 7-19. The model has a total of five identical zones and nine possible sensor locations (S1-S9). The nine sensor locations are in the return ducts for the five zones and at the four zonal interfaces.
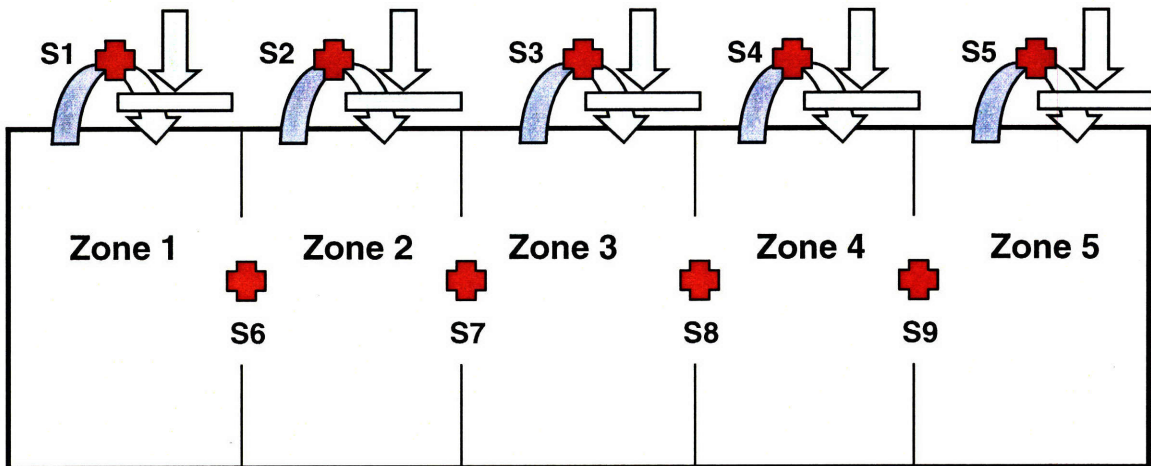

Figure 7-19 The convention center model

The algorithm uses the n X m matrix *zonedose* that describes the dosage that results at each (m) sensor locations for a one gram release in all (n) zones. This matrix is constructed using the underlying network model and a dynamic programming algorithm as was described in Section 5.3.

Zonedose

Release Zone	Sensor Locations								
	S1	S2	S3	S4	S5	S6	S7	S8	S9
Z1	4.3E-04	7.5E-06	1.3E-07	2.2E-09	3.9E-11	1.9E-04	3.2E-06	5.6E-08	9.6E-10
Z2	7.2E-06	4.2E-04	7.0E-06	1.2E-07	2.1E-09	1.8E-04	1.8E-04	3.0E-06	5.2E-08
Z3	1.2E-07	7.0E-06	4.2E-04	7.0E-06	1.2E-07	3.0E-06	1.8E-04	1.8E-04	3.0E-06
Z4	2.1E-09	1.2E-07	7.0E-06	4.2E-04	7.2E-06	5.2E-08	3.0E-06	1.8E-04	1.8E-04
Z5	3.9E-11	2.2E-09	1.3E-07	7.5E-06	4.3E-04	9.6E-10	5.6E-08	3.2E-06	1.9E-04

A one gram release in zone 3 leads to a dosage of 7E-6 g-min/m^3 at sensor location 2

Figure 7-20 *Zonedose* matrix is the dose at each sensor location for a release in each zone

When the sensitivity of the sensor is divided by the entries in *zonedose* the n X m matrix *detectmass* is formed. The entries in *detectmass* are the quantity of agent that needs to be released in zone (n) in order for the sensor at location (m) to alarm.

Detectmass

Release Zone	Sensor Locations								
	S1	S2	S3	S4	S5	S6	S7	S8	S9
Z1	4.0E-02	2.3E+00	1.3E+02	7.6E+03	4.3E+05	9.1E-02	5.3E+00	3.1E+02	1.8E+04
Z2	2.4E+00	4.1E-02	2.4E+00	1.4E+02	7.9E+03	9.7E-02	9.7E-02	5.6E+00	3.3E+02
Z3	1.4E+02	2.4E+00	4.1E-02	2.4E+00	1.4E+02	5.6E+00	9.7E-02	9.7E-02	5.6E+00
Z4	7.9E+03	1.4E+02	2.4E+00	4.1E-02	2.4E+00	3.3E+02	5.6E+00	9.7E-02	9.7E-02
Z5	4.3E+05	7.6E+03	1.3E+02	2.3E+00	4.0E-02	1.8E+04	3.1E+02	5.3E+00	9.1E-02

At least 2.4 grams of agent need to released in zone 3 to cause an alarm at sensor position 2

Figure 7-21 *Detectmass* is the mass that needs to be released for a given sensor to alarm

Each release defined in *detectmass* would lead to a corresponding dosage distribution within the building. By using the lethality curve, or probit slope, for a particular agent the percentage of people in each zone that would receive a lethal dose is determined. Multiplying the lethality by the number of people in each zone and then summing over all the zones gives the number of untreated fatalities for each release. A new n X m matrix is created that defines the number of untreated casualties that would result in the maximum undetectable release of agent in each of the n zones for all m sensor locations.

The next step in the analysis is a combinatorial optimization routine that minimizes the maximum number of casualties that would result for the various sensor combinations. The maximum number of sensor locations considered is thirty (airport case) and we are considering those cases where we are limited to two sensors, therefore the maximum number of sensor combinations is 30 choose 2:

$$\frac{30!}{28!*2!} = 435$$

Because this is a rather moderate number of sensor combinations each one can be considered explicitly. The optimization routine considers each sensor combination and determines what release causes the highest number of fatalities while evading detection from either sensor. The sensor combination that minimizes this worst-case release is then selected as the optimal combination for the available resources.

Fatalities

		S1	S2	S3	S4	S5	S6	S7	S8	S9
	Z1	395	2573	6882	11852	16833	729	3616	8245	13227
	Z2	2968	395	2968	9415	16320	729	729	4345	11132
	Z3	9455	2968	395	2968	9455	4345	729	729	4345
	Z4	16320	9415	2968	395	2968	11132	4345	729	729
	Z5	16833	11852	6882	2573	395	13227	8245	3616	729

Sensor Locations (header spanning above S1–S9)

Release Zone (vertical label beside Z1–Z5)

A 2.4 grams release in zone 3 causes 2,968 untreated fatalities

Figure 7-22 *Fatalities* is the number of untreated fatalities that would occur for an undetectable release

In the example, sensor set {1, 4} and sensor set {2, 5} are both optimal combinations and minimize the worst-case scenarios. The worst-case for this simulation results in 2968 untreated fatalities and occurs due to a 2.4 gram release in either zone two or zone three for sensor set {1, 4}. The two thousand nine-hundred and sixty-eight fatalities correspond to 11.9% of the convention centers 25,000 inhabitants based on a constant population density of 1 person per 20 ft^2.

For all the simulations the population density in a room is set to a constant ratio of the square footage. The least expensive sensors are considered corresponding to HHA sensors with sensitivity equivalent to 10,000 spores. The contaminant in the simulations is anthrax and the infectivity model used is given in Figure 7-23 (Glassman, 1966).
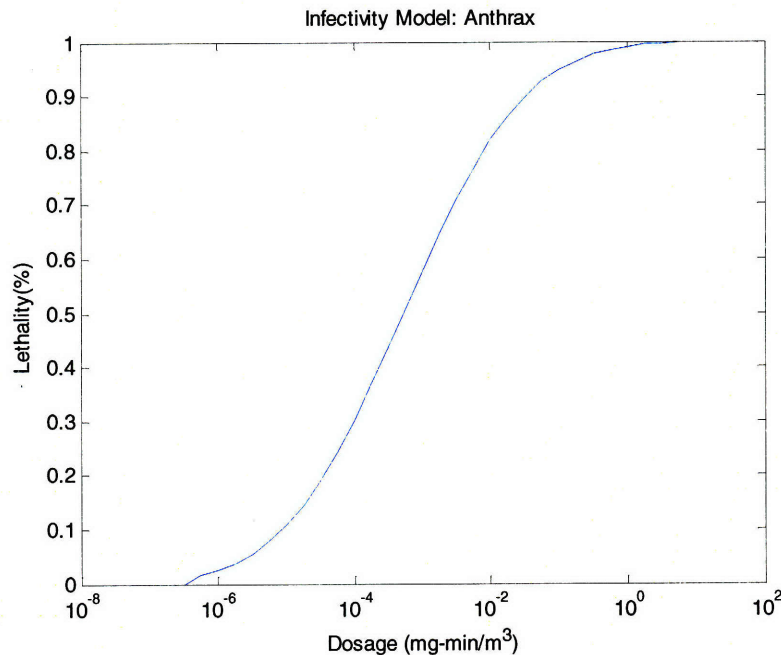
Figure 7-23 Infectivity model for anthrax

For the office building model the optimal sensor allocation for two inexpensive sensors is shown in Figure 7-24.
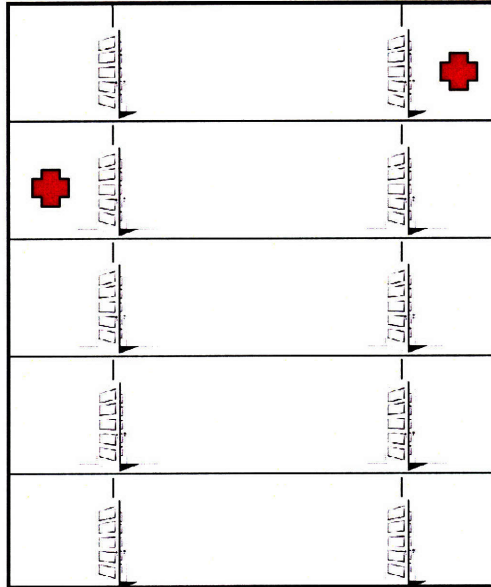
Figure 7-24 Optimal sensor placement for an office building with 2 sensors

The worst-case undetectable release for this sensor layout is a .2 gram release of anthrax in the fourth floor office level. A release of this size and location is expected to result in 320 untreated fatalities, equivalent to 8.7% of the total building population.

The optimal positioning for two low-cost sensors in the airport model is given in Figure 7-25
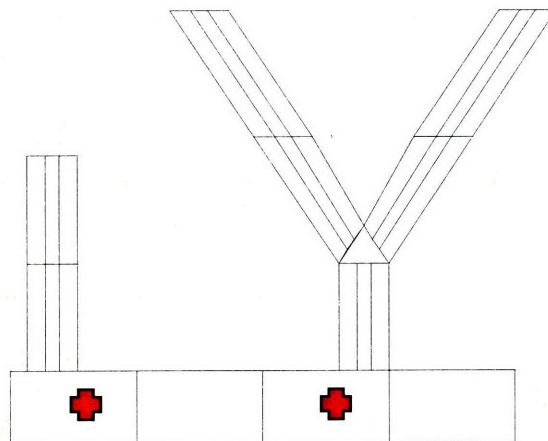
Figure 7-25 Optimal sensor positioning for two sensors in an airport terminal

The worst-case undetectable release for the optimal sensing solution consists of a 1.6 gram release in zone 25 (the lower right zone in the main terminal). This release would lead to 1122 untreated casualties, or 7.3% of the 15,000+ occupants. The optimal sensor locations are identical to the locations used in the set coverage problem.

7.2.2. EFFECT OF BUILDING CONDITIONS

In approximating the performance of a limited set of sensors in a particular building the analysis tools developed in Section 7.1.4 are useful. Recall that the number of zones covered by a particular sensor in a linear building layout was given by:

$$Covered\ zones = 1 + 2 * floor(Log_A(sensitivity * \frac{dil}{mass}))$$ (7-7)

If the situation is such that there are a limited number of sensors that will be used in a particular building the above equation can be rearranged to solve for the maximum release mass that would evade detection.

$$Mass = dil * sensitivity * A^{\frac{(1-Z)}{2}}$$ (7-8)

Z is the total number of AHU zones in the building divided by the number of sensors available and then rounded up. The 2 in $A^{(1-Z)/2}$ is appropriate for linear zone arrangements but needs to be adjusted depending upon the building layout. In general the maximum undetected release is equal to:

$$Mass = dil * sensitivity * A^{-n}$$ (7-9)

where:

n= maximum nodes between any node and a sensor node

For the convention center model the inputs are d = 2491, sensitivity = .000017, A = .017, and n=1. The predicted maximum undetected release mass is therefore:

2491*.000017*.017^-1 = 2.49 grams

This is extremely close to the calculated max release of 2.4 grams of anthrax. For the office building, ignoring the dose reduction within the stairwell, the inputs are: d= 335, A=.077, n=1, and the maximum undetected release is:

335*.000017*.077^-1 = .1 grams

And for the airport model d= 687.5, A = .0065, n=1, and the maximum predicted undetectable release is:

$$687^*.000017^*.0065^\wedge{-}1 = 1.8 \text{ grams}$$

The predicted maximum release for both the airport and office building roughly approximate their calculated values, with the office building off by a bit because the dilution through the stairwell transport zones is ignored.

How well a group of sensors can defend a particular building is proportional to the average zone dilution, the sensitivity of the sensors, and the building mixing parameter to the power of the number of zones that each sensor covers. This reinforces the conclusions from Section 7.1.4 that stated that a larger number of inexpensive sensors will typically outperform a few higher sensitivity sensors in most situations.

7.3. SUMMARY

The network model representation of large buildings appears to be an efficient method for analyzing potential building threats over a large number of conditions. It is easy to modify important factors such as dilution and intra-zonal airflows and then understand the impact on optimal sensor architectures.

During the sensitivity-cost analysis it became evident that, given the sensor models used, the less expensive sensors were favored more often then the more expensive sensors. This held true even with the sensor models having a 10X improvement in sensitivity for every 1.5X increase in cost. In Section 7.1.4 the equation is derived that relates the number of zones covered by a sensor (and thus the price we would pay) to the sensitivity of the sensor. The primary factor determining the preference for sensors of different costs and sensitivity was found to be how well mixed the building is. Buildings that are well-mixed tend to display a preference for a small number of high sensitivity sensors, while buildings that are poorly-mixed are better covered by many cheaper sensors.

When a limited number of sensors are available to protect a facility, one likely placement criteria is to place the sensors so that they limit the worst-case release that would go undetected. Section 7.2 discussed the implementation of this strategy for the three baseline models. A first-order estimate of the maximum attack that would evade detection was derived in Equation (7-8). From this equation the building operator can determine what size release constitutes an undetectable threat which informs the design of the building's physical security.

102

8. SUMMARY

The purpose of this exercise was to create a reduced-order model that can be used to quickly determine the preliminary sensing requirements for large buildings. Intra-zonal airflow rates are not calculated directly, as is common in other network models, but instead are taken as input parameters into the model and are then used to calculate the contamination transport equations. Intra-zonal airflows are highly variable and this construct makes it easy to parametrically vary the airflows and understand the impact on the optimal sensing solution.

In calculating the contamination transport equations the assumption is made that large air-handling zones are poorly-mixed. This assumption sets a reasonable lower bound on the spread of contamination through large AHU zones and thus an upper bound on the building's sensing requirements.

A building is subdivided into large AHU zones and smaller transport zones and is formulated as a network model. The nodes in the network model represent potential sensor locations and the path lengths between zones are the reduction in dose as an aerosolized contaminant flows between sensing locations. Concepts from network theory such as set coverage and dominant sets are then used to determine the optimal sensing solution for a particular building.

Section 8.1 discusses the important results gleaned from the development of the reduced-order model including the relationship of building parameters to sensor effectiveness. Section 8.2 details future improvements that could be made to the reduced-order model. Section 8.3 discusses the contributions of this work towards the goal of a simplified analysis methodology.

8.1. RESULTS DISCUSSION

The factors influencing the sensing requirements in buildings include the building's airflows and architectural layout. In Section 4 the dose in a release zone was calculated to be:

$$Dose \sim (\int mgen) / (f_S Q_R + Q_{OA})$$
(8-1)

for a well-mixed zone and:

$$Dose \sim m_i \left(\frac{1}{Q_R f_S + Q_{OA}} - \frac{1}{Q_S} \right) \qquad (8\text{-}2)$$

in a poorly-mixed zone. The ($Q_R f_S + Q_{OA}$) term was defined as a zone's dilution and is the rate at which contaminated air is removed from the zone either through inflows of clean fresh air (Q_{OA}) or the cleaning of contaminated air as it is circulated through the buildings HVAC filters ($Q_R f_S$). For a poorly-mixed zone 1/(1/dil − 1/Qs) is defined as the zone's poorly-mixed dilution and is always larger then a zone's well-mixed dilution.

It is the ratio of intra-zonal airflows to dilution that determines how efficiently contaminants are spread throughout a building. The dosage multiplier between neighboring AHU zones equals the air exchange rate in the direction of contamination transport divided by the dilution rate in the downstream zone.

$$Dose_2 \sim Dose_1 * \frac{Q_X}{(f_S Q_R + Q_{OA})} \quad \text{(well-mixed)} \qquad (8\text{-}3)$$

$$Dose_2 \sim Dose_1 * Q_X \left(\frac{1}{Q_R + Q_{OA}} - \frac{1}{Q_S} \right) \quad \text{(poorly-mixed)} \qquad (8\text{-}4)$$

A network model was constructed with the nodes equivalent to sensor locations and dose multipliers ($Dose_2/Dose_1$) equal to the path lengths between nodes. Building characteristics such as stairwells and hallways are also included as nodes in the network model due to their important role in contamination transport. These transport zones oftentimes interconnect multiple AHU zones and have short unidirectional path lengths due to high intra-zonal airflows and low dilution.

The structure of a building, principally the number and layout of its AHU zones, determines the structure of its network model. As discussed in Section 7.1.4, increasing the connectivity of a building's network model likely decreases the number of nodes required to form a dominant set. A smaller domination number for a graph indicates that fewer sensors would be required to fully cover the building.

The sensing requirements for a particular building depend on the "size" and "connectivity" of the building. From a contamination transport perspective the "size" of a building depends upon the building's dilution and the number of zones. A building's "connectivity" has a direct relationship to the intra-zonal airflow rates and the connectivity

104

of the underlying network model. Qualitatively, the number of sensors needed to cover a building increase with the "size" of the building and decreases as "connectivity" increases.

In Section 7.1.4 the number of zones covered by a sensor was determined for a one-dimensional network model with uniform zone dilutions and intra-zonal airflow rates.

$$Covered\ zones = 1 + 2 * floor(Log_A(sensitivity * \frac{dil}{mass})) \qquad (8\text{-}5)$$

where:

$$A = Q_X(\frac{1}{dil} - \frac{1}{Q_S}) \qquad (8\text{-}6)$$

Equations (8-5) and (8-6) show that Qx and the poorly-mixed zone dilution have a proportional influence on a sensor's effectiveness. A 10% rise in the intra-zonal airflow rate and a 10% gain in the poorly-mixed dilution will result in no change in path length or the number of zones covered. However, the number of zones covered by a sensor varies logarithmically with the ratio of Qx to poorly-mixed dilution. A small change in their ratio, (A), typically has a small effect on coverage, but as the ratio approaches one the change in coverage can be severe. As the intra-zonal airflow approaches the dilution rate very little contamination reduction occurs between zones and a sensor covers a larger number of zones. In Figure 8-1 we see the affect that the variable A has on $Log_A(sens*d/m)$ for the hypothetical case of sensitivity = .000017, dilution = 2000, and mass =1 gram.
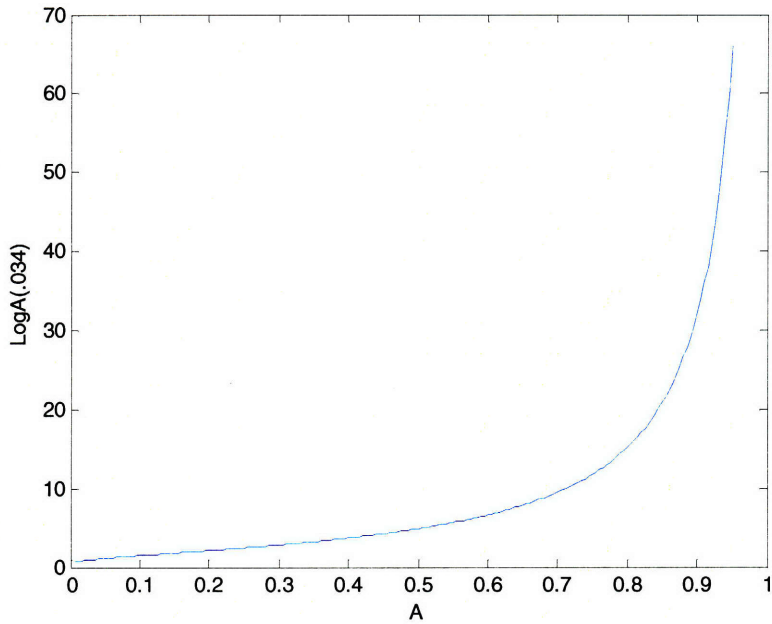
Figure 8-1 The effect of Qx(1/d-1/Qs) on zones covered

In Equation (8-5) the interconnectivity of the network model is expressed through the multiplier (2*). In the linear example the multiplier is two because the sensor covers zones on either side of the sensing zones. In theory, in networks where the nodes posses' high in-degree centrality an incremental increase in directional coverage could yield an exponential increase in the total zones covered. Buildings with this type of geometry are expected to be rare.

Linear model

Interconnected model
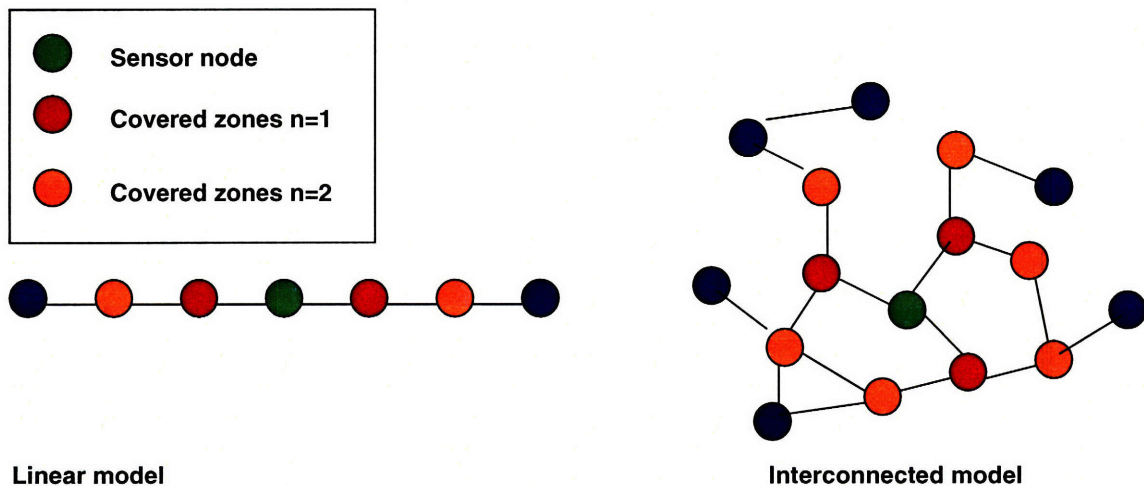
Figure 8-2 A sensor in the interconnected model covers more zones

Each building is unique; however some general guidelines for sensor placement can be deduced based upon the gross building airflow characteristics. For buildings with a strong directional airflow it is best to place sensors in zones at the end of the airflow path. Strong directional airflows may occur in tall buildings with large indoor / outdoor temperature differences (like the office building model), in buildings with the majority of outdoor leakage paths in a particular location (like the airport model), or in instances with strong wind pressures from a consistent bearing. The network model for these buildings resembles a tree-like structure with short path lengths due to high Q_x values relative to zone dilutions between upstream zones and downstream zones. Placing sensors in the downstream "leaves" efficiently covers upstream zones because the directional path lengths are relatively short.

For buildings without strong directional airflows the best locations for sensor placement are typically towards the center of the building. The center of the building is the zone with the lowest eccentricity in the network model implementation. Absent of transport zones or highly directional airflows, the network center should be approximately equivalent to the geographic center of the building. In buildings requiring multiple sensors the optimal sensor positions will minimize the maximum distance from any zone in the building to a sensor location.

8.2. FUTURE WORK

Additional work is needed to study certain assumptions made in the reduced-order model, to explore ways to further simplify the modeling approach, and to examine whether a similar approach would be useful for a concentration dependant sensing solution.

A future addition to the model might include the ability to account for deposition and resuspension of particulates. The current model assumes contaminants are aerosolized, which allows for contamination flow between zones to be represented as an equivalent intra-zonal airflow. Deposition is a concentration dependant phenomenon and depends on many factors including particle size distribution and electrostatic charge. The resuspension of particulates also depends on a variety of factors particularly the level of activity in a zone. It is unclear whether deposition and resuspension will significantly impact fixed dose dependant sensors. Studies indicate that the primary effect of these phenomena is a persistent low level of contaminant concentration in a

zone for a period of time well after the release. While this is not likely to impact the dose dependant model, it should be examined in more detail.

In general, a more detailed analysis is needed to understand the boundaries of the reduced-order model. Section 4.4 discussed some of the limitations of the model but did not attempt to quantify the limits. In particular, more work is needed to understand when the poorly-mixed assumption should be used instead of the well-mixed assumption.

This thesis provides only a cursory description of certain concepts from graph theory such as dominating sets. Finding the minimum dominating set for a graph bears many relationships to the sensor placement problem. It is possible that further constructs from graph theory could be used to better classify building types and quickly determine the sensing needs in large buildings. The idea of visualizing a building as a two-dimensional network has been considered previously in disciplines such as space syntax theory but has not been applied to this class of problems.

A related path that could further simplify the analysis process would involve grouping buildings into several classes based on physical type and use. A sample of buildings from each class would then be examined in more detail and the similarities in network structure within building classes could be determined. If enough similarities exist between buildings of a particular class then general rules-of-thumb could be developed that simplify the analysis of future buildings.

The methodology presented here only considers the requirements for dose dependant bio-defense sensors. Dose dependant sensors are a logical starting point because they are cheaper, more readily available, and less prone to false alarms then concentration dependant sensors. In the longer-term, however, the natural trend will likely be towards concentration dependant sensors which have the potential to provide greater defensive capabilities. It is unclear whether the network constructs developed here would applicable to concentration dependant sensors, and is an area that should be explored in further detail.

8.3. CONTRIBUTIONS

Research today focuses on creating ever more complex building models utilizing techniques such as computational fluid dynamics. Even the more simplified multi-zone models are moving in this direction. Recent releases of CONTAM, the multi-zone model

developed by NIST, have included a feature that allows users to define 1D convection/diffusion zones in which contaminant concentration can vary along a user-defined axis. Additional complexity not only increases the models' run-time but increases the time it takes to construct the model and analyze the results.

Very large buildings can be millions of square feet in size and have highly variable airflow patterns that depend upon numerous factors. Creating detailed airflow models requires considerable time and effort and only provides a single snapshot of the building's conditions. Coarser models that consider only the gross building characteristics are faster to build and execute and can provide the level of specificity necessary to make informed decisions.

The reduced-order model is a tool that can help simplify the analysis of large indoor spaces. The flexibility of the model combined with fast simulation times allows the user to understand how variations in building conditions influence the number and placement of sensors needed to detect an attack. And the network based architecture of the reduced-order model is a new and intuitive method for conceptualizing how a building's structural layout affects the placement of sensors.

Potentially more valuable then the actual model are the quantifiable insights into how simple building properties affect sensing requirements. The number of zones covered by a single sensor was calculated as function of the building's HVAC properties, the connectivity of the HVAC zones, and the intra-zonal airflow rates. The optimal tradeoff between a sensor's sensitivity and cost was also characterized under various building conditions. Being able to quantify how building properties directly influence sensing requirements circumvents the need to conduct time consuming analysis of a building's airflow conditions.

The eventual goal is to be able to estimate the number and placement of sensors based solely on the building's architectural layout and the properties of its mechanical system. Ideally a building operator will be able to enter information about the type of building, its location, and some basic information about its mechanical system into a model and generate a realistic set of requirements. This thesis is only a first step towards realizing that goal.

Altmel, I. Kuban, Necati Aras, Evren Guney, and Cem Ersoy. "Effective coverage in sensor networks: Binary integer programming formulations and heuristics". IEEE ICC 2006 proceedings 4014-4019

ASHRAE handbook. Fundamentals. Atlanta, Ga. : American Society of Heating, Refrigerating, and Air-Conditioning Engineers, c2001-

ASHRAE Standard 62.1-2004 "Ventilation for Acceptable Indoor Air Quality"

ASHREAE Standard 52.2-1999 "Filter Performance Test Standard"

Beghein, C., Y. Jiang, and Q. Y. Chen. "Using large eddy simulation to study particle motions in a room." Indoor Air V. 15 (2005) 281-290

Chakrabarty, Krishnendu, S. Sitharama Iyengar, and Hairong Qi. "Grid Coverage for Surveillance and Target Location in Distributed Sensor Networks." IEEE Transactions on Computers V. 51 N. 12 1448-1453

Davis, Christopher J. "Nuclear Blindness: An Overview of the Biological Weapons Programs of the Former Soviet Union and Iraq." Emerging Infectious Diseases V.5 N.4

De Neufville, Richard. Airport Systems Planning, Design, and Management New York, McGraw-Hill, 2003

Drivas, Peter J., Peter A. Valberg, Brian L. Murphy, and Richard Wilson. "Modeling Indoor Air Exposure from Short-Term Point Source Releases." Indoor Air V. 6 (1996) 271-277

Ferro, Andrea R., Royal J. Kopperud, and Lynn M. Hildemann. "Source Strengths for Indoor Human Activities that Resuspend Particulate Matter". Environ. Sci. Technol. (2004), V.38, 1759-1764

Feustel, Helmut E., and Brian V. Smith. "COMIS 3.0 – User's Guide." Lawrence Berkley National Laboratory (1997)

http://www.flychicago.com/ohare/concessionsohare/pdf/Terminal123.pdf (2008)

http://www.flydenver.com/maps/inside/index.asp (2008)

Glassman, H.N., "Industrial Inhalation Anthrax," Bacteriol. Rev. 30: 657-659, 1966.

Gross, Jonathan L., and Jay Yellen, Graph Theory and Its Applications Boca Raton, Chapman & Hall (2006).

Haghighat, Fariborz, and Ahmed Cherif Megri. "A Comprehensive Validation of Two Airflow Models – COMIS and CONTAM". Indoor Air V.6(1996) 278-288

Haynes, Teresa W., Stephen T. Hedetniemi, and Peter J. Slater. Fundamentals of Domination in Graphs. New York. Marcel Dekker, Inc. (1998)

Hiller, B. and Hanson, J. The Social Logic of Space. Cambridge University Press (1984)

JAMA. "Anthrax as a Biological Weapon, 2002; Updated Recommendations for Management". Journal of the American Medical Association, May 1, 2002 V. 287, N 17.

Liu, X., and Z. Zhai. "Location identification for indoor instantaneous point contaminant source by probability-based inverse Computational Fluid Dynamics modeling." Indoor Air V.18 (2008) 2-11

Miller, Judith, "U.S. Deploying Monitor System for Germ Peril," The New York Times, January 22, 2003, p.A1

Richmond-Bryant, J., A. D. Eisner, L. A. Brixey, and R. W. Wiener. "Transport of airborne particles within a room." Indoor Air V.16 (2006) 48-55

www.sanjose.org (2007)

Schaelin A., V. Dorer, J. Maas, A. Moser. "Improvement of multizone model predictions by detailed flow path values from CFD calculations". ASHRAE Transactions 1994;100(Part 2):709-720

Thatcher, Tracy L., and David W. Layton. "Deposition, Resuspension, and Penetration of Particles within a Residence". Atmospheric Environment V. 29, N. 13 (1995) 1487-1497

Upham, R. "A validation study of the airflow and contaminant migration computer model CONTAM as applied to tall buildings". University Park Pa: The Pennsylvania State University: 1997.

Van Broekhoven, Scott B. *Unpublished Data* (2002)

Walton, George N., and W. Stuart Dols. "CONTAM 2.4b User Guide and Program Documentation." NISTIR 7251 (2006)

Wang, L. and Chen, Q. 2007. "Validation of a coupled multizone and CFD program for building airflow and contaminant transport simulations". HVAC&R Research, 13(2), 267-281

Wikipedia "World Trade Center Design with Floor and Elevator Arrangement" http://en.wikipedia.org/wiki/World_Trade_Center (2008)

Wilkening, Dean A. "Sverdlosk revisited: Modeling human inhalation anthrax." Proceedings of the National Academy of Sciences 2006;103;7589-7594

Yamamoto, Toshiaki, David S. Ensor, and Leslie E. Sparks. "Evaluation of Ventilation Performance for Indoor Space." Building and Environment V.29 N.3 (1994) 291-296

Zhang, T, and Q. Chen. "Identification of contaminant sources in enclosed spaces by a single sensor." Indoor Air V.17 (2007) 439-449